Extraction of bioactives from marine by-products using Deep Eutectic Solvents for Dry Eye Disease treatment

Maha Abdallah

Dissertation presented to obtain the
Ph.D degree in Sustainable Chemistry

Instituto de Tecnologia Química e Biológica António Xavier | Universidade Nova de Lisboa

Oeiras,
March, 2022

"Nothing in life is to be feared; it is only to be understood."

- Marie Curie

Extraction of bioactives from marine by-products using Deep Eutectic Solvents for Dry Eye Disease treatment

Maha Abdallah

Dissertation presented to obtain the Ph.D degree in

Sustainable Chemistry

Instituto de Tecnologia Química e Biológica António Xavier | Universidade Nova de Lisboa

Oeiras, March 2022

DISSERTATION: July 2022

SUPERVISOR:

Doctor Naiara Fernández
Principle Scientist, Natural Bioactives and Nutraceuticals Process Technology Lab, Food and Health Division, iBET - Instituto de Biologia Experimental e Tecnológica

CO-SUPERVISOR:

Professor Maria do Rosário Beja Gonzaga Bronze
Associate Professor, Faculdade de Farmácia, Universidade de Lisboa
Senior Scientific Advisor
Head of Natural Bioactives and Nutraceuticals Characterization Lab, Food and Health Division, iBET - Instituto de Biologia Experimental e Tecnológica

CO-SUPERVISOR:

Doctor Ana Alexandra Figueiredo Matias
Invited Researcher, Natural Bioactives and Nutraceuticals Process Technology Lab, Food and Health Division, iBET - Instituto de Biologia Experimental e Tecnológica

The work included in this thesis was developed at:

- Food and Health Division, Instituto de Biologia Experimental e Tecnológica; Oeiras, Portugal.

- Instituto de Tecnologia Química e Biológica António Xavier, Universidade Nova de Lisboa; Oeiras, Portugal

- Faculdade de Ciências e Tecnologia, Universidade Nova de Lisboa; Caparica, Portugal

- Institute for Thermal Separation Processes, Hamburg University of Technology; Hamburg, Germany

- Instituto Universitario de Oftalmobiología Aplicada, University of Valladolid; Valladolid, Spain

Table of Contents

List of Figures

List of Tables

ACKNOWLEDGEMENTS

First and foremost, I want to thank my supervisor Dr. Naiara Fernández for the guidance, understanding, and motivation. Her support and knowledge have encouraged me throughout my research and daily life. I would also like to express gratitude to Professor Maria do Rosário Bronze and Dr. Ana Matias for the scientific support and suggestions that enabled the writing of the research articles and finally this thesis.

I gratefully acknowledge Junior-Professor Pavel Gurikov for his scientific guidance and for having me at the Hamburg University of Technology in Germany. I also want to thank Dr. Simon Müller and Andrés González de Castilla for support and resources that they provided to complete the research work.

I would like to thank the Applied Ophthalmology Institute in Spain, namely the supervisors Dr. Amalia Enríquez-de-Salamanca, Dr. Yolanda Diebold, Dr. María J. González-García and my colleagues Luna Krstić and Nikolaos Katsinas for the scientific assistance that I received during my secondment

I gratefully acknowledge the continuous support in acquiring training and knowledge from the supervisors and colleagues at the Food and Health Division at iBET. I want to especially thank my colleagues at the Natural Bioactives and Nutraceuticals Process Technology Lab, Ana Nunes, Agostinho Alexandre, Miguel Batista, Melanie Matos, João Baixinho, Martim Cardeira, Viktoriya Ivasiv, Inês Prazeres and every colleague who joined the team. I am grateful to sharing my PhD experience with you, for the help in the lab work, and most importantly for the friendships, understanding, encouragement, and all the good moments that we shared in the last years. Being part of your team made my PhD experience and my move to Portugal so pleasant and memorable.

Looking back to this period of my life, I am mostly grateful for my parents, my sister Rima Abdallah, and my family who were a great support during the last years. They always showed me the value of education and gave me the emotional support I needed to pursue my PhD. Thank you for your constant care, compassion, and for continuously making me feel less far from home during my PhD. I want to especially thank Simon Nabbout for always being a shoulder to lean on

during many years. I am in awe of the valuable support, advices, and for pushing me forward whenever I was in doubt.

I would like to thank everyone who was present during my PhD period, for the partnerships and collaborations from the start until the end, and the kind donations of marine raw materials that enable the completion of my work. Finally, I would like to acknowledge ITQB-NOVA for accepting my PhD work and providing the resources to accomplish this project and obtain my degree.

Summary

Dry eye disease (DED), results from tear film instability, inflammation, ocular surface damage and has significantly increased worldwide. Different risk factors are associated to this disease including aging, climate change, use of contact lens, hormonal changes, use of electronic screens, among others. The development of cures is highly essential for the treatment of DED. Currently, the most common therapy is the use of artificial and biological tear substitutes that aim for osmo-protection, lubrication and stabilization of the ocular surface.

Deep eutectic solvents (DES) have been widely investigated as an alternative approach to the use of conventional extraction methods, as they are more eco-friendly and cheaper comparing to conventional solvents. They are prepared by combining a hydrogen bond donor and hydrogen bond acceptor near the eutectic temperature and at molar ratio and include lactic acid, fructose, urea and terpenes (menthol, thymol, camphor, and borneol). The thermodynamic and physicochemical properties of these solvents are evaluated in order to define these solvents as “deep” eutectic mixtures. The simulation of the solid-liquid equilibrium phase diagram is done using the Universal Functional Activity Coefficient function and the Conductor-like Screening Model for Real Solvents software, which are compared to the real solid-liquid phase diagram of the solvents obtained using differential scanning calorimetry. In addition, the physicochemical properties are determined to assess the structure and the presence of hydrogen bonding and compare the behavior of these solvents with the components used for their preparation and confirm their behavior as a non-ideal mixture.

In this study, the extraction process was implemented using the prepared DES to extract bioactive ingredients from the marine by-products: including codfish bones, mussels and tuna vitreous humor. The obtained extracts were characterized to analyze their composition in proteins, lipids, ash, hyaluronic acid and chondroitin sulfate. The results were compared to extracts composition obtained using conventional methods that were prepared to confirm the viability of the use of DES as alternative extracting solvents. Bioactivity studies were done to evaluate the potential application of selected compounds in therapeutic formulations for the DED treatment. In vitro testing on human corneal epithelial cell line and dry eye-associated microorganisms were used. The cellular viability of the testing samples was studied on Caco-2 and human corneal cell lines. Moreover, the reactive oxygen species scavenging capacity and the potential inflammatory

response of the testing samples were assessed on human corneal epithelial cell line. Additionally, antimicrobial properties of the samples against dry eye-associated gram-positive bacteria (*Staphylococcus aureus*) and gram-negative bacteria (*Pseudomonas aeruginosa*) were evaluated to furtherly study the use of the samples as preservatives that ensure a safe shelf life increase in ophthalmic formulation.

Sumário

A síndrome do olho seco resulta da instabilidade do filme lacrimal, inflamação e de danos provocados na superfície ocular e tem aumentado significativamente no mundo. Diferentes fatores de risco estão associados a essa doença, incluindo o envelhecimento, mudanças climáticas, uso de lentes, alterações hormonais, uso de écrans electrónicos entre outros fatores. Atualmente, o tratamento mais comum consiste na utilização de lágrimas artificiais que podem garantir osmo-proteção, lubrificação e estabilização da superfície ocular.

Os DES têm sido estudados como alternativa aos solventes convencionais por serem mais ecológicos e baratos. São preparados combinando um dador e um aceitador de ligação de hidrogênio na temperatura eutéctica, como o ácido lático, frutose, ureia e terpenos (mentol, timol, cânfora e borneol). As propriedades termodinâmicas e físico-químicas dos DES são avaliadas para definir os solventes como “profundos”. Assim, a simulação do diagrama de fases de equilíbrio sólido-líquido é feita usando a função Universal Functional Activity Coefficient e o software Conductor-like Screening Model for Real Solvents, e são comparados com o diagrama de fase real sólido-líquido obtido quando se usa a calorimetria de varrimento diferencial. As propriedades físico-químicas são estudadas para avaliar a estrutura e a presença de ligações de hidrogênio e comparar o comportamento desses solventes com os compostos puros que foram utilizados para os preparar, e assim poder confirmar os seus comportamentos como misturas não ideais.

Neste trabalho foi implementado um processo para extração de ingredientes bioativos a partir de subprodutos marinhos: incluindo espinhas de bacalhau, mexilhão e humor vítreo de atum, usando os solventes eutéticos preparados com ácido lático, frutose, uréia e terpenos (mentol, timol, cânfora e borneol). Os extratos foram caracterizados na sua composição em proteínas, lipídos, cinzas, ácido hialurônico e sulfato de condroitina. Os resultados foram comparados com a composição dos extratos obtidos por métodos convencionais, para confirmar a viabilidade do uso de DES como solventes de extração alternativos. Foram feitos estudos da bioatividade para avaliar o potencial de aplicação dos compostos selecionados em formulações terapêuticas para o tratamento da doença dos olhos secos. Foram realizados testes in vitro com células epiteliais da córnea humana e com microrganismos associados aos olhos secos. A

viabilidade das amostras foi analisada na linha celular Caco-2 e na linha de células epiteliais da córnea humana. A capacidade de eliminação de espécies reativas de oxigênio e a resposta potencial inflamatória foram estudadas nas células epiteliais da córnea humana. Além disso, as propriedades antimicrobianas das amostras contra bactérias gram-positivas associadas ao olho seco (*Staphylococcus aureus*) e bactérias gram-negativas (*Pseudomonas aeruginosa*) foram estudadas para avaliar o seu uso como conservantes, garantindo um aumento seguro do tempo de vida da formulação oftálmica.

Abbreviation List

AAPH	2,2′-azobis(2-methylpropionamidine) dihydrochloride
ANOVA	Analysis of Variance
ARD %	Average Relative Deviation Percentage
BCA	Bicinchoninic Acid
Bor	Borneol
Cam	Camphor
CAMHB	Cation-Adjusted Mueller Hinton broth
CB	Codfish Bones
CE	Capillary Electrophoresis
CFU	Colony-Forming Unit
CHL-ED	Chloramphenicol-based Eye Drop
COSMO-RS	Conductor-like Screening Model for Real Solvents
CPC	Cetylpyridinium Chloride
CS	Chondroitin Sulfate
Da	Dalton
DED	Dry Eye Disease
DES	Deep Eutectic Solvent
di-0s	Non-sulfated Chondroitin Sulfate Disaccharide
di-4s	Chondroitin Sulfate Disaccharide (GlcAβ1-3GalNAc(4s))
di-6s	Chondroitin Sulfate Disaccharide (GlcAβ1-3GalNAc(6s))
di-HA	Hyaluronic Acid Disaccharide

DMEM	Dulbecco’s Modified Eagle Medium
DMSO	Deuterated Dimethyl Sulfoxide
DSC	Differential Scanning Calorimetry
DSS	2,2-Dimethyl-2-Silapentane-5-Sulfonate
ED	Eye Drop
EH	Enzyme Hydrolysis
EDTA	Ethylenediaminetetraacetic Acid
ELISA	Enzyme-Linked Immunoassay
FBS	Fetal Bovine Serum
FCS	Fucosylated Chondroitin Sulfate
FL	Disodium Fluorescein
Fru	Fructose
FTIR	Fourier-Transform Infrared Spectroscopy
GAG	Glycosaminoglycan
Gal	Galactosamine
GalNAc	N-Acetylgalactosamine
GlcA	Glucuronic Acid
GlcN	Glucosamine
H_2DCF-DA	2’,7’-dichlorodihydrofluorescein diacetate
HA	Hyaluronic Acid
HA-ED	Hyaluronic Acid-based Eye Drop
HBA	Hydrogen Bond Acceptor

HBD	Hydrogen Bond Donor
HCE	Human Corneal Epithelial
HPLC	High-Performance Liquid Chromatography
ICAM-1	Intercellular Adhesion Molecule-1
IdoA	Iduronic Acid
IL	Interleukin
Lac	Lactic Acid
MBC	Minimum Bactericidal Concentration
Men	Menthol
MIC	Minimum Inhibitory Concentration
MM	Mussel Meat
NEAA	Non-Essential Amino Acids
NMR	Nuclear Magnetic Resonance
ORAC	Oxygen Radical Absorbance Capacity
PBS	Phosphate Buffered Saline
PE	Precipitated Extract
PenStrep	Penicillin-Streptomycin
PMS	Phenazine Methosulfate
RD %	Relative Deviation Percentage
ROS	Reactive Oxygen Species
SAX	Strong Anion Exchange
SDS-PAGE	Sodium Dodecyl Sulphate – Polyacrylamide Gel Electrophoresis

SEM	Standard Error of the Mean
SF	Soluble Fraction
SLE	Solid–Liquid Equilibrium
TEAC	Trolox Equivalents Antioxidant Capacity
TGA	Thermogravimetric Analysis
Thy	Thymol
TMS	Tetramethylsilane
TNF-α	Tumor necrosis factor-α
TSA	Trypticase Soy Agar
TSB	Trypticase Soy Broth
TVH	Tuna Vitreous Humor
UNIFAC	UNIversal Functional Activity Coefficient
Ur	Urea
UV-B	Ultraviolet-B
XTT	2,3-bis-(2-methoxy-4-nitro-5-sulfophenyl)-2H-tetrazolium-5-carboxanilide

Symbols

A_1-A_9	Optimized parameters for the proposed models
e_r	Percentage relative error
M_w	Molecular weight
n	Refractive index

P	Pressure
T	Temperature
V	Volume
x	Molar ratio
γ	Activity coefficient
ΔH	Enthalphy
η	Viscosity
ρ	Density
σ	Surface tension
σ_1-σ_6	Optimized parameters for the proposed models
ω	Acentric factor

Subscripts

c	Critical
coeff	Coefficient
cr	Crystallization
D	Degradation
E	Eutectic
exp	Experimental
f	Fusion/melting
g	Glass

i	Compound i
L	Computed theoretically using models
m	modified Lydersen-Joback-Reid (for eutectic mixtures)
M	modified Lydersen-Joback-Reid (for pure compounds)
ref	reference

Superscripts

R	Residual
L	Computed theoretically using models
C	Combinatorial

Chapter I:
Introduction

This chapter was published by Elsevier as:

Abdallah, M. M., Fernández, N., Matias, A. A., & do Rosário Bronze, M. (2020). Hyaluronic acid and Chondroitin sulfate from marine and terrestrial sources: Extraction and purification methods. Carbohydrate Polymers, 243, 116441. DOI: 10.1016/j.carbpol.2020.116441

Abstract

Deep eutectic solvents (DES) have been widely investigated as new alternatives to conventional solvents as they are more eco-friendly and cheaper. They are prepared by combining a hydrogen bond donor and hydrogen bond acceptor, near the eutectic temperature and molar ratio. The thermodynamic behavior must be strongly non-ideal in order to define these solvents as “deep” eutectic mixtures. The physicochemical characterization is essential to define the structure and the chemical interactions and to obtain relevant properties for final purpose of these solvents. DES can be used for different industrial, biomedical and pharmaceutical applications. In the current study, DES are designed, prepared, and characterized experimentally and theoretically. They are then applied for the extraction of bioactive ingredients from marine by-products (codfish bones, mussels, and tuna vitreous humor), including hyaluronic acid (HA) and chondroitin sulfate (CS). These two polysaccharides have been evaluated in diverse therapeutic applications, including the dry eye disease (DED), a multifactorial disease resulting from tear film instability, inflammation, and ocular surface damage. Hence, they are one of the most commonly used natural compounds in DED artificial tears. Extensive research has already been published regarding the efficient extraction of natural HA and CS from marine and terrestrial by-products at a high yield and purity. In general, the vitreous humor is the main used source of HA, while the cartilage is the most common source for CS. The developed methods differ in the extraction conditions, enzymes and/or solvents used and the purification technique. In this work, DES were used for the extraction of HA and CS from marine by-products for their potential application in DED treatment. The extracts are then characterized chemically and in vitro to evaluate their bioactivity for their potential therapeutic application in ocular therapy.

Keywords: Deep eutectic solvents; natural compounds; characterization; hyaluronic acid; chondroitin sulfate; marine and terrestrial biomass; extraction techniques; dry eye disease; ocular therapy.

1. Development of sustainable processes

Nowadays, industries seek the development of green processes and technologies in all applications. The design of chemical products and processes that do not involve hazardous substances is highly increasing [1]. This led to significant advantages, including environmental benefits and innovative approaches [2]. Some of the main trends that focus on the implementation of green chemistry include the use of alternative solvents (such as ionic liquids and supercritical fluids), the valorization of renewable feedstock (biomass), the development of new synthesis pathways (photocatalytic reaction), among others [3]. Hence, these sustainable processes ensure not only an environmental protection, but also provide economic advantages.

1.1. Deep eutectic solvents as novel alternative solvents

Deep eutectic solvents (DES) describe the systems formed of eutectic mixtures of two or more components prepared by combining hydrogen bond acceptor (HBA) and hydrogen bond donor (HBD) molecules [4]. Abbott *et al.* first described a novel eutectic solvent composed of quaternary ammonium salts and urea having a lower melting point than the pure substances, which is mainly due to the complexation an interactions involved in the system [5]. HBA can be categorized into ionic compounds, such as tetraalkyl quaternary ammonium and phosphorous salts, and non-ionic compounds, such as monoterpene ketones. Common HBD include alcohols, glycols, carboxylic acids, and phenols [6]. Some of these compounds can act as both a HBD and HBA, such as organic acids and monoterpenoids, as shown in Figure 1. The research focus on the application of DES has remarkably increased in various fields for their use as alternatives to conventional solvents and ionic liquids [7]. This is mainly due to the importance of implementing low-cost and environmental-friendly processes, since the eutectic solvents have shown to have promising and advantageous characteristics [8, 9]. They have similar physicochemical properties in comparison to the ionic liquids, including high dissolution capacity, low vapor pressure and low melting point [10, 11]. Nonetheless, the DES have shown additional advantages since their compounds are remarkably cheaper, thermally stable, low- to non-toxic, more commonly biodegradable and require no further purification stages [11, 12]. Therefore, their potential for industrial production scale-up is bigger in comparison to ionic liquids.

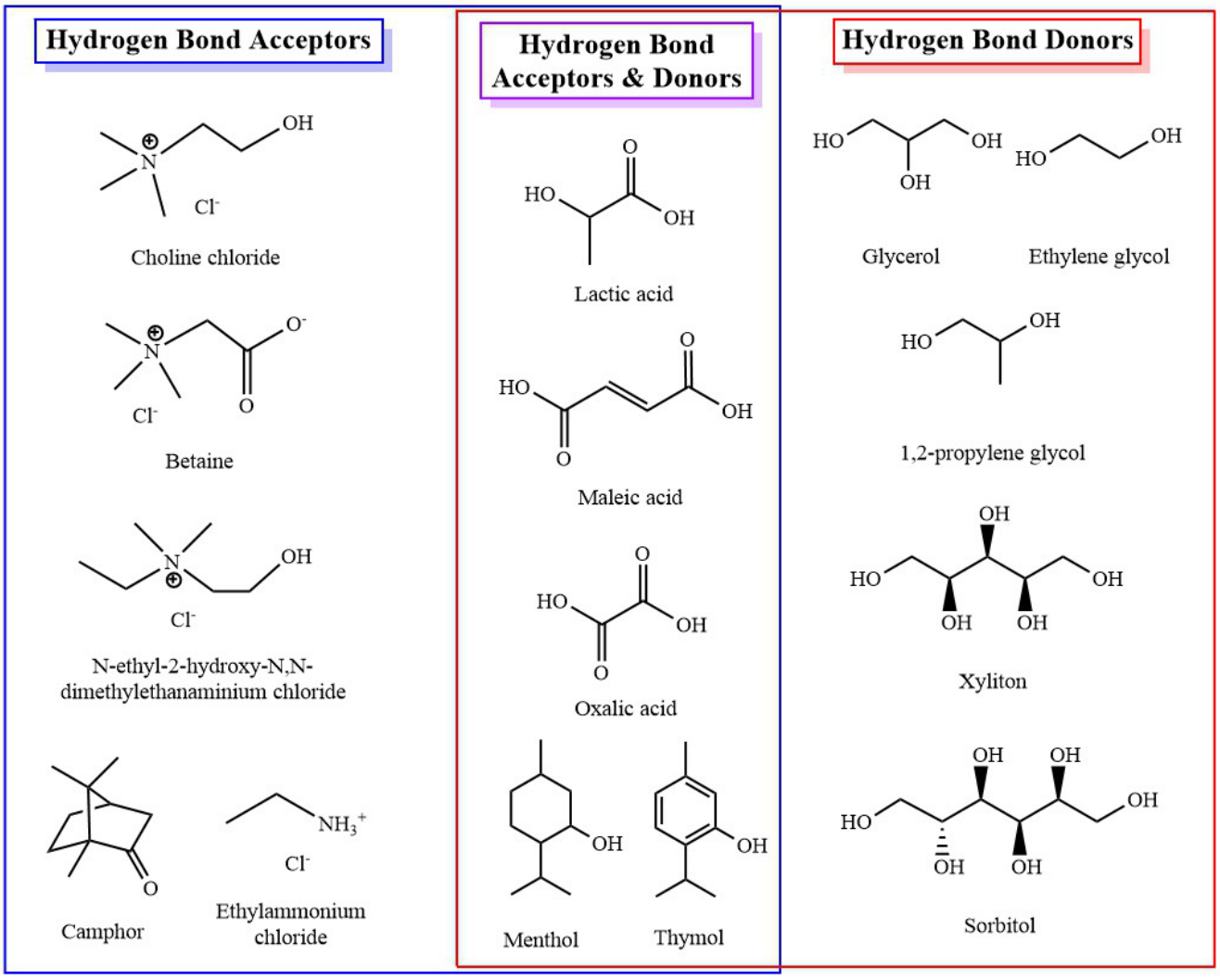

Figure 1: Some examples of deep eutectic solvents constituents of hydrogen bond donors and acceptors [6].

DES are characterized by the eutectic point, an invariant isobaric point of the mixture, comprising the molar ratio and a minimum melting temperature [13]. The eutectic point can be identified using the solid-liquid equilibrium phase diagram of the system, through the intersection of the melting curves of the compounds, as shown in Figure 2 [13, 14]. DES display different characteristics of a thermal transition, depending on the compounds in the system, the molecular

interactions and the cooling/heating rates. They generally undergo glass transition, which could be common even under low cooling rates, such as 5 °C/min [13, 15]. Nonetheless, the interactions and the molecular dynamics within the systems define the “deepness” of the DES in comparison to other regular eutectic mixtures [14, 16]. The thermodynamic analysis can clarify their interactions in the liquid phase and their behavior at specific molar ratio and temperature, to understand what differentiates them from non-deep eutectic mixtures. DES can be characterized using the solid-liquid equilibrium (SLE) phase diagram to study the ideal and real behavior of the systems [17]. The melting properties of the pure components involved should be obtained in order to evaluate the ideal solubility curve. The SLE phase diagrams can be computed using different tools, such as COSMO-RS and PC-SAFT and a comparison between the predictions assuming an ideal and real curve can be done to evaluate the systems [14]. Moreover, experimental studies of the SLE phase diagram could be achieved to confirm the real behavior, predicted by the simulation tools [18].

In general, the interactions of these systems are Van der Waals interactions and hydrogen bonding, which leads to a significant melting point drop (Figure 2) [13, 19, 20]. This melting point drop is due not only to charge delocalization between the components that enable the hydrogen bond formation, but also to the lattice energies of the interacting compounds and the entropy changes upon DES formation [5, 8, 21]. As it has been described by Abbott et al., the charge transfer occurring between the individual compounds is the main reason for the significant melting point depression of the eutectic system at a specific molar ratio [5]. Therefore, the stronger the hydrogen bond in the system, the deeper the reduction in the melting point.

DES can be further characterized by analyzing their physical properties, including the viscosity, density, refractive index, surface tension, miscibility and polarity [10, 18, 22, 23]. These properties are highly dependent on the structure of the components in the system and their molar ratio. Therefore, they have shown to be promising alternatives to molecular solvents due to their advantageous tunability that allows the optimization of the yield, solubility, selectivity, toxicity, bioactivity, stability, among others, depending on their application [24, 25].

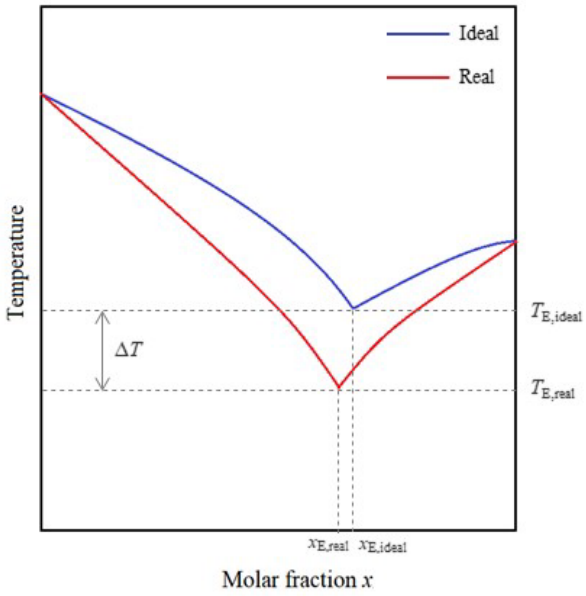

Figure 2: Schematic representation of binary phase solid-liquid equilibrium phase diagram of an ideal eutectic mixture (blue line) and real eutectic mixture (red line).

Previous studies and ongoing research have shown the various applications of versatile DES in many areas [13], as sustainability-oriented, pharmaceutical, biochemical and industrial applications, as summarized in Table 1. One of the most important roles of DES is their multifunctional role in solubilization, extraction and purification of high added-value products from biomass [8, 26]. For instance, DES were efficiently applied in the pre-treatment of lignocellulosic biomass. In these types of raw materials, cellulose represents the main component and the skeleton part of the biomass and is encapsulated by lignin and hemicellulose by strong intermolecular forces [27]. The pre-treatment of biomass using DES can efficiently and selectively ensure the destruction of lignocellulose structure and the removal of hemicellulose and lignin, to enhance the contact of cellulose with target chemical agents and enzymes [26, 27, 36–39, 28–35]. Furthermore, DES were also employed in the solubilization of cellulose for its efficient conversion into platform products, such as regenerated materials and cellulose derivatives of esters, ethers, and grafted copolymers [10, 27, 40–42]. Other studies are focused on the use of DES for the efficient extraction of different bioactive compounds from biomass, including proteins,

phenolic compounds as flavonoids, pesticides and polymers such as pectin, inulin, κ-carrageanan, xylan, agar and agarose, chitin and chitosan, among others [9, 10, 51–60, 43, 61–70, 44, 71, 45–50]. For instance, Vieira et al. compared the yield of extraction of phenolic compounds from *Juglans regia L*. using different DES and a conventional method using ethanol. According to their work, choline chloride:butyric acid resulted in a higher extraction yield in comparison to the conventional method and other tested chlorine chloride-based DES [70]. Similar results were obtained by Zhuang et al. for the extraction of flavonoids from *Platycladi Cacumen* using different combinations of DES. A greater yield was obtained using choline chloride:laevulinic acid in comparison to other tested DES and a conventional method [72]. Chitin was also extracted using DES from shrimp shells with a recovery yield higher than 85% using choline chloride:lactic acid [71]. Furthermore, to ensure a high yield of the extraction using DES, various techniques have been implemented, such as heating, stirring and the use of ultrasound and microwave assistance [52, 73–75]. For instance, choline chloride- and betaine hydrochloride-based DES were employed for the dissolution of α-chitin using conventional heating, microwave irradiation and ultrasonication. The results demonstrated that the use of microwave and ultrasonication decreased the time and temperature required for the process [76].

In addition, the use of DES in ecofriendly and purification processes is shown to be highly efficient due to their chemical characteristics [77]. One of the main separation applications include gas capture [78–87], desulfurization [22, 88–91], and metal separation processes [92–95]. As greenhouse gas pollution highly increased globally, the need for technologies of CO_2 and other gases capture has also increased [96]. DES prove to be efficient alternative solvents for capturing greenhouse gases, namely CO_2 and SO_2 [85–87]. This is mainly due to their low vapor pressure, high stability, convenient biodegradability, which replace the need for the conventional adsorption solvents, such as monoethanolamine and methyldiethanolamine, that exhibit a high vapor pressure, high toxicity and partial degradation [87]. In addition, previous studies have shown that the maximum capacity and absorption rate of the DES vary based on the type and molar ratio of HBA and HBD components, as they lead to varying viscosity, density and surface tension [97].

Furthermore, the use of DES in pharmaceutical and biomedical applications has shown increased attention [98]. They were proven to be efficient solvents for drug solubilization [99–101]. One study demonstrated that the solubility of the local anesthetic drug lidocaine was

enhanced using selected DES, due to the involved intermolecular hydrogen bonding interactions taking place between the drug and DES [100]. Additional research include the study of the protein folding, stability and structure within DES [102–108] and also their use in genomics to assess controlled DNA folding [104, 106, 107]. Moreover, DES increased the stability of DNA-conjugated activated esters, due to the strong binding of DES components with the chemical bases of DNA, such as guanine, adenine and thymine [109]. Furthermore, *in vitro* and *in vivo* studies demonstrated the potential therapeutic effects of DES [101, 110–115]. Hayyan et al. confirmed that their cytotoxicity can differ based on variations of the HBA and HBD combination and their corresponding molar ratio [110]. Further studies are important to reduce the toxicity effect of the tunable DES to ensure their implementation in therapeutic applications in drugs and formulation. Therefore, great attention has been paid to DES that are formed using natural metabolites (such as organic acids, alcohols, sugars, and terpenes) for their use in therapeutic applications [7, 8, 116–118].

The need for greener methodologies in chemical synthesis has increased the need for alternative solvents that can be adopted in various industrial processes and DES have been widely proposed as ecofriendly alternatives in such applications [117, 119]. Various studies focused on the use of DES in polymer synthesis, including polycondensation, electrochemical polymerization, free-radical polymerization and ring-opening polymerization reactions [120–124]. For instance, DES-assisted synthesis of poly(octanediol-co-citrate) polyesters was done by the incorporation of quaternary ammonium and phosphonium salts into the polymer network [125] and the itaconic acid free-radical copolymerization was done by in situ crosslinking of DES for the synthesis of hydrogels [126]. Furthermore, DES were also used in the synthesis of nanoparticles [127–131]. Studies have also shown the use of arabic gum with DES to synthesize coated gold nanoparticles and ultra-thin gold nano-sheets [132, 133]. Consequently, the high solubility of metal oxides, solid halogens and small organic molecules have substantially enlarged the efficient use of DES in the synthesis of highly functional nanomaterials, with improved chemical stability and optical properties [131].

DES were also employed in metallurgy and electrodeposition, to produce a range of useful tools through metal processing, dissolution and deposition [134–140]. Electrodeposition mainly involves the formation of a metal coating on an electrode surface by the reduction of metal cations

on the cathode using an electrical potential. This process allows the adjustment of surface functionalities, including its corrosion, hardness, resistance, brightness, magnetism, among others [141]. Hence, DES have shown a strong potential for their use in electrodeposition applications due to their electrical conductivity in comparison to nonaqueous solvents [142]. An example is the preparation of nickel metal coatings, through the dissolution of nickel chloride dehydrate salts in DES, such as choline chloride:urea and choline chloride:ethylene glycol [143]. It was demonstrated that the morphology of nickel coatings obtained using DES baths differ from aqueous plated nickel coatings, due to the differences in the process thermodynamics and kinetics [144]. Furthermore, the use of DES in redox flow batteries [142, 145–148] and solar cells [149–153] has been also increasingly studied. DES are promising solvents for use in renewable energy storage in redox flow batteries, due to their strong thermal and electrochemical stability, low viscosity at room temperature and high ionic conductivity [148]. A study showed that Li^+ cations highly interact with the C=O group of DES components, such as urea [148]. This interaction demonstrates that DES does not react with the electrode surface of a lithium battery and defines the cycling performance of lithium iron phosphate batteries [148, 154]. Moreover, DES were widely applied in photovoltaic dye-sensitized solar cells, due to their efficient, biodegradable and low-cost features. Nguyen et al. demonstrated that devices composed of choline chloride: ethylene glycol, increase the short circuit current value, while the ones composed of choline chloride:urea electrolytes improve the open circuit voltage values [155]. It was also proven that the molecular structures and interactions of DES play an important role in the enhancement of the open circuit voltage and short circuit current values [150, 151, 155]. Hence, these novel solvents widen the choices of electrolyte that can be used in the design of dye-sensitized solar cells, for future low-cost and ecofriendly large-scale industrial production.

Table 1: The different areas and applications of deep eutectic solvents.

Area	Applications	Reference
Biomass valorization	Pre-treatment and hydrolysis of biomass	[26, 27, 36–42, 28–35]
	Extraction of phenolic compounds, proteins, pesticides, polysaccharides, among other bioactive compounds	[9, 10, 51–60, 43, 61–70, 44, 71, 45–50]
Sustainability-oriented and purification processes	Gas capture	[78–87]
	Desulfurization	[22, 88–91]
	Metal separation	[92–95]
Pharmaceutical and biomedical processes	Drug solubility	[99–101]
	Controlled DNA folding	[104, 106, 107]
	Protein folding and stability	[102–108]
	In vitro and *in vivo* bioactivities	[101, 110–115]
Synthesis reactions	Polymerization	[120–126]
	Nanoparticles synthesis	[127–133]
Power systems	Electrodeposition of metals	[134–140]
	Redox flow batteries	[142, 145–148]
	Solar cells	[149–153]

Consequently, DES are promising alternative solvents displaying continued progress in different applications. Their physicochemical properties have been extensively studied and tailored by changing the nature and molar ratios of the components. These solvents were employed in broad areas of applications, and their status as green low-cost alternative biodegradable solvents promoted their strong involvement in sustainable and therapeutic fields. Further research is required to understand the structure, interactions and dynamics of these systems to optimize their behavior, according to the target application.

1.2. Valorization of residues

Biomass consists of organic matter obtained from living organisms. It is composed of proteins, lipids and polysaccharides, which enables them to be employed as feedstock for new products in green industries [156]. An example of biomass is the food wastes, which represent residues that are obtained from edible biomass. They can be generated from different stages of the food life cycle, starting from agriculture, manufacturing and processing to household consumption [157, 158]. The worldwide food waste is estimated to be approximately 1.6 billion tons globally [159]. A study calculated that 39% of food wastes takes place in the manufacturing industry, 42% from households, 14% from food services sector, and 5% from distribution [157]. Moreover, it was shown that 88% of the total marine fish production (estimated to be 179 million tons in 2018) is consumed by humans, and the rest is discarded [160]. Hence, both marine and terrestrial wastes obtained from food wastes were largely investigated for their valorization in significant industrial processes due to their low-cost abundance, safety and environmental advantages [161].

It has been shown that one of the main approaches for reducing environmental damage is through the application of a circular economy [162]. This topic is currently one of the most targeted research focuses among scientists. Its main goal is the restoration of resources, including residues, in applications of values for environmental and economical purposes. Hence, when natural materials reach the end of their life cycle, they can be reused in beneficial applications, including the isolation of bioactive molecules [162, 163]. Consequently, the high amount of wastes produced by food industries, can be valorized through the implementation of valorization processes.

Over the years, the use of both marine and terrestrial residues was evaluated in diverse industrial technologies, including cosmetics, as pharmaceutically active ingredients, valuable agro-chemicals and food and feed ingredients [3, 43, 156]. They have been widely employed as a source for the isolation of natural bioactive compounds that are used as natural products in pharmaceutical and cosmetic industries [164]. Hence, various techniques were developed for the efficient extraction of valuable ingredients from biomass sources [165]. Many compounds used in pharmaceutical applications were originally isolated from natural sources, including vitamin C, salicylic acid, pilocarpine, taxol, quinine and different glycosaminoglycans [166–168]. Among

glycosaminoglycans hyaluronic acid (HA) and chondroitin sulfate (CS) are widely used in pharmaceutical and medical applications.

1.3. Hyaluronic acid and Chondroitin sulfate from marine and terrestrial sources: extraction and purification methods

Glycosaminoglycans (GAGs) are linear polysaccharides formed of covalently linked disaccharide units. Their disaccharide repeating unit components are an amino sugar (hexoamines including D-glucosamine and D-galactosamine) and a uronic acid (D-glucuronic acid and L-iduronic acid). They are present in mammalian tissues as gel-like materials, mainly on the cell surfaces and the extracellular matrix. They include four main classes of compounds: HA and CS, fucosylated chondroitin sulfate (FCS), heparin/heparan sulfate, dermatan sulfate and keratan sulfate, as shown in Table 2 [169]. GAGs are generally bound covalently to a core protein to form a proteoglycan presenting different physiological functions. They differ on the chain length, linkage to the protein, extent of sulfation and proportion of the uronic acids, among others [170].

Considerable research has been done to investigate the therapeutic and potential applications of GAGs and they have been used in biomedical, cosmetic, veterinary, food and pharmaceutical applications[171–174]. Hence, HA and CS have demonstrated biocompatible, anti-inflammatory, biodegradable, non-immunogenic and non-toxic properties that have increased their application in different fields (Highley, Prestwich, & Burdick, 2016; Schiraldi et al., 2010). They have also been employed in tissue engineering as they have shown to promote cell growth and differentiation [175]. As they are important components of the extra-cellular matrix of cells, they have been incorporated in scaffold design to improve biocompatibility, tissue regeneration and cell adhesion [176].

Recently, great attention has been given to the use of biomass, including animal wastes and by-products, as a potential source for the isolation of both HA and CS. They have been extracted from various tissues such as rooster and wattle combs, umbilical cords, swine, porcine and bovine cartilage [177–179]. They can be obtained with varying structure and characteristics, such as the sugar composition and the extent of sulfation, depending on the method of extraction and the species of origin [176, 180, 181]. Terrestrial and marine biomass such as animal residues,

wastes and by-products have been extensively investigated in the past decades due to its long-term economic and environmental benefits as it is the most abundant renewable resource. [182, 183]. It has been estimated that over 50% of the tissues of fish (head, fin, skin…) are discarded as waste, which leads to problems in the waste management and highly affect the environment [184].

Table 2: Chemical structure of GAGs (Rn=H or SO3-) [185–189].

GAG	Chemical structure of the disaccharide or trisaccharide units	Systematic name(s)
Hyaluronic acid	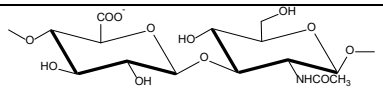	D-GlcA-*β*1-4-D-GalNAc-α1-4
Chondroitin sulfate	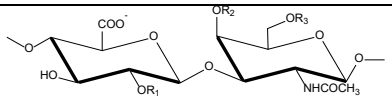	Its different systematic names are shown in Table 2
Fucosylated chondroitin sulfate	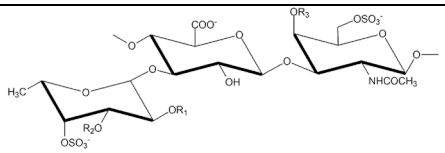	Composed of GlcA, GalNAc and the fucose branch α-L-fucose, with different sulfation positions R.
Dermatan sulfate	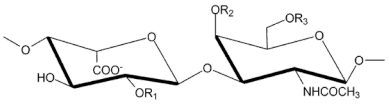	IdoA-GalNAc(4s) IdoA-(2s)-GalNAc(4s) IdoA-GalNAc(4s,6s)
Keratan sulfate	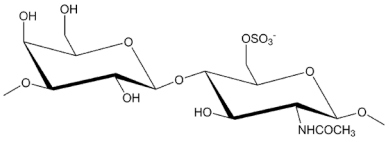	D-Gal-*β*1-4-D-GalNAc(6s)-*β*1-3
Heparin	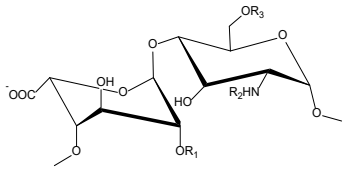	D-GlcA-*β*1-4-D-GlcNAc-α1-4 D-GlcA-*β*1-4-D-GlcNAc(6s)-α1-4 D-GlcA-*β*1-4-D-GlcN(s)-α1-4 D-GlcA-*β*1-4-D-GlcN(s,6s)-α1-4 L-IdoA-α1-4 -D-GlcN(s)-α1-4 L-IdoA(2s)-α1-4 -D-GlcN(s)-α1-4
Heparan sulfate		D-GlcA-α1-4-D-GlcN(s)-α1-4 D-GlcA-α1-4-D-GlcN(s,6s)-α1-4 L-IdoA(2s)-*β*1-4 -D-GlcN(s)-α1-4 L-IdoA(2s)-*β*1-4 -D-GlcN(s,6s)-α1-4

1.3.1. Hyaluronic acid

HA is a polysaccharide formed of disaccharide repeating units comprised of N-acetyl-D-glucosamine (GalNAc) and D-glucuronic acid (GlcA) [190]. It is the only GAG that is not sulfated and not bound to proteins [191]. It is usually comprised of 100 to 20,000 repeating units and has a molecular weight between 10^5 and 10^8 Da, in contrast the other GAGs which are smaller in size [192, 193]. In the human body HA, is abundant in the intracellular matrix of connective tissues (200-500 µg/g in the dermis), the umbilical cord (4100 µg/g) and in the fluid of space-filling tissues such as the synovial fluid (1400-3600 µg/mL) and the vitreous humor (140-500 µg/mL) [194].

HA plays an essential role in tissue hydration and permeation and in the transport of macromolecules between cells and invasive bacteria, due to its swelling property and its ability to absorb a large amount of water molecules [195]. The structure and characteristics of HA, as well its physicochemical and biological properties give it its valuable features such as biocompatibility, viscoelasticity, lubricity and immunostimulatory. It has been employed in joint injections, ocular surgeries, osteoarthritis treatment, plastic surgeries and skin treatments such as major burns and anti-aging products [196, 197]. In the biomedical field, HA has been applied in tissue culture scaffolds [198]. It has shown to be a potential compound in the development of tailored nanocomposites by combining it with chitosan, for wound and chronic ulcer dressing, due to the anti-bacterial properties [199–202]. Furthermore, it has been used in as dermal fillers and the treatment of osteoarthritis, vascular diseases and in cancer progression [194, 203].

HA has been extracted from various mammalian and marine animals. The concentration, purity and yield differ based on the source as well as the technique used. HA can also be produced by microbial and chemical synthesis. It is biosynthesized using bacteria *Streptococcus zooepidemicus* microbial fermentation [204]. Chemically assembled oligosaccharides include di- to decasaccharides [205–207]. Its chemical synthesis has shown to be challenging due to glycosylation and deprotection difficulties. In a method applied by Lu *et al.* [208] to obtain HA decasaccharides, a high glycosylation yield was ensured by using the trichloroacetyl group as a nitrogen protective group for the glucosamine groups, as well as by adding Lewis acid trimethylsilyl triflate to inhibit trichloromethyl oxazoline formation. The process was done under mild basic conditions to enable deprotection by the removal of base-labile protective functional

groups. The design and preparation of biomaterials from HA, such as hyaluronic nanofibers, using a green technology is a potential protecting and stabilizing agent with antitumor effects [209, 210].

1.3.2. Chondroitin sulfate

CS is a GAG formed by repeated disaccharide GalNAc and GlcA [190]. It has a shorter chain than HA as it comprises 20 to 100 repeating units [211]. It is mainly present in the extracellular matrix of tissues and plasma membranes [212]. This polymer has a significant heterogeneity in the length and the structure that differs based on the different sulfate positions, as shown in Table 3 [213, 214]. For example, in embryonic cartilage of the chicken, the sulfate group is mainly present on the carbon 4 of hexosamine, and with growth, the formation of chondroitin 6-sulfate increases [215]. It also displays variation in the molecular weight as it ranges between 10^4 to10^5 Da depending on the source and the tissue [216].

CS is a major GAG of cartilage and its presence in the extracellular matrix of connective tissue is highly essential as it provides elasticity in articular cartilage, inflammation, hemostasis, cell development regulation, cell adhesion, differentiation and proliferation [217]. It has been highly used in osteoarthritis treatment due to its anti-inflammatory action and its highly negative surface charge, capable of hydrating tissues by absorbing water [218]. It is also used in tissue engineering as CS hydrogels proved to accelerate wound healing [219]. Therefore, safe and pure CS is required for clinical applications.

CS can been extracted from various terrestrial and marine animals, such as cartilage, fish bones and fins [220–223]. Its concentration and composition differ based on the origin and it varies between terrestrial and marine sources. For instance, CS from tracheal cartilage is mainly constituted by CS-A, which structure is shown in Table 3, while CS-C and CS-D are the main constituents of the shark cartilage [224]. Since the sulfation group may occur on different positions, there exists a total of 16 different possible disaccharides [225]. The CS-B has a sulfated positions 4 of N-acetylgalactosamine and 2 of glucuronic acid. Dermatan sulfate having a similar structure with iduronic acid in the place of glucuronic acid (its epimer) at carbon position 5 [172]. Moreover, fucosylated CS is structurally distinct and is commonly extracted from the wall of sea cucumber [226]. It is different from the mammalian chondroitin sulfates as it contains side chains with O-sulfated fucosyl residues that are attached to the O-3 of the glucuronic acid unit [227, 228].

CS has been synthesized and extracted using various techniques, but its synthesis is challenging and complex due to the inclusion of specific sulfation patterns. Hence, chemical and bio-synthesis techniques can be employed to obtain CS with a specific structure, molecular weight and sulfation pattern. CS can also be produced by biological fermentation using fungi and bacteria, such as *Escherichia coli, Pasteurella multocida* and *Bacillus subtilis* [217, 229, 230].

The chemical synthesis of CS oligosaccharides is time consuming as it requires many steps. Various CS structures and chain length can be generated from a base disaccharide unit which is converted to either a donor or an acceptor. Glycosylation reaction takes place followed by a radical reduction of the N-trichloroacetyl group and oxidation of the para-methoxybenzylidene group. Then the assembly of CS with different sulfation patterns takes place under specific conditions and following a specific sequence of reactions [231].

Table 3: CS classes and sulfation pattern.

Chondroitin Sulfate name	Chemical structure of the repeating disaccharide	Systematic name	Disaccharide common name	Sulfated position
CS-O Di-OS	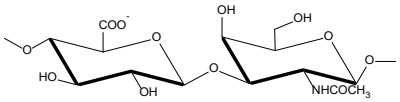	GlcA*β*1-3GalNAc	ΔDi-0s	Non-sulfated
CS-A CS-4 Di-A	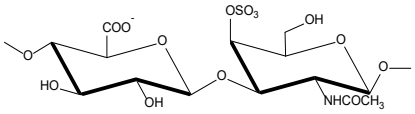	GlcA*β*1-3GalNAc(4s)	ΔDi-4s	Carbon 4 of the N-acetylgalactosamine
CS-B Di-B	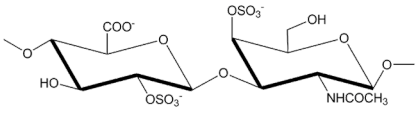	GlcA(2s)*β*1-3GalNAc(4s)	ΔDi-2,4s	Position 4 of N-acetylgalactosamine and 2 of glucuronic acid
CS-C CS-6 Di-C	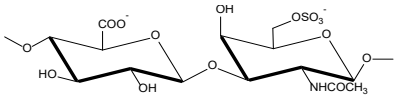	GlcA*β*1-3GalNAc(6s)	ΔDi-6s	Carbon 6 of the N-acetylgalactosamine
CS-D Di-diS$_D$	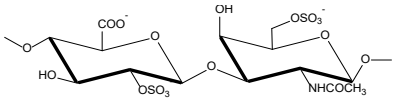	GlcA(2s)*β*1-3GalNAc(6s)	ΔDi-2,6s	Position 6 of N-acetylgalactosamine and 2 of glucuronic acid
CS-E Di-diS$_E$	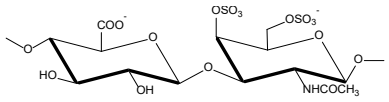	GlcA*β*1-3GalNAc(4s,6s)	ΔDi-4,6s	Carbons 4 and 6 of the N-acetylgalactosamine
Di-triS	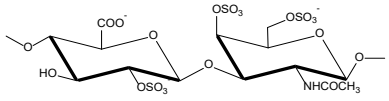	GlcA(2s)*β*1-3GalNAc(4s,6s)	ΔDi-2,4,6s	Positions 4 and 6 of N-acetylgalactosamine and 2 of glucuronic acid

1.3.3. Extraction of hyaluronic acid and chondroitin sulfate

1.3.3.1. Sources

1.3.3.1.1. Marine biomass

Nowadays, the isolation of valuable compounds from marine sources is highly investigated for many potential applications. Different approaches, including enzyme hydrolysis (EH), have been developed for the recovery of different compounds, such as proteins and polysaccharides, from marine plants and organisms [232].

HA and CS were extracted from marine sources to ensure the maximum exploitation of marine wastes as they have shown to be a potential source for the extraction of valuable compounds, as shown in Table 4 and Table 5. They can be extracted from different parts of the organisms, such as cartilage, head, eyes, fins and skin [180]. One of the main sources used for extraction is the cartilage, which is a tissue matrix composed mainly of collagen and a network of proteoglycans containing GAGs, such as CS and HA [233].

CS is found in the cartilage of shark, catshark, skate, octopus, squid, blue shark and the bones of monkfish, codfish, spiny dogfish, salmon, tuna and sturgeon [234–236]. Higashi et al. [237] showed that the whole fins of different shark species are a source of CS, including *Isurus oxyrinchus*, *Prionace glauca*, *Scyliorhinus torazame*, *Dasyatis akajei*, *Dalatias licha*, *Mitsukurina owatoni*. The structure and the sulfation pattern of CS differs between the marine sources based on the repeating glucuronic acid and N- acetylated galactosamine unit, which can be sulfated on carbon 4 and/or 6, and on the position 2 of glucuronic acid and 6 of galactosamine [238].

HA was extracted from various sources as shown in Table 5, including mollusc bivalve, liver of stingray, and the vitreous humor of swordfish and shark.

Table 4: Extraction techniques of CS from different marine sources.

Marine Source	Body part	Extraction method	Separation/purification method	Yield	Reference
Small-spotted catshark	Head, skeleton and fins	Alcalase (EH)	Ultrafiltration-diafiltration	4.8% in head 3.3% in fins 1.5% in skeleton	Blanco, Fraguas, Sotelo, Pérez-Martín, & Vázquez, 2015
Blackmouth Catfish	Cartilage	Alcalase (EH)	Ultrafiltration-diafiltration	3.5-3.7% of wet weight cartilage	J. Vázquez et al., 2018
Sea cucumbers		Papain (EH)	Dialysis followed by anion exchange chromatography	FCS isolated from 4 sea cucumbers (% by weight) *P. graeffei* 11.0% *H. vagabunda* 6.3% *S. tremulus* 7.0% *I. badionotus* 9.9%	Chen et al., 2011
Monkfish, codfish, spiny dogfish and tuna	Bones	Papain (EH)	Dialysis followed by anion exchange chromatography	(% w/w) in bones of: Monkfish 0.34% Codfish 0.011% Dogfish 0.28% Tuna 0.023%	Maccari et al., 2015

Tilipa		Papain (EH)	Dialysis		Vasconcelos Oliveira et al., 2017
Zebrafish	-	Papain (EH)	Anion exchange chromatography	80% CS of the total GAGs extracted CS-O 17.5% CS-A 59.4% CS-C 23.1%	Souza et al., 2007
Different fish species	Fins, head and skeleton	Alcalase (EH)	Dialysis followed by ultrafiltration-diafiltration	g*S. canicula* fins 3.9% *S. canicula* head 5.8% *S. canicula* skeleton 1.9% *P. glauca* head 12.1% *R. clavata* skeleton 13.7% (w/w dry cartilage)	Novoa-Carballal et al., 2017
Blue shark	Cartilage	Neutrase, alcalase, papain, bromelain and acid protease (EH)	Anion exchange chromatography	Highest yield using neutrase 88.4% of total CS recovered	Xie et al., 2014

		Alcalase (EH)	Ultrafiltration-diafiltration	12.08% (w/w dry cartilage)	J. A. Vázquez, Blanco, Fraguas, Pastrana, & Pérez-Martín, 2016
	Fins	Actinase (EH)	Anion exchange chromatography	Total GAG amount 44.9 mg/g dry weight	Higashi, Takeuchi, et al., 2015
Chinese sturgeon	Cartilage	Pepsin (EH)	Anion exchange chromatography	26.51%	Zhao et al., 2013
Shortfin mako shark		Alcalase (EH)	Filtration through a membrane of 3 kDa molecular-weight cut-off	57% (w/v)	S.-B. Kim et al., 2012
	Fins	Actinase (EH)	Anion exchange chromatography	Total GAG amount 7.71 mg/g dry weight	Higashi, Takeuchi, et al., 2015
Ray	Cartilage	Papain (EH)	Dialysis	7.49% ray cartilage	Garnjanagoonchorn et al., 2007
Shark	Fins	Papain (EH)	Dialysis	15.05%	Garnjanagoonchorn et al., 2007
Skate	Cartilage by-products	Alkaline process	Ultrafiltration-diafiltration	41 g/L of extracted CS	Miguel A. Murado, Fraguas, Montemayor, Vázquez, & González, 2010
	Cartilage	Alcalase (EH)	Protein removal by centrifugation	47.44% (w/w)	Song et al., 2017

			Ethanol purification	23.3%	Jeong, 2016
		Papain (EH)	Ultrafiltration-diafiltration	13 g/L of extracted CS	Lignot, Lahogue, & Bourseau, 2003
Spotted dogfish	Cartilage	Papain (EH)	Anion exchange chromatography	1.5% weight of CS on dry basis. CS-O 8.3% CS-A 41% CS-C 32% CS-D 8.3%	Gargiulo, Lanzetta, Parrilli, & De Castro, 2009
Salmon	Cartilage	Actinase (EH)	Ion Exchange chromatography	Total CS 24% (w/w) CS-O 11% CS-A 28.4% CS-C 52.8% CS-E 7.8%	Takai & Kono, 2003
	Bones	Papain (EH)	Dialysis followed by anion exchange chromatography	0.10%	Maccari et al., 2015
Different shark species	Fins	Actinase (EH)	Anion exchange chromatography	Total GAG amount (mg/g dry weight): Birdbreak dogfish 12.2 Cloudy catshark 11.7 Small tooth sand tiger 9.85 Red stingray 43.8	Higashi, Takeuchi, et al., 2015

				Frilled shark 16.6 Silver Chimaera 22.0 Spotless smooth-hound 39.8 Kitefin shark 8.46 Goblin shark 37.3	
Squid	Fins, arms, skin, head, eyes and mantle	Actinase (EH)	Anion exchange chromatography	CS (mg/g dry tissue) Fin 2.973 Arms 1.555 Skin 3.482 Head 2.475 Eyes 2.297 Mantle 0.021	Tamura et al., 2009
	Cornea	Papain (EH)	Ion exchange chromatography	CS 5% (w/w) CS-O 11% CS-A 49% CS-D 28% CS-C 20%	Karamanos, Manouras, Tsegenidis, & Antonopoulos, 1991
Carp	Scales	Actinase (EH)	Ion exchange chromatography	157.37 µg/mg	Sumi et al., 2002
Thornback skate		Alkaline process	Ultrafiltration-diafiltration	15% w/w CS extracted	Miguel A. Murado et al., 2010

Sea snake	Skins and meat	Trypsin and papain (EH)	Dialysis followed by ion exchange chromatography	10.1% sulfated groups	Bai et al., 2018
Octopus		Actinase E (EH)	Anion exchange chromatography	19.2%	Higashi, Okamoto, et al., 2015

Table 5: Extraction techniques of HA from different marine sources.

Marine Source	**Body parts**	**Extraction method**	**Separation/purification method**	**Concentration**	**Reference**
Swordfish	Eyeballs	Alkaline process	Ultrafiltration-diafiltration and protein electrodeposition	0.055 g/L of vitreous humor	M.A. Murado, Montemayor, Cabo, Vázquez, & González, 2012
Shark	Eyeballs	Alkaline process	Ultrafiltration-diafiltration and protein electrodeposition	0.3 g/L of vitreous humor	M.A. Murado et al., 2012
Mollusc bivalve		Papain (EH)	Anion exchange chromatography	0.81 mg HA/g dry weight of tissue	Volpi & Maccari, 2003
				4.2 mg HA/g dry weight of tissue	Kanchana, Arumugam, Giji, & Balasubramanian, 2013
Stingray	Liver	Papain (EH)	Anion exchange chromatography	6.1 mg HA/g dry weight of tissue	Sadhasivam, Muthuvel,

					Pachaiyappan, & Thangavel, 2013
Tuna	Eyeballs	Actinase (EH)	Dialysis		Mizuno et al., 1991
		Mycolysin (EH)	Dialysis	0.42 g/L vitreous humor	Amagai, Tashiro, & Ogawa, 2009

1.3.3.1.2. Terrestrial biomass

The generation of terrestrial by-products is highly increasing especially in slaughterhouses and food industries. It has been estimated that the average of animal wastes is 275 kg of bovine and 2.3 kg of pig per tons of total weight of killed animals, which accounts for 27.5% and 4% of the animal weight, respectively [262]. In addition, poultry farms generate millions of tons of wastes annually [263]. Therefore, terrestrial biomass and animal by-products have attracted great attention for the isolation of valuable compounds including HA and CS, as shown in Table 6 and Table 7.

HA was extracted from different animal sources such as rooster comb, the vitreous humor, umbilical cord and synovial fluid. Some of the highest concentrations of extracted HA were found in the rooster comb (39.8 g/kg), wattle tissue (17.9 g/kg) [264], and cattle, pig and sheep synovial fluid (up to 40 g/L) [265]. It has also been extracted from the vitreous humor of different terrestrial animals, such as pig, monkey and bovine [257, 266, 267]. The most investigated terrestrial source of HA is the rooster comb [264, 268–271].

CS was extracted mainly from the cartilage of different animals, such as buffalo, antler, sheep and crocodile [272–275]. Moreover, results have shown a significant extraction yield of CS from buffalo cartilages, including nasal, tracheal and joints, containing a high amount of CS (around 60 mg/g) which has been isolated by enzymatic treatment. Therefore, different amounts of CS, having specific structure and sulfation pattern, have been extracted based on the source and the extraction method.

Table 6: Extraction techniques of CS from different terrestrial sources.

Terrestrial Source	Body parts	Extraction method	Separation/purification method	Yield	Reference
Crocodile	Cartilage	Papain (EH)	Dialysis	14.84%	Garnjanagoonchorn et al., 2007
Buffalo	Tracheal, nasal and joint cartilage	Papain (EH)	Dialysis	Tracheal 62.05 ± 0.5 mg/g Nasal 60.47 ± 1.19 mg/g Joint 60.76 ± 0.38 mg/g	Sundaresan et al., 2018
Bovine	Nasal cartilage	Papain (EH)	Ion exchange chromatography	7.8%	T Nakano et al., 2000
Chicken	Claw cartilage	Papain (EH)	-	2.47%	Dewanti Widyaningsih et al., 2016
	Kneel		Dialysis	14.08%	Garnjanagoonchorn et al., 2007
	Kneel cartilage	Alcalase (EH)	-	40.09%	Shin, You, An, & Kang, 2006
Sheep	Cartilage	Use of organic solvents	Ethanol purification	Recovery rate of 7.6%	Zhujun et al., 2008
Antler	Cartilage	Papain (EH)	Anion exchange chromatography	95.1% of total uronic acid	C.-T. Kim et al., 2014
Pig laryngeal	Cartilage	Papain (EH)	Tricloroacetic acid deproteinization and ion exchange chromatography		Li & Xiong, 2010

Table 7: Extraction techniques of HA from different terrestrial sources.

Terrestrial Source	Body parts	Extraction method	Separation/purification method	Concentration	Reference
Wattle		Papain (EH)	Dialysis and cellulose acetate electrophoresis	17.9 µg/ mg	Takuo Nakano et al., 1994
Rooster	Comb	Pronase (EH)	Chloroform treatment and ion exchange chromatography	Yield > 90% with respect to hexuronic acid	Swann, 1968
		Use of sodium acetate	Dialysis	1 mg/g of frozen rooster comb	Kang et al., 2010
		Use of organic solvent and sodium acetate	Centrifugation		Kulkarni et al., 2018
		Use of organic solvent and sodium acetate	Chloroform treatment		Boas, 1949
		Papain (EH)	Dialysis and cellulose acetate electrophoresis	39.8 µg/ mg	Takuo Nakano et al., 1994
Chicken	Comb	Papain (EH)	Ethanol purification and centrifugation	15 g hexuronic acid/mg dry tissue	Rosa et al., 2012
Bovine	Eyes	Use of organic sodium salt	Dialysis	469.9 µg/ mL vitreous humor	Gherezghiher et al., 1987

	Synovial fluid	Use of quaternary ammonium salt	Dialysis	250 mg/L synovial fluid	Matsumura, De Salegui, Herp, & Pigman, 1963
Pig	Eyes		Ultrafiltration-diafiltration and protein electrodeposition	0.04 g/L vitreous humor	M.A. Murado et al., 2012
	Synovial fluid	Trypsin and pronase (EH)	Chloroform treatment and filtration		Cullis-Hill, 1989
Cattle	Synovial fluid	Trypsin and pronase (EH)	Chloroform treatment and filtration		Cullis-Hill, 1989
Sheep	Synovial fluid				Cullis-Hill, 1989
Owl monkey	Eyes	Use of organic solvents	Chloroform treatment		Balazs, 1977
		Use of organic sodium salt	Dialysis	291.8 µg/ mL vitreous humor	Gherezghiher et al., 1987
Eggshell membrane		Pepsin, trypsin and papain (EH)	-	Using each enzyme: Pepsin 38.79 mg HA/ g eggshell Papain 39.02 mg HA/ g eggshell Trypsin 44.82 mg HA/ g eggshell	Ürgeová & Vulganová, 2016

		Use of isopropanol and sodium acetate	Silica gel and activated carbon purification	5.3 mg HA/ g eggshell	Khanmohammadi, Khoshfetrat, Eskandarnezhad, Sani, & Ebrahimi, 2014

1.3.3.2. Methods of extraction

Various techniques were developed and optimized to extract HA and CS using detergents, enzymes and/or solvents to breakdown the structure and isolate the GAGs from other polysaccharide complexes present in the tissues [193]. In general, the methods are based on the chemical hydrolysis of the tissue to ensure the disruption of the proteoglycan core, followed by the elimination of proteins to recover the GAGs.

1.3.3.2.1. Digestion using enzymes

The most commonly used techniques for the isolation of GAGs involve the ED using papain, trypsin, pepsin and pronase, as shown in the Tables 3-6. These enzymes have been applied for the degradation of the tissue and the breakdown of the protein fractions to isolate the undamaged HA and CS molecules.

Papain is one of the most commonly used enzymes to isolate HA and CS. In general, the tissues were at first defatted using acetone, then treated with the enzyme. The mixture was then boiled to denature the enzyme and the GAGs were precipitated using ethanol saturated with sodium acetate [220]. This technique was applied with minor modifications for the extraction of CS from various fish (tuna, codfish, monkfish, dogfish and salmon) [234], tilapia [241], buffalo cartilages [272], skate cartilage [250], spotted dogfish cartilage [251], squid cornea [254], crocodile and ray cartilage, shark fin and chicken keel [233] and bovine nasal cartilage [273]. Moreover, CS was isolated from thornback skate (*Raja clavata*) by ED using papain combined with chemical hydrolysis using an alkaline hydroalcoholic solution [247]. In addition, papain was also employed to extract HA from mollusc bivalve, rooster and chicken combs and wattle [220, 264, 279]. In the isolation of HA from the terrestrial by-products, the tissues were defatted using

ethanol followed by delipidation with chloroform and methanol, prior to the hydrolysis using papain. This enzyme was also used with trypsin to isolate sulfated GAGs from sea snake (*Lapemis curtus*) [256] and in the hydrolysis of proteoglycans from hammerhead shark fins [283]. As shown in Table 3, sea cucumber has been used as a source of FCS, which was isolated based on a method developed by Vieira et al. It is based on the enzymatic hydrolysis using papain in the presence of EDTA and cysteine, followed by precipitation using cetylpyridinium chloride (CPC) [226, 228].

A method developed by Sumi et al. [255] was applied on carp scales based on enzyme hydrolysis using the protease actinase E followed by the elimination of polypeptides and the precipitation of the GAGs from the aqueous solution by the application of dialysis and a cation-exchange column for purification. This method is more time-consuming in comparison to the other enzymatic methods as it requires heat treatment, dialysis and ion exchange separation. Digestion using actinase E was also applied for the isolation of CS from salmon [252], diamond squid [253], octopus [235], and the fins of several shark species such as blue shark, shortfin mako shark, birdbreak dogfish, cloudy catshark, small tooth sand tiger, red stingray [237]. HA was also extracted using actinase E from the vitreous humor of tuna fish eyes, followed by membrane dialysis and CPC precipitation [260].

Another method applied by Blanco *et al.* is based on the enzymatic hydrolysis using the endoprotease alcalase in a thermostatted reactor followed by alkaline proteolysis and purification by ultrafiltration-difiltration. This technique was applied to isolate CS from small-spotted catshark (*Scyliorhinus canicula*) [239] and blackmouth catshark (*Galeus melastomus*) [240]. In a study done by Kim et al., alcalase and flavourzyme were used to purify CS from shortfin mako shark (*Isurus oxyrinchus*) cartilage [246].

In another study, the use of different enzymes was investigated: neutrase, alcalase, papain, bromelain and acid protease, for the extraction of CS from blue shark cartilage [236]. Moreover, alcalase has been employed in the hydrolysis of tissues for CS and HA extraction [248, 257]. CS was also isolated from chicken kneel cartilage by ultrasound treatment and alcalase hydrolysis, and from Tilapia by-products using a combination of ultrasound-microwave followed by protease hydrolysis [284, 285]. In contrast, CS was isolated from Chinese sturgeon (*Acipenser sinensis*) cartilage by de-fatting using petroleum ether, then the study of different extraction

conditions by hydrolysis using aqueous NaOH and acidic, neutral and alkaline proteases, papain, pancreatin, and pepsin [245]. In another study, the enzymatic hydrolysis with three enzymes (papain, pepsin and trypsin) was investigated on eggshell membranes to determine the optimum temperature and pH conditions for the extraction of HA. The results have shown that trypsin is more effective than papain and pepsin [281].

Other enzymes were employed for tissue digestion for HA and CS extraction, including proteases, pronase and trypsin. For instance, HA was extracted from the vitreous humor of fish eyes using a protease from *Streptomyces griseus* [261]. HA was isolated from human synovial fluid of a patient with rheumatoid arthritis, using pronase in a phosphate buffer followed by dialysis [286] and from rooster comb using pronase [268]. In addition, trypsin was used to isolate CS from cartilage proteoglycans [287] and HA from animals synovial fluid [265]. Pepsin has also been used for HA isolation [288].

1.3.3.2.2. Use of organic solvents and inorganic salts

The extraction of GAGs can be done using organic solvents and sodium salts, mainly sodium acetate, as shown in Tables 3-6. The application of organic solvents is based on the isolation of proteoglycans by the solubilization of the cell-matrix components (Chascall et al., 1994) and it has been mainly used in the isolation of HA.

HA was extracted from rooster combs using organic solvents and sodium acetate. At first, homogenization using acetone is done to de-fat the tissues, followed by the extraction using a sodium acetate solution for several times. Chloroform and chloroform-amyl alcohol were then used repeatedly to ensure protein removal. Dialysis was applied followed by the addition of the sodium acetate solution and precipitation using ethanol [269–271].

HA was also isolated from the vitreous humor of owl monkey eyes [267]. At first, the blood is removed from animal tissue to extract HA followed by the deproteinization of HA extract. Then, treatment with chloroform is done to form a two-phase mixture to perform liquid-liquid extraction for the purification of the system.

Furthermore, quaternary ammonium salts have shown the ability to form water-insoluble molecules due to presence of long alkyl chains polyanions [290]. CPC is the most commonly used in the extraction processes. In a study, HA was isolated from bovine synovial fluid using CPC by

the formation of HA-CPC complex (Matsumura, De Salegui, Herp, & Pigman, 1963). The precipitate was then washed with water, NaCl solution and ethanol followed by dialysis. Additionally, HA was extracted from the vitreous humor of fish eyes using CPC to obtain a HA-CPC complex which was dissociated by suspension in NaCl solution, followed by a treatment using mycolysin and Tris-HCl buffer. This technique was showed to be effective when working with the vitreous humor to obtain high yield and high molecular weight HA [261].

A method was based on the extraction of HA from eggshells by a treatment using acetic acid followed by the use of a water-jacketed contactor placed on a magnetic stirrer that maximizes HA extraction by contacting the eggshells with aliquots of acetic acid solution supplied using a peristaltic pump. Precipitation of HA was done using isopropanol followed by centrifugation and suspension in a sodium acetate solution [282].

1.3.3.3. Purification methods

Various purification methods have been employed at the final stage of extraction to ensure a higher purity of HA and CS. Ultrafiltration-diafiltration is highly applied method for purification and it is a size-based separation to remove the impurities and concentrate the HA and CS in solution [250, 291, 292]. For instance, purification of HA isolated from the vitreous humor of swordfish and shark [257] was done using a plate polysulfone membranes with a molecular weight cut-off at 100, 300 and 675 kDa. Protein electrodeposition was performed at a current between two platinum electrodes of 10 to 40 mA and HA is obtained with a purity higher than 99.5%. In addition, this technique was applied in the purification of CS extracted from skate cartilage [250] and HA obtained from fermentation [292]. Moreover, it was also employed for a selective purification and protein permeation in the extraction process of CS from catshark (*Scyliorhinus canicula*) head, skeleton and fins and from blue shark (*Prionace glauca*) head wastes using polyethersulfone membrane of 30 kDa cut-off for the catshark and 30 and 100 kDa cut-off for the blue shark [239, 244].

Additional purification techniques include dialysis and ion exchange. Dialysis has also been used for HA and CS purification from impurities in solution. For instance, it has been used as a final step for the purification of HA extracted from fish eyes [261], CS from pig laryngeal cartilage [278] and buffalo cartilages [272]. On the other hand, anion exchange chromatography has been employed for protein separation and purification [226, 234, 242]. Furthermore, ion

exchange resins such as silica gel, alumina and activated carbon, are also employed for the purification of CS and HA [249, 292]. Silica gel has been employed to improve the purity of CS extraction [293]. It has been shown that alumina is an effective adsorbent of endotoxins as it removed 99% of endotoxins and 88% of proteins. Furthermore, activated carbon and silica gel were used to remove impurities in the HA extraction from eggshells [282]. In a study, different activated carbons were tested (Darco KB-B, Norit CN1, Norit C Extra USP, Norit A Supra EUR…) for the removal of high molecular weight proteins from HA obtained by fermentation, for its further application to biomaterials. Results show that Norit CN1 has the highest removal percentage of proteins with 97% and a 90% removal of endotoxins [292].

1.3.3.4. Methodology and matrices comparison

Various methods were applied in the extraction of HA and CS using enzymes, solvents or other treatment compounds for an efficient isolation at a high purity. Nevertheless, these methods are expensive for large scale extractions, as they could require lyophilization of the raw materials and the final product, enzyme proteolysis, ultrafiltration-diafiltration, among other techniques [168]. In addition, the purity of the final product is challenging at an industrial scale and depends on the technique applied. In fact, some animal sources contain a relatively low amounts of the GAGs, mainly HA, and may not be feasible for industrial applications [217, 239]. For instance, fermentation processes of HA using mutants of C streptococci and Lancerfield group A are more commonly applied in industries using to replace HA from natural sources [196]. They have been applied in batch, fed-batch and continuous operations [294]. The culture process has been optimized to obtain the most suitable medium, pH, aeration and agitation conditions, bioreactor type, lysozyme or hyaluronidase added [295–297]. For CS, industrial scale biotechnological production processes have not been applied, which could be mainly due to the low yields of the pathogenic microorganisms cultivation [217]. The production of CS for commercial use is obtained from terrestrial and marine by-products of bovine, chicken, porcine, skate, shark, cartilaginous and bony fish, or a mix of these sources to obtain a CS with mixed properties [298]. However, the final CS product may present contaminants and biological effects, and may lack a controlled structure and reproducibility and a consistent grade of purity [299].

Hence, the extraction methods present different advantages and disadvantages when taking into account the cost, yield and environmental impact. In general, the economically feasible

methods yield to a lower purity in contrast to the methods with a higher purity that require more steps and a larger amount of reagents and thus are more time-consuming. For instance, the use of enzymes is expensive and a significant amount is require to hydrolyze the tissues. It is also challenging as it requires a specific buffer and treatment conditions for 24h for the hydrolysis process. Moreover, a heat treatment is needed to de-nature the enzyme. For instance, an amount of 60 mg of papain is required for each 1g of de-fatted tissue to treat [234]. A CS yield of 0.011-0.34% (w/w of different fish bones), 14.84% (dry weight of crocodile cartilage) and 15.05% (dry weight of shark fins) were obtained when applying this enzyme in the extraction process [233, 234]. In contrast, organic solvents such as chloroform and methanol were used prior to the application of papain for the extraction of HA from chicken combs for the separation of proteins and lipids [279]. Chloroform was also used without the use of enzyme, as a solvent in the extraction of HA from rooster combs [270, 271]. This method was employed as an alternative to the use of enzymes and hence eliminates the heating step required for enzyme denaturation. Even though chloroform is a cheaper alternative for the enzymes, it is a toxic compound and thus has a negative environmental impact. On the other hand, the enzyme alcalase was less commonly applied and it showed a significant CS yield of 57% (w/v) from shortfin mako shark [246], 23.3% and 47.44% (w/w) from skate cartilage [248, 249], 40.09% from chicken kneel cartilage [277] and 1.9 to 12.1% (w/w dry cartilage) from different fish by-products [243]. Furthermore, the application of the enzymatic digestion using actinase E showed a yield of CS of 24% (w/w) from salmon cartilage [252], 41.2% (w/w) from shortfin mako shark [237] and 19.2% from octopus [235]. The application of ultrafiltration-diafiltration was done to ensure a high purity of HA and CS. This method is done as a final step or to eliminate the use of solvents (such as ethanol, chloroform, sodium acetate solution…) or ion exchange separation in the final stage. However, it requires the use of a membrane filter with specific pore size, a pump and a pressure sensor. A yield of 12.08% of CS (w/w dry blue shark cartilage) [244] was obtained, 0.055, 0.3 and 0.04 g/L of HA from the vitreous humor of swordfish, shark and pig, respectively [257].

The amount of HA extracted from vitreous humor of marine animals (55 mg/L in swordfish, 300 mg/L in shark [257] and 420 mg/L in tuna [261] is shown to be higher than that of terrestrial sources (250 mg/L in bovine [280] synovial fluid , 0.47 mg/Land 0.29 mg/L in vitreous humor in bovine and monkey [266] and 40 mg/L in pig [257]).

On the other hand, CS was extensively extracted from the cartilage of marine and terrestrial animals. For instance, the yield is shown to be 14.84% (dry weight) from crocodile cartilage [233], 2.4% from chicken claw cartilage [276] in contrast to 26.51% from Chinese sturgeon cartilage [245] and 24% from salmon cartilage [252]. Therefore, the extraction methods differ in the cost, environmental impact, yield of HA/CS and the level of purity obtained. The yields obtained not only depend on the enzyme used, but also on the following purification steps and the source of marine and terrestrial by-products.

1.3.3.5. Conclusion

Nowadays, the amount of generated terrestrial and marine wastes has significantly increased. The use of the by-products in the extraction of valuable biopolymers has received a great attention in the last decade for various applications. For instance, HA and CS are essential bioactive compounds which have been used in several biomedical and pharmaceutical applications and extensive research was done to ensure their efficient isolation at a high yield and purity. Different marine and terrestrial animal contain a significant amount of GAGs which require specific techniques to separate them and isolate HA and CS. In general, the cartilage is the most commonly used source for CS, while the vitreous humor is mainly used as a source of HA. The methods were based on the general steps of tissue hydrolysis, impurities (such as proteins) removal and purification of HA and CS. They differ in the amount of HA and CS recovered by using the specific enzymes and/or solvents, and also the source of biomass used. The most commonly applied method is the enzymatic digestion using papain, which has been shown to be efficient for the isolation of GAGs. This leads to specific yield, molecular weight and sulfation pattern of the isolated HA and CS. The optimization of the current extraction methods, as well as the development of novel techniques, is highly essential to ensure the efficient isolation of the target bioactive polymers at high purity using a low-cost, green and less time-consuming technique.

These extracted bioactive compounds can be potentially studied for their use in therapeutical applications, such as the dry eye disease (DED).

2. Dry eye disease

Dry eye disease (DED) is a multifactorial disease resulting from tear film instability, inflammation and ocular surface damage, leading to symptoms of visual impairment, pain and discomfort [300, 301]. Its core etiology involves a vicious cycle: the tear film instability and hyperosmolarity activate pro-inflammatory interleukins and chemokines production, leading to cornea and conjunctiva damage and the loss of the tear film homeostasis [301]. The tear film plays an important role in the lubrication, nutrition, wound healing and immunological defense of the eye [302]. Its instability is at the basis of the disease and the starting point of inflammation. In addition, the loss of its homeostasis promotes ocular surface inflammation and damage, hyperosmolarity and neurosensory abnormalities [302, 303]. Furthermore, the alteration of the tear film can be attributed to the chronic blockage of the Meibomian glands, shown in Figure 3, that induces inflammation, eye irritation and ocular surface disease [304–306]. This DED pathological process causes alterations in the ocular surface morphology and it also stimulates ocular oxidative stress [307]. This leads to reactive oxygen species production and antioxidant enzymes decrement, thus creating a physiological imbalance between antioxidative enzymes and the reactive oxygen species [308]. Moreover, the chronic inflammation induces a goblet cell loss and the apoptotic process at the conjunctival and corneal level [309]. In patients suffering from Sjögren syndrome, a systemic autoimmune disease which targets the lacrimal and salivary glands, the tear production is significantly reduced, which promotes chronic dry eye [310]. In this disease, the glandular inflammation and the malfunction of acinar epithelial cells induces the apoptosis of acinar cell mass [310, 311]. Consequently, the alteration of the ocular surface by apoptosis, along with the hyperosmolar environment, stimulate the corneal nerve fibers and the lacrimal gland, leading to blinking, burning sensation and other DED symptoms [309, 312].

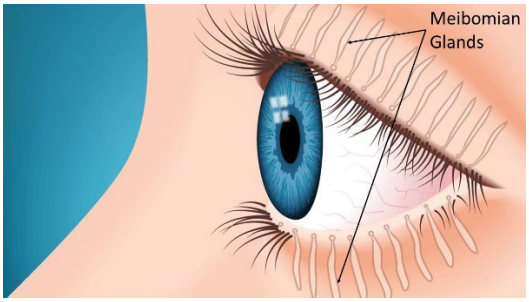

Figure 3: Meibomian glands of the eyelids in which a chronic blockage leads to alteration of the tear film and inflammation.

Different risk factors are associated to this disease including aging, climate change, dry environment, use of contact lens, hormonal changes (particularly for menopausal and postmenopausal women), use of electronic screens, among others [313–315]. It has been shown to be gender dependent as its prevalence is 70% higher in women than men and becoming more significant with age. This is mainly due to sex-specific autosomal factors and sex steroids [315–317]. In addition, the DED is more common in office environments that include intense computer use and air conditioning [318]. These factors lead to aqueous-deficient dry eye with reduced secretion of tear fluid with increased tear fluid evaporation. These DED pathogenic mechanisms do not have to be mutually exclusive; nevertheless, many patients display a combination of both [315].

The multifactorial etiology of DED made its diagnosis more challenging, which leads to an increased need for efficient diagnostic tools. The tools could be classified according to the parameter to be measured, such as the tear film stability, osmolarity, composition and volume, among other parameters [319]. More accurate diagnosis is reached when the results obtained combine more than one parameter tested. Nevertheless, the diagnosis that relies only on the symptoms of the patient is shown to be inadequate. This is mainly due to the fact that the symptoms of the DED are similar to ones shown in other ocular diseases, such as allergic or cicatricial conjunctivitis, and filamentary or neurotrophic keratitis [320], in addition to the discordance between the signs and the symptoms of the DED as only 57% of symptomatic patients present objective signs [321, 322]. Hence, several diagnostic tools are available and they

differ based on their sensitivity and specificity depending on the patient's disease severity, specific characteristics, among different other factors [301, 322]. At first, a questionnaire can be implemented to do a screening and grading of the patient's symptoms [322]. Based on the results, if the patient displays positive symptoms score, the less invasive tests can be done to assess the homeostatic markers, which include tear osmolarity, ocular surface staining, and tear breakup time [319, 322]. Following the results of any of the tests, if homeostatic markers are found in either eye, further tests that are more invasive can be done. These include tear volume assessment and meibography, which confirm the severity of the disease and its sub-classification for its proper treatment [322].

Current therapies for the DED are limited due to variation in the dry-eye diagnostic parameters. In general, most therapies aim to decrease inflammation and enhance different components in the tear film [312]. Table 8 displays some of the treatments that can be used for the management of the DED according to the Tear Film & Ocular Surface Society Dry Eye Workshop (TFOS DEWS) II Management and Therapy Report [323]. Currently, the most common therapy is the use of artificial and biological tear substitutes that aim for osmo-protection, lubrication and stabilization of the ocular surface [312, 324]. They have been applied for tear production and stimulation in order to alleviate ocular surface pain and discomfort. Artificial tears can be comprised of HA, CS, polyvinyl alcohol, polyethylene glycol, polyacrylic acid, polyvinylpyrrolidone, dextran, carboxymethyl cellulose, hydroxypropyl methylcellulose, and hydroxypropyl-guar [323, 325–327]. These ingredients are shown to enhance the tear viscosity and increase the tear film thickness. For instance, HA and CS were proven to play a vital role in tissue hydration, permeation viscoelasticity, lubricity and immune-stimulation [195]. Furthermore, biological tears can be formed from autologous, allogenic and umbilical cord serum, mucolytics and TRPV1 receptor antagonists [322, 325, 326, 328–330]. One of the techniques used for tear conservation is punctal occlusion, in which the tear drainage system is blocked to preserve the natural tears on the ocular surface [331]. Moisture chamber spectacles and humidifying devices that are placed locally can be used to slow the tear evaporation and enhance humidity or local air quality, by minimizing the presence of airflow over the ocular surface [332, 333]. Topical secretagogues, including aqueous and mucin secretagogues, have shown to stimulate secretion in the ocular surface, leading to improved film stability [334, 335]. Oral secretagogues, such as the cholinergic agonists cevimeline and pilocarpine, are used mainly for tear stimulation for

patients suffering from the Sjögren syndrome associated to the DED [336, 337]. Androgens and insulin-like growth factor 1 have shown to simulate lipid secretion *in vitro* of meibomian gland cells [338]. Another technique to induce tear secretion is through nasolacrimal reflex stimulation. Through this therapeutic strategy, the nervous system is stimulated through mechanical or chemical methodology in order to upregulate the tear production [339].

Different therapies are attributed to the meibomian gland dysfunction, such as lubricants, warm compresses, thermal pulsation, intense pulsed light therapy, intraductal probing and debridement scaling [323, 340–345]. The treatments aim to decrease the obstruction from the terminal duct and ductal system of the meibomian glands in the management of meibomian gland dysfunction, and they have shown to successfully improve the signs of the patients [306, 314, 323].

Other therapies focus on the use of anti-inflammatory agents for the management of the DED. Glucocorticoids, including corticosteroids have shown to be efficient in the management of inflammatory DED [346]. For instance, the use of topical methylprednisolone leads to the suppression of inflammatory cytokine and the activation of mitogen-activated kinase [347]. In addition, sex steroids, such as androgens, estrogens and progestins have shown improvements in the ocular surface tissue regulation [348]. However, these glucocorticoids present side effects, including cataracts, ocular hypertension, opportunistic infections, among others [349]. Non-glucocorticoid immunomodulators have also been used for their anti-inflammatory effect in the management of the DED. These include cyclosporine A, pranoprofen, ketorolac, diclofenac, indomethacin, lubricin, among others [350–354]. Furthermore, the lymphocyte function-associated antigen-1 (LFA-1) integrin with its cognate ligand intercellular adhesion molecule-1 (ICAM-1) can interact with ocular cells to decrease inflammation. Lifitegrast is an LFA-1 antagonist which blocks the ICAM-1 binding to LFA-1, and inhibits T cell mediated inflammation in DED. Hence, it is shown to be efficient in the improvement of DED signs and symptoms [355–358].

In many cases, the patient suffering from DED undergoes treatment by surgical approaches. For instance, tarsorrhaphy (partial suture of the eyelids) can help decrease tear evaporation and ocular surface desiccation [359]. Additional DED therapies can be also linked to dietary modification as nutritional supplementation, such as omega-3 and -6 fatty acids, and

vitamin D, have proven to improve DED symptoms [360, 361]. Moreover, the modification of the unfavorable ambient conditions (low humidity, high/low air temperature, high air movement, smoke), as well as the limitation of digital device use and contact lens wear, have proven to enhance tear stability and decrease its evaporation. Hence, the modification of these external factors must be implemented in parallel to any prescribed treatment for DED patients in order to ensure a suitable, efficient and helpful therapy.

Table 8: Current proposed DED treatments according to different therapeutic aims.

Aim	Treatment	Reference
Tear replacement	Artificial and biological tear substitutes	[323–330]
Tear conservation	Punctal occlusion	[331]
	Moisture chamber spectacles and humidifiers	[332, 333]
Tear stimulation	Topical and oral secretagogues	[334, 335]
	Androgens and insulin-like growth factor 1	[336–338]
	Nasolacrimal reflex stimulation	[339]
Meibomian gland dysfunction therapy	Ocular lubricants	[327, 345, 362]
	Warm compresses	[344]
	Thermal pulsation	[343]
	Intense pulsed light	[340, 363]
	Intraductal probing	[342]
	Debridement scaling	[341]
Anti-inflammatory therapy	Glucocorticoids and non-glucocorticoid immunomodulators	[346, 348, 350–354, 364]
	Lifitegrast	[355–358]

Recent studies have shown that the use of natural compounds improves the symptoms of the DED [315, 365]. Many compounds used in pharmaceutical applications were originally isolated from natural sources, such as plants and biomass [166]. Medicinal plant extracts have been used in the DED management as they have shown to decrease inflammation and

osmolarity, enhance tear film stability and tear production [366]. These include flavonoid compounds extracted from *Buddleja officinalis*, apricot kernel extract from *Prunus armeniaca*, goji berry extract from *Lycium barbarum*, standardized ethanol extract from *Rhynchosia volubili*, among others [367–370]. Another study shown that the topical application of mixed medicinal plant extracts, such as *Schizonepeta tenuifolia*, *Angelica dahurica*, and *Rehmannia glutinosa Liboschitz*, contributed to alleviate DED due to their antioxidant effect [371, 372]. Several eye drops containing natural compounds have been employed for the improvement of DED symptoms. For instance, one study showed that eye drops made from natural extracts enhanced antioxidant proteins expression level [373]. Another work showed that eye drops composed of natural extracts containing musk, bee venom, and deer antlers restored the tear mucin layer and the damaged ocular surface and also increased tear film volume in DED animal models [374]. Moreover, the use of an eye drop containing *Plantago ovata* mucilage was shown to improve the tear film break-up time in DED patients [375]. Therefore, the application of natural compounds in the management of DED is shown to be significantly increasing during the last years, due to their provenly potent therapeutic effects.

Glycosaminoglycans are one of the most commonly used natural compounds in DED artificial tears, including HA and CS. They are hydrophilic molecules with significant functions in the body as they play an important role in the hydration and the elastoviscosity of tissues [174, 175]. They have shown non-immunogenic and biocompatible effects that increased its application in the pharmaceutical and medical fields. Previous studies have proven that HA eye drops have a better performance than non-HA eye drops, including artificial tears and normal saline [326, 376]. Moreover, the topical application of HA and CS display significant improvement in the corneal epithelial barrier in patients suffering from the DED [377, 378]. Hence, these molecules were increasingly studied in the last years and were combined with different compounds for DED ophthalmic formulations. The presence of lipids in eye drops can help to restore the disturbance in tear composition. The tear lipid layer is composed of phospholipids, cholesterol, triglycerides and free fatty acids produced by the meibomian glands [379, 380]. This layer is essential for tear film stability as it forms a hydrophobic boundary between the aqueous and gaseous tear film and prevents rapid evaporation of the tears. Hence, to obtain comparable physiological composition of the tear film, the presence of lipids along with the aqueous and mucin layers is essential [381]. A study has proven that both HA and CS-containing eye drops significantly improved tear

production in DED patients [326, 327, 378]. Another study also confirmed the efficacy of mineral oil and HA combination in eye drops for DED management [382]. Furthermore, protein variations in tears are also observed in DED patients, including patients with Sjorgen's syndrome [383, 384]. Tears of dry eye patients have significantly lower levels of lactoferrin, lipocalin-1 and lipophilin A and C, and higher levels of serum albumin [385]. A study show that the use of selenium-binding lactoferrin is efficient in the treatment of the dry eye, leading to reduction of oxidative stress and prevention of corneal damage [386]. Further bioactive compounds were used in eye drop formulations to enhance DED symptoms of patients, including cationic emulsion of polyvinyl alcohol and povidone, povidone–iodine nanoemulsion, carboxymethyl cellulose, hydroxypropyl-guar, and among others [387–389].

Different eye drops having versatile bioactive ingredients have been studied for an efficient treatment of the DED. Further studies must be done to ensure an efficient topical application of eye drops at an optimal composition of glycosaminoglycans, proteins, lipids, among other bioactive ingredients, depending on the symptoms and the condition of the patient.

3. Objective of the work

The main objective of this work was to implement an alternative procedure to extract bioactive ingredients as HA and CS from marine by-products (codfish bones, mussels, tuna vitreous humor) for their potential application in DED treatment. These extracts must be characterized chemically and in vitro to evaluate their bioactivity. The biocompatibility studies can prove their potential therapeutic application as natural ingredients in ocular therapy.

The chapters of this thesis are therefore arranged according to this sequence of steps in order to complete the objectives of the research work.

Chapter II:
Physicochemical characterization and simulation of the solid-liquid equilibrium phase diagram of eutectic solvent systems

This chapter was published by MDPI as:

Abdallah, M. M., Müller, S., González de Castilla, A., Gurikov, P., Matias, A. A., Bronze, M. D. R., & Fernández, N. (2021). Physicochemical Characterization and Simulation of the Solid–Liquid Equilibrium Phase Diagram of Terpene-Based Eutectic Solvent Systems. Molecules, 26(6), 1801. DOI:10.3390/molecules26061801

Abstract

The characterization of eutectic solvent systems is performed to describe their solid-liquid phase transitions. Physical characterization is done experimentally for all solvent systems to evaluate the density, viscosity, surface tension and refractive index. For the terpene-based solvent systems, the values are compared to computed correlations for deep eutectic solvents (DES) to show that the average relative deviation percentage is 19.1, 12.0 and 1.4% for the density, surface tension and refractive index, respectively. The chemical interactions are analyzed using FTIR and NMR to study the intermolecular hydrogen bonding in the systems. The thermodynamic parameters, including the degradation, glass transition and crystallization temperatures, are measured using DSC and TGA. Based on these data, the solid-liquid equilibrium phase diagrams are calculated for the ideal case and predictions are made using the semi-predictive UNIFAC and the predictive COSMO-RS models, the latter with two different parametrization levels. For each system, the ideal, experimental and predicted eutectic points are obtained. The deviation from ideality is studied and it is shown that the systems could be considered DES.

Keywords: Deep eutectic solvents; natural compounds; physical characterization; simulation; equilibrium phase diagram; chemical interactions

1. Introduction

DES have been widely investigated as new alternatives and analogues to ionic liquids. In many cases, they are more eco-friendly and cheaper alternatives to ionic liquids and conventional solvents. They are prepared by combining a hydrogen bond donor and hydrogen bond acceptor near the eutectic point (eutectic temperature and molar ratio) at a temperature above the melting temperature of the homogenous mixture formed. The resulting system should have a considerably lower melting point compared to its ideal eutectic and the melting point of its individual constituents [5, 10, 96] as they are characterized by the presence of hydrogen bonding and strong non-ideal attractive interactions [117, 390].

The use of non-toxic compounds has been highly investigated for the preparation of DES. Terpenes are produced by living organisms, including bacteria, fungi, algae and plants. They comprehend a chemical space of approximately 30,000 secondary metabolites that are divided into isoprene units and differ in the role and structure. The monoterpenes (C_{10}, 2 isoprene units) and sesquiterpenes (C_{15}, 3 isoprene units) are the more volatile groups and are formed in vegetation [391, 392]. Monoterpenes include menthol, thymol, linalool, borneol, eucalyptol, camphor, 1,8-cineole, α-pinene, limonene and citral. They are found in essential oils of different plants, such as mentha, thyme, lemon, juniper, lavender, eucalyptus, marjoram, rosemary, pine, salvi and geranium among others [393]. This class of compounds have been widely used in pharmaceutical applications for the development of drugs due to their bioactive properties. For instance, menthol and borneol have been employed in ocular applications, including the dry eye disease [344, 394–396]. Thymol has been employed as skin permeation enhancer of the drug meloxicam [397]. Furthermore, ibuprofen has been combined with terpene eutectic systems to increase its transdermal permeation [398].

In order to check whether the mixture in question is a DES, the thermodynamic behavior should be strongly non-ideal. For this test, the simulation of the solid-liquid equilibrium (SLE) phase diagram of the two solids is done. An eutectic mixture can be considered “deep” when the real eutectic temperature is significantly lower than the ideal one ($T_{E,\,real} < T_{E,\,ideal}$) [8, 399, 400]. In this work, eutectic mixtures are prepared by combining four terpenes shown in Table 9, to prepare the eutectic systems menthol:borneol (Men:Bor), thymol:borneol (Thy:Bor), menthol:camphor (Men:Cam) and thymol:camphor (Thy:Cam). The physical properties such as melting temperature, viscosity and density are obtained experimentally. The refractive index and surface tension are computed using empirical correlations developed to estimate the properties of the eutectic mixtures [401, 402]. Furthermore, the thermodynamic properties are obtained to calculate the SLE phase diagram, from which the eutectic molar composition and temperature can be determined. In addition, the chemical properties of the prepared DES are studied to assess the structure and the presence of hydrogen bonding. The SLE phase diagrams are calculated using the UNIversal Functional Activity Coefficient (UNIFAC) [403] and the Conductor-like Screening Model for Real Solvents (COSMO-RS) [404, 405].

Table 9: Chemical structure of the compounds used in DES preparation.

Compound	Chemical structure
Menthol	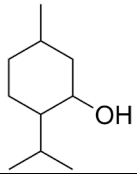
Thymol	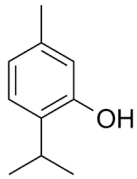
Borneol	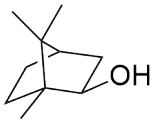
Camphor	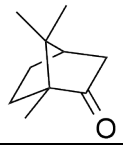
Lactic acid	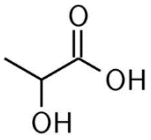
Fructose	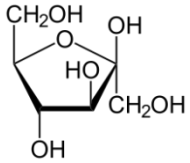
Urea	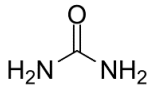

2. Materials and Methods

2.1. Materials

The chemicals used were the following: DL-menthol (CAS [89-78-1], ≥95 %), D-fructose (CAS: 57-48-7), urea (CAS: 57-13-6), DL-camphor (CAS [76-22-2], ≥96 %)) from Sigma-Aldrich (St. Louis, MO, USA), DL-lactic acid (aqueous solution, 85.0-90.0 %, CAS: 50-21-5), thymol (CAS [89-83-8], ≥98 %) and L-borneol (CAS [464-45-9], ≥97 %)) from Alfa Aesar (Haverhill, MA, USA). Deuterated dimethyl sulfoxide (DMSO, CAS [67-68-5]) and chloroform ($CDCl_3$, CAS [865-49-6]) and tetramethylsilane (TMS, CAS [75-76-3]) used in NMR experiments was purchased from Sigma-Aldrich (St. Louis, MO, USA).

2.2. Eutectic mixtures preparation

To prepare the eutectic mixtures, the pure terpene components were mixed at the chosen concentration, magnetically stirred and heated to 80 ºC for around 15 min until a homogenous transparent liquid system is obtained.

2.3. Analysis of the physical properties

The viscosity and density of the terpene-based mixtures close to the eutectic point were obtained using an Anton Paar viscometer (SVM 3001, Graz Austria) in a range of temperatures between 293 and 323 K. The temperature reproducibility was 0.03 K. The measurements were performed in triplicates for each sample. The lactic acid-based mixtures were prepared based on the literature [75, 406–408]. Their viscosity was studied using a rheometer (MCR 102, Anton Paar). The equipment was fitted with a parallel plate geometry (PP50-61752) with a gap of 0.8 mm and a constant shear rate of 10 s^{-1} was used. At first, the samples were pre-equilibrated at 50 ºC, then a temperature scan was done from 50 to 20 ºC at a 1 ºC /min cooling rate. The density was obtained by measuring the mass of 1 mL of the systems at 25 ºC.

To measure the surface tension, a tensiometer (KSV Sigma 702) and Du Noüy ring method were employed. The measurements were done at a temperature of 298 K in a thermostat bath (Lab Companion RM0525G). Three replicates were done for each mixture close to the eutectic point. An Abbe refractometer was used to determine the refractive index of the eutectic mixtures using natural light.

The surface tension (σ) and refractive index (n_D) were estimated using empirical models that had been proposed as universal approximations to estimate these properties for the eutectic systems [401, 402], according to Eq. (1) and (2).

$$\sigma_L = 393.4\ln(\rho) - 5.3\times10^{-5}\omega^{P_c} - 3.72\times10^{-2}T_c\ln\left(\rho^2\left[V_c + \frac{-50.3}{\omega^2}\right]\right) + \frac{1.132M_w\sqrt{T}}{P_c\ln\left(\frac{V_c\rho}{\sqrt{T}}\right)} + 108.9 \quad (1)$$

$$n_D = 5.17\times10^{-2}\omega^3 - 11.625\frac{\omega^2}{Mw} + 2.27\times10^{-3}P_c + 1.3668 + \frac{25.89\omega}{T} \quad (2)$$

M_w is the molecular weight (g/mol), T is the temperature (K) and ω, P_c, V_c and T_c are the acentric factor, critical pressure, volume and temperature, respectively, and ρ_L is the density (g/mL) and was computed based on Eq. (3) [409].

$$\rho_L = -1.13\times10^{-6}T_c^2 + 2.566\times10^{-3}T_c + 0.2376\omega^{0.2211} - 4.67\times10^{-4}V_c - 4.64\times10^{-4}T \quad (3)$$

The critical properties parameters of the compounds were obtained based on the Modified Lydersen and Joback-Reid model [410, 411], as shown in Eqs. (4) to (14).

$$T_{b,i} = 198.2\ K + \sum nT_{bM,i} \quad (4)$$

$$T_{c,i} = \frac{T_{b,i}}{0.5703 + 1.0121\ K^{-1}\sum nT_{bM,i} - 1K^{-2}(\sum nT_{bM,i})^2} \quad (5)$$

$$P_{c,i} = \frac{M_{w,i}\ \times (1\ bar^3\frac{mol}{g})}{[0.2573\ bar + \sum nP_{M,i}]^2} \quad (6)$$

$$V_{c,i} = 6.75\ cm^3 + \sum nV_{M,i} \quad (7)$$

$$\omega_i = \frac{(T_b - 43\ K)(T_c - 43\ K)}{(T_c - T_b)(0.7T_c - 43\ K)}\log\left(\frac{P_c}{1.01325\ bar}\right) - \frac{(T_c - 43\ K)}{(T_c - T_b)}\log\left(\frac{P_c}{1.01325\ bar}\right) + \log\left(\frac{P_c}{1.01325\ bar}\right) - 1 \quad (8)$$

T_b is the normal boiling temperature (K), $T_{c,i}$, $P_{c,i}$ and $V_{c,i}$ are the critical temperature (K), pressure (bar) and molar volume (cm^3/mol) of the component i, n is the number of each functional group in the compound, M_w is the molecular weight of compound *i* (g/mol), and ω_i is the acentric factor.

$\Delta T_{bM,i}$, $\Delta T_{M,i}$, $\Delta P_{M,i}$ and $\Delta V_{M,i}$ are the contribution to the critical properties in the modified Lydersen-Joback-Reid method of compound i and they were computed based on the chemical groups present in each compound, according to the data in Table 10 [410, 411].

The critical properties of the eutectic mixtures were obtained based on the Lee-Kesler mixing rules [412]:

$$T_{c,ij} = \sqrt{T_{c,i} \times T_{c,j}} \quad (9)$$

$$V_{c,ij} = \frac{1}{8}\left(V_{c,i}^{1/3} + V_{c,j}^{1/3}\right)^3 \quad (10)$$

$$V_{cm} = y_i^2 V_{c,i} + 2y_i y_j V_{c,ij} + y_j^2 V_{c,j} \quad (11)$$

$$T_{cm} = \frac{1}{V_{cm}^{0.25}}\left(y_i^2 V_{c,i}^{0.25} T_{c,ij} + 2y_i y_j V_{c,ij}^{0.25} T_{c,ij} + y_j^2 V_{c,j}^{0.25} T_{c,j}\right) \quad (12)$$

$$P_{cm} = (0.2905 - 0.085\omega_m)\frac{RT_{cm}}{V_{cm}} \quad (13)$$

$$\omega_m = y_i\omega_i + y_j\omega_j \quad (14)$$

$T_{c,ij}$ and $V_{c,ij}$ are the critical temperature (K) and volume (cm^3/mol) of the compounds *i* and *j*. y_i and y_j are the molar ratio of compounds *i* and *j*, respectively, in the eutectic mixture. *R* is the gas constant (83.14 cm^3·bar/g mole·K). T_{cm}, P_{cm} and V_{cm} are the critical temperature (K), pressure (bar) and molar volume (cm^3/mol) of the eutectic mixtures and are used to compute the theoretical physical properties (density, surface tension and refractive index) of the eutectic mixtures.

Table 10: The contribution to the critical properties in the modified Lydersen-Joback-Reid method.

	Groups	ΔT_{bM} (K)	ΔT_M (K)	ΔP_M (bar)	ΔV_M (cm^3/mol)
Without rings	-CH3	23.58	0.0275	0.3031	66.81
	-CH2-	22.88	0.0159	0.2165	57.11
	>CH-	21.74	0.0002	0.114	45.7
	>C<	18.18	-0.0206	0.0539	21.78
	-CH2	24.96	0.017	0.2493	60.37
	-CH-	18.25	0.0182	0.1866	49.92
	-C<	24.14	-0.0003	0.0832	34.9
	-C-	26.15	-0.0029	0.0934	33.85
	=CH	0	0.0078	0.1429	43.97
	=C-	0	0.0078	0.1429	43.97
	-OH (alcohol)	92.88	0.0723	0.1343	30.4
	-O-	22.42	0.0051	0.13	15.61
	>C=O	94.97	0.0247	0.2341	69.76
	-CHO	72.24	0.0294	0.3128	77.46
	-COOH	169.06	0.0853	0.4537	88.6
	-COO-	81.1	0.0377	0.4139	84.76
	HCOO-	0	0.036	0.4752	97.77
	-O (others)	-10.5	0.0273	0.2042	44.03
	-NH2	73.23	0.0364	0.1692	49.1
	>NH	50.17	0.0119	0.0322	78.96
	>N-	11.74	-0.0028	0.0304	26.7
	-N-	74.6	0.0172	0.1541	45.54
	-CN	125.66	0.0506	0.3697	89.32
	-NO2	152.54	0.0448	0.4529	123.62

	-F	-0.03	0.0228	0.2912	31.47
	-Cl	38.13	0.0188	0.3738	62.08
	-Br	66.86	0.0124	0.5799	76.6
	-I	93.84	0.0148	0.9174	100.79
With Rings	-CH2-	27.15	0.0116	0.1982	51.64
	>CH-	21.78	0.0081	0.1773	30.56
	-CH-	26.73	0.0114	0.1693	42.55
	>C<	21.32	-0.018	0.0139	17.62
	-C<	31.01	0.0051	0.0955	31.28
	-O-	31.22	0.0138	0.1371	17.41
	-OH (phenol)	76.34	0.0291	0.0493	-17.44
	>C=O	94.97	0.0343	0.2751	59.32
	>NH	52.82	0.0244	0.0724	27.61
	>N-	0	0.0063	0.0538	25.17
	-N-	57.55	-0.0011	0.0559	42.15

The errors were obtained to assess the accuracy of the models used to compute the physical parameters in comparison to the experimental results. The errors were calculated using Eq. (15) and (16) to get the relative deviation (RD%) and the average relative deviation (ARD%), respectively.

$$\mathrm{RD\%} = 100\left(\frac{\rho_{\mathrm{L}\,i} - \rho_{\mathrm{exp}\,i}}{\rho_{\mathrm{exp}\,i}}\right) \tag{15}$$

$$\mathrm{ARD\%} = \frac{100}{\mathrm{N}}\sum_{i}^{n}\left|\frac{\rho_{\mathrm{L}\,i} - \rho_{\mathrm{exp}\,i}}{\rho_{\mathrm{exp}\,i}}\right| \tag{16}$$

2.4. Fourier-transform infrared spectroscopy analysis

Fourier-transform infrared spectroscopy (FTIR) (Class 1 Laser Product Nicolet 6100, San Jose, CA) was used to assess the structure of the pure compounds as well as the prepared

eutectic mixtures. FTIR absorption spectra were recorded with 4 cm^{-1} resolution and with 40 scans of the sample in the range 4000 to 600 cm^{-1}.

2.5. ^{1}H-NMR analysis

NEO500 spectrometer, Bruker, Rheinstetten, Germany, coupled to a temperature probe (BTO2000) was used to analyze the pure terpenes and the prepared eutectic mixtures. For the pure compounds, 5 mg of the solids were solved in 650 µL of $CDCl_3$ with TMS in the NMR tube. Before acquisition, the samples were equilibrated for 15 min using a Thermocouple-T to adjust and monitor the temperature. Proton chemical shifts were calibrated in reference to TMS (0 ppm). To analyze the eutectic solvent systems, DMSO was placed in a sealed capillary tube inside the NMR tube containing 300 µL of the solvent systems, to avoid the interference of DMSO in the hydrogen bonding in the systems. Equilibration was done for 15 min to ensure the required temperature, and the samples were locked using the frequency of the DMSO (2.8 ppm). The spectra were recorded at 298 to 323 K for the pure compounds and 298 to 313 K for the eutectic systems, with an increment of 5 K. For both pure compounds and eutectic systems, the spectra were obtained at 500 MHz with a 30º pulse angle, 4.5 s pulse delay, and 16 scans.

2.6. TGA and DSC analysis

The thermal degradation temperatures were determined using thermogravimetric analyzer TGA (TA instrument model TGA Q50). Samples were placed in the crucible under nitrogen atmosphere (flow rate of 50 mL/min) and heated up to 773 K at a rate of 2 K/min.

The thermodynamic properties were obtained using differential scanning calorimetry (DSC) (TA Instrument model DSC Q200) under anhydrous high-purity nitrogen at 50 mL/min. Samples were sealed in aluminum pans. For borneol and camphor, the temperature was cooled to 193 K, then heated from 193 to 503 K, cooled to 193 K and heated back to 503 K at a rate of 6 K/min. For thymol, menthol, the same cycles and cooling rate was applied with the cooling and heating temperatures of 193 and 333 K, respectively. The computed parameters were determined in the second reheating cycle.

To obtain the experimental SLE, the eutectic mixtures at different molar ratios were studied on DSC by cooling with a rate of 6 K/min conducted until 193 K. A heating cycle was done until a temperature that was approximately 10 K higher than the liquidus temperature of the

sample. The sample was then cooled back to 193 K and reheated to the same temperature as in the first cycle. The DSC measurements were obtained in the third cycle.

2.7. SLE phase diagram calculation

The SLE phase diagram of the terpene-based solvent systems was plotted using COSMO-RS and MATLAB in order to obtain the suitable range of the components molar ratio and the operating temperature at which these solvents could act as DES.

The shown SLE phase diagrams were based on the following simplified thermodynamic relation Eq. (17), in which the less relevant change in calorific capacity (ΔC_p) was neglected [413, 414]:

$$\ln\left(x_i^L \gamma_i^L\right) = \frac{\Delta H_f}{RT} \cdot \left(\frac{T}{T_f} - 1\right) \quad (17)$$

where x_i^L and γ_i^L are the molar ratio and the activity coefficient of component i, respectively. ΔH_f is the enthalpy of fusion (J/mol), R is the gas constant (8.314 J/mol·K), T and T_f are the temperature of the system and the melting temperature (K) of a pure component, respectively. The SLE simulation was done using two software applications: MATLAB and COSMOthermX19. The use of the two models was compared to the ideal SLE in which the activity coefficient was equal to unity.

2.7.1. UNIFAC function computations

UNIFAC is based on the fragmentation of the molecules into their functional groups to let these groups interact with each other to calculate the activity coefficient γ_i^L [415–417]. It was computed as a function of the combinatorial and residual activity coefficients γ_i^C and γ_i^R, respectively as shown in Eq. (18).

$$\ln\left(\gamma_i^L\right) = \ln\left(\gamma_i^C\right) + \ln\left(\gamma_i^R\right) \quad (18)$$

The combinatorial activity coefficient depends on the size and spatial conformation of the molecules present in the system. On the other hand, the residual activity coefficient accounts for the energetic interactions obtained using the group activity coefficients of both the mixture and the pure substances [415, 418].

The coefficient γ_i^C was computed based on the Flory-Huggins expression and the Staverman-Guggenheim correction term [413, 419], as shown in Eq. 19:

$$\ln \gamma_i^C = 1 - J_i + \ln J_i - 5q_i \left(\ln \frac{\phi_i}{\theta_i} + 1 - \frac{\phi_i}{\theta_i} \right) \quad (19)$$

where the quantity J_i, the molecule volume and surface area fractions ϕ_i and θ_i, respectively were computed as following:

$$J_i = \frac{\phi_i}{x_i} \quad (20)$$

$$\phi_i = \frac{x_i r_i}{\sum x_i r_i} \quad (21)$$

$$\theta_i = \frac{x_i q_i}{\sum_j x_j q_j} \quad (22)$$

where q_i and r_i are the molecular surface area and volume, respectively, and they were obtained as shown in Eq. 23 and 24:

$$q_i = \sum \nu_k^{(i)} R_k \quad (23)$$

$$r_i = \sum \nu_k^{(i)} Q_k \quad (24)$$

where ν_k corresponds to the number of subgroups of type *k* in the component *i*, R_k and Q_k are the subgroup parameters defined as the Van der Waals group volumes and surface areas, respectively. These values were obtained from a database (Dortmund Data Bank) [420]. The lactic acid-based systems were not evaluated as the functional groups present in the systems were not all available in the database of Dortmund Data Bank and the simulation of the ideal and real curves using the UNIFAC function was not applicable.

On the other hand, the coefficient γ_i^R was computed based on the Eq. 25:

$$\ln \gamma_i^R = \sum \nu_k^{(i)} \left(\ln \Gamma_k - \ln \Gamma_k^{(i)} \right) \quad (25)$$

where Γ_k and $\Gamma_k^{(i)}$ are the group activity coefficients of the subgroup *k* in the mixture and in the pure substance *i*, respectively and they can be computed using Eq. 26 by calculating the sums over all the different groups:

$$\ln \Gamma_{\mathrm{k}} = Q_{\mathrm{k}}[1 - \ln(\sum_{\mathrm{m}} \Theta_{\mathrm{m}}\psi_{\mathrm{mk}}) - \sum_{\mathrm{m}} \frac{\Theta_{\mathrm{m}}\psi_{\mathrm{km}}}{\sum_n \Theta_{\mathrm{n}}\psi_{\mathrm{nm}}}] \quad (26)$$

where ψ_{m} and Θ_{m} correspond to the group interaction parameter and the area fraction of the group m, respectively. They were computed based on Eq. 27 and 28. Θ_{m} was obtained similarly to the Θ_{i} factor calculated in the combinatorial coefficient.

$$\Theta_{\mathrm{m}} = \frac{X_{\mathrm{m}}Q_{\mathrm{m}}}{\sum_n X_{\mathrm{n}}Q_{\mathrm{n}}} \quad (27)$$

where X_{m} corresponds to the molar fraction of the group m in the mixture and can be obtained as shown in Eq. 28:

$$X_{\mathrm{m}} = \frac{\sum_j \nu_{\mathrm{m}}^{(i)} x_j}{\sum_j \sum_n \nu_{\mathrm{n}}^{(i)} x_j} \quad (28)$$

The group interaction parameter ψ_{m} depends on the temperature of the system and it was given according to Eq. 29:

$$\psi_{\mathrm{m}} = \exp(-\frac{a_{\mathrm{mn}}}{T}) \quad (29)$$

The parameter a_{mn} is the binary group interaction parameter and it does not depend on the temperature and it is not symmetric [416]. Therefore, a_{mn} has a different value than a_{nm}. These binary interaction parameters were obtained by fitting a wide range of experimental phase equilibrium data [420].

An own implementation of UNIFAC (on MATLAB 2019a) was used in this work. The parameters of UNIFAC were published by Hansen et al. (1991), Gmehling et al. (1993) and Oracz et al. (1996) [420–422].

2.7.2. COSMO-RS simulation

COSMO-RS was also used to calculate the SLE phase diagrams. It relies on quantum chemistry and statistical thermodynamics in order to predict the properties of the target fluid mixtures from first principles [405, 423]. The activity coefficient was calculated by taking into consideration the surface charge of the molecules, computed based on quantum chemistry instead of the chemical groups present in the molecules. This allows for a much more predictive application of the model straight from the structure of the molecules [424]. The conformers of the

terpene used were generated using COSMOconf software (version 3.0). The COSMOthermX19 parameterization was applied at the BP-TZVP and BP-TZVPD-FINE levels.

3. Results and Discussion

3.1. Physical properties of the eutectic systems

In order to compute the theoretical physical parameters, the critical properties of the eutectic systems are shown in Table 11 and Table 12. The physical parameters obtained both theoretically and experimentally for a temperature of 298 K are shown in Table 13. The viscosity and density are an important physical property required for the design and optimization of various chemical processes employing the solvents, such as heat exchangers, separation units and agitation equipment, among others [425, 426]. The binary system Men:Bor (128.07 mPa/s) was shown to be more viscous than the other terpene-based systems, followed by Thy:Bor (45.47 mPa·s). Thus, the eutectic solvents with borneol in the system have a higher viscosity than those with camphor. The lactic acid-based solvent systems are much more viscous than the terpene-based systems. The viscosity was shown to be 746.70 and 732.91 mPa/s for Lac:Fru and Lac:Ur, respectively at room temperature (25 °C). At the extraction temperature of 50 °C, this value decreased to 113.40 and 187.93 mPa/s for Lac:Fru and Lac:Ur, respectively, which would be more favorable in extraction processes.

Moreover, the density highly depends on the structure of the components of the system [23]. It is essential to determine this parameter in extraction processes as it affects the kinetic rate and the driving force between the solvent and the solid particles [22, 427]. The difference in the densities between each combination of DES is affected by the molecular organization and packing within the system [7]. The values were obtained experimentally and were shown to be between 0.9152 to 0.9717 g/mL for the terpene-based systems. The density of the lactic acid-based solvent systems was shown to be 1.2 g/mL. Therefore, they are much denser than terpene-based solvent systems. The RD% was shown to lie between 17.3 to 22.65 %, as shown in Table 14. The ARD% of the density computed using the proposed model was 20.07%. Based on the previous works, the values of the RD% for the density were shown to be similar as the values range from -13 to 22 % [409]. In contrast, the ARD% obtained based on the current study of the four eutectic

systems was higher than the one shown in previous work, which can be explained by the fact that in the previous work, the model was applied to DES that are mainly based on quaternary ammonium salts [409].

Table 11: Critical properties of the pure compounds.

Compound i	$\Delta T_{bM,i}$ (K)	$\Delta T_{M,i}$ (K)	$\Delta P_{M,i}$ (bar)	$\Delta V_{M,i}$ (cm^3/mol)	$T_{b,i}$ (K)	$T_{c,i}$ (K)	$P_{c,i}$ (bar)	$V_{c,i}$ (cm^3/mol)	ω_i
Menthol	315.61	0.1709	2.1991	475.29	513.81	719.56	25.90	482.04	0.509
Borneol	292.95	0.1185	1.7583	403.71	491.15	726.35	37.97	410.46	0.404
Thymol	327.19	0.1514	1.8910	414.21	525.39	749.90	32.55	420.96	0.511
Camphor	311.58	0.1237	1.9841	480.47	509.78	749.46	30.30	487.22	0.342
Lactic acid	303.77	0.2033	1.0777	235.73	501.97	683.20	50.54	242.48	1.025
Fructose	642.89	0.4233	1.7634	428.9	841.09	1026.30	44.12	435.65	2.219
Urea	241.43	0.0975	0.5725	167.96	439.63	666.64	87.22	174.71	0.596

Table 12: Critical properties of the eutectic mixtures.

Eutectic mixture *i:j*	V_{cm} (cm^3/mol)	T_{cm} (K)	P_{cm} (bar)	ω_m
Men:Bor	460.16	721.39	32.57	0.48
Men:Cam	484.11	731.46	31.77	0.44
Thy:Bor	425.98	740.58	35.45	0.53
Thy:Cam	453.69	749.49	34.92	0.43
Lac:Fru	272.67	738.19	41.89	1.23
Lac:Ur	228.33	679.47	52.12	0.94

The surface tension is a physical property that describes the inclination of a fluid, which defines its minimal surface area. It plays a vital role in the permeability of the solvent and the design of processes. Its value increases with the decrease of the temperature and the kinetic molecular energy of the liquid [402, 428]. It was shown to be in the range of 29.04 to 31.75 mN/m

for the terpene-based solvent systems. The computed values are shown to be similar to the experimental values, as the RD% values ranging from -20.96 to 18.59 %. These values were in correlation with previous works which showed that most of the investigated systems had a surface tension value lower than 50 mN/m [402]. Furthermore, the values were shown to be 44.62 and 43.96 mN/m for Lac:Fru and Lac:Ur, respectively. These results were higher than those of the terpene-based solvent systems, but were comparable to those found in the literature as the surface tensions of choline chloride:phenylacetic acid (1:2 in molar mass) and 1-butyl-3-methyl-imidazolium tetrafluoroborate had been reported to be 41.86 and 44.81 mN/m, respectively [5, 429]. The ARD% value was shown to be much higher (66.88 %) for the study of surface tension than for the other parameters. This is mainly due to the high difference between the theoretical and experimental values of the lactic acid-based solvent systems. Hence, the employed models are more accurate for the study of terpene-based solvent systems.

The refractive index of the eutectic solvent systems had been investigated as a useful tool to identify compounds, assess the purities of substances and verify the concentrations of mixtures [24, 430]. It is a fundamental parameter to measure the electronic polarizability of a molecule and understand the intermolecular interactions and the behavior in solutions [431]. For the lactic acid-based solvent systems, the values were shown to be 1.4590 and 1.4368 for Lac:Fru and Lac:Ur, respectively. The refractive index values of the terpene-based eutectic mixtures were shown to be in the range of 1.4635 to 1.5105, which were in accordance with previous studies [401], and were similar to the estimated values using the models as the RD% for this parameter was the lowest, ranging from -2.05 to 3.53 % and the ARD% value was 1.72 %. Thus, based on the results obtained for the study of the 4 terpene eutectic mixtures, the proposed models were mostly fit for the computation of the refractive index, as a lower ARD% was obtained in comparison to the other properties.

Table 13: Experimental and theoretical properties of the eutectic systems.

		Experimental				Theoretical		
Eutectic systems	**M_w (g/mol)**	**Viscosity η_{exp} (mPa/s)**	**Density ρ_{exp} (g/mL)**	**Surface tension σ_{exp} (mN/m)**	**Refractive index $n_{D,\,exp}$**	**Density ρ_L (g/mL)**	**Surface tension σ_L (mN/m)**	**Refractive index n_D**
Men:Bor (7:3)	155.66	128.07 ± 0.24	0.9152 ± 0.0005	29.04 ± 0.03	1.4670 ± 0.0005	1.1116	25.37	1.4708
Men:Cam (3:2)	154.65	19.23 ± 0.01	0.9178 ± 0.0001	29.41 ± 0.08	1.4635 ± 0.0008	1.1063	23.25	1.4671
Thy:Bor (7:3)	151.43	45.63 ± 0.20	0.9716 ± 0.0001	31.75 ± 0.01	1.5105 ± 0.0002	1.1500	29.19	1.4795
Thy:Cam (1:1)	151.23	21.10 ± 0.02	0.9675 ± 0.0001	30.35 ± 0.06	1.4970 ± 0.0003	1.1350	32.25	1.4731
Lac:Fru (5:1)	105.39	746.70 ± 16.37	1.2540 ± 0.0011	44.62 ± 0.07	1.4590 ± 0.0009	1.5490	119.92	1.5026
Lac:Ur (4:1)	84.08	732.91 ± 9.61	1.2390 ± 0.0009	43.96 ± 0.03	1.4368 ± 0.0006	1.4993	126.56	1.4956

Table 14: Error parameters RD% and ARD%.

	Relative average deviation percent RD%						Average relative deviation ARD%
	Men:Bor	**Men:Cam**	**Thy:Bor**	**Thy:Cam**	**Lac:Fru**	**Lac:Ur**	
Density ρ	21.5	20.5	18.4	17.3	22.65	20.09	20.07
Surface tension σ	-12.7	-21.0	-8.1	6.3	167.4	185.9	66.88
Refractive index n_D	0.26	0.25	-2.05	-1.59	2.67	3.53	1.72

3.2. FTIR and ^{1}H NMR analysis

The eutectic mixtures and the pure components used to prepare them were analyzed using FTIR to assess their chemical structure, as shown in Figure 4. Menthol, thymol and borneol are terpene alcohols and exhibited an O−H stretching vibration at 3270, 3170 and 3300 cm^{-1}, respectively. In contrast, camphor displayed a strong absorption band at 1739 cm^{-1}, which is a characteristic of ketones having a C=O stretching vibration. Furthermore, symmetrical and asymmetrical $-CH_2$ stretching vibrations correspond to the bands at 2958 and 2867 cm^{-1}, respectively. These bands were superimposed upon the O−H stretching. These terpene molecules present a hydrogen bond between the oxygen atoms and the hydroxyl groups. The O−H stretching vibration peaks shifted to higher wavenumbers in comparison to the pure compounds due to the hydrogen bonding that took place through the O−H groups [432]. For the lactic acid-based solvent systems, the spectra of the prepared solvents exhibited similar absorption profiles to those of the pure components, with lactic acid having the dominant vibrating peaks in solvent systems as it has a higher molar ratio (5:1 and 4:1 of Lac:Fru and Lac:Ur, respectively). A strong absorption band was observed in lactic acid and the solvents at 1718 cm^{-1}, which was a relative to the C=O stretching vibration present in the lactic acid. In contrast, the broad absorption peak at 3361 cm^{-1} corresponded to the O–H bond in a carboxylic acid of the pure lactic acid and in the prepared solvents. This stretching bond was also visible in the spectra

of fructose at 3394 cm^{-1}. It can be observed in both systems Lac:Ur and Lac:Fru that the wavenumber of the O−H stretching bands shifted in comparison to the pure compounds as hydrogen bonding occurred. Moreover, the peaks 1050 and 976 cm^{-1} were relative to the strong absorption of the C–O stretching bands. For urea, the bands at 1460, 1589 and 1672 cm^{-1} represent the C–N, N–H and C=O stretching vibrations, respectively [433, 434]. The N–H and C=O peaks were shifted to higher wavenumbers in Lac:Ur to 1628 and 1714 cm^{-1}, respectively, due to hydrogen bonding that took place.

Furthermore, the eutectic mixtures and the pure components were analyzed using ^{1}H-NMR. The temperatures measured lied between 298 to 323 K at an increment of 5 K to study the chemical shifts that take place due to the H-bonded protons for the inter- and intramolecular bonds [98, 435]. It had been shown that as the temperature of the sample is increased, a decrease in the intermolecular bonding takes place, which led to an upfield shift of the H-bonded protons [436], as shown in Figure 5. A temperature coefficient (T_{coeff}) was obtained to study the magnitude of the shift and the type of H-bonding associated. This coefficient was calculated as the slope of the linear correlation of the chemical shifts (δ) as a function of the temperature, as shown in Figure 6. In nonpolar solvents, a T_{coeff} value more negative than -0.005 ppm/K indicates intermolecular H-bonding takes place, while a T_{coeff} value less negative than -0.003 ppm/K indicates intramolecular H-bonding [437]. In Figure 5, the upfield shift of each –OH functional group was present in each system as the temperature increased. Figure 6 and Table 15 show that the T_{coeff} values obtained for each system range between -0.0212 to -0.012 ppm/K, suggesting an intermolecular H-bond is happening. As for the pure terpenes, an upfield shift of the –OH functional group was also observed when the temperature is increased. However, the extent of the chemical shift was lower than that observed in the eutectic systems, as T_{coeff} ranged between -0.004 to -0.009 ppm/K, as shown in Table 15. Thus, the molecular interaction taking place in the pure compounds differed from that in the eutectic systems. This suggests that significant hydrogen bonding occurs between two different molecules, hence the eutectic systems do not behave as an ideal mixture.

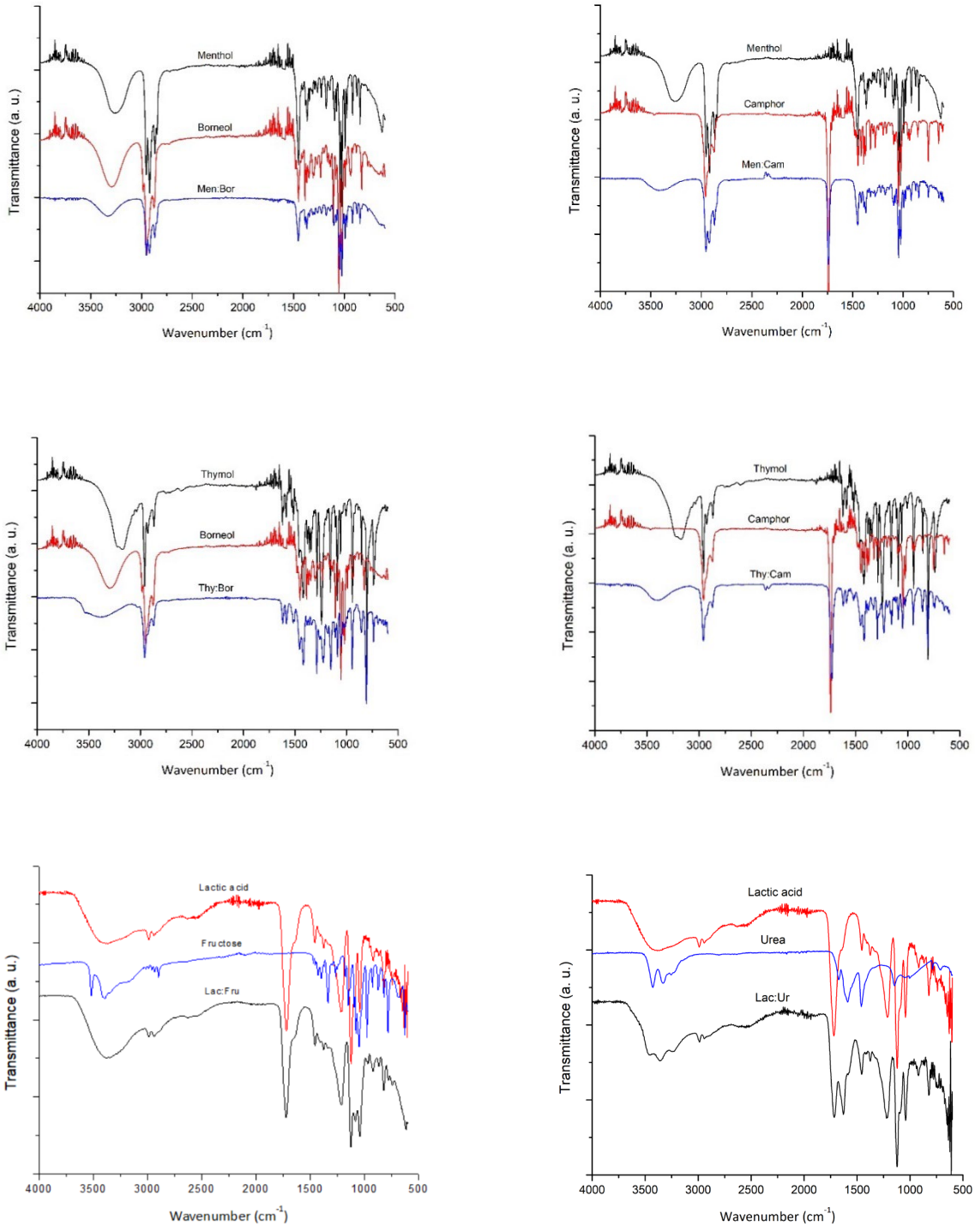

Figure 4*: FTIR spectra of the pure compounds and the eutectic systems.*

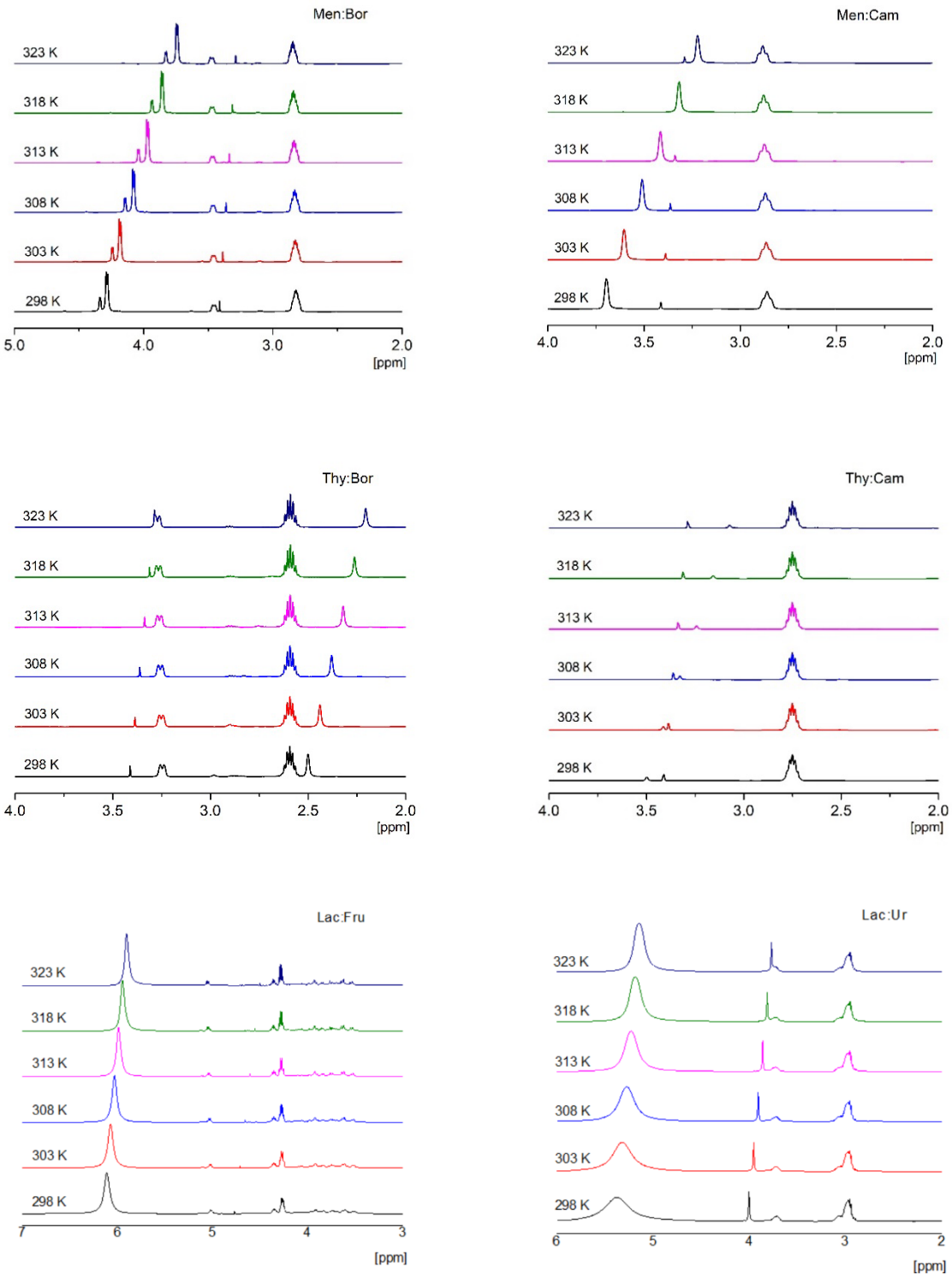

Figure 5: Magnified ^{1}H-NMR spectra of the eutectic systems as a function of temperature.

(a)

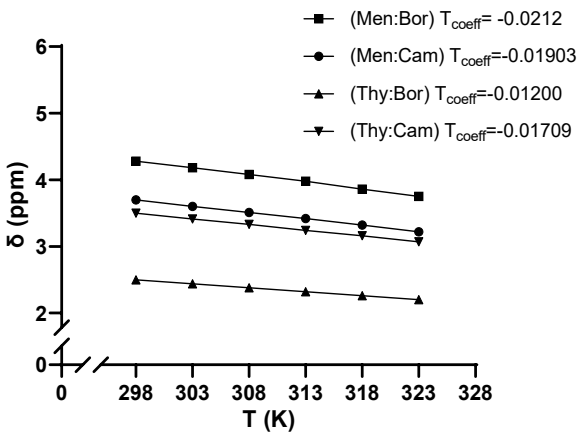

(b)

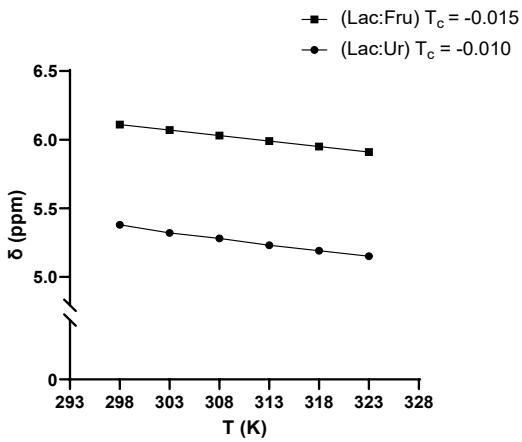

Figure *6*: *Plot of the chemical shifts (δ) of the OH protons as a function of temperature for (a) terpene-based and (b) lactic acid-based eutectic system.*

Table 15*: The temperature coefficient T_{coeff} of each pure compound and eutectic systems.*

Compound	T_{coeff}
Menthol	-0.005
Borneol	-0.004
Thymol	-0.006
Camphor	-0.005
Lactic acid	-0.008
Fructose	-0.009
Urea	-0.009
Men:Bor	-0.021
Men:Cam	-0.019
Thy:Bor	-0.012
Thy:Cam	-0.017
Lac:Fru	-0.015
Lac:Ur	-0.010

3.3. TGA and DSC analysis

The thermodynamic properties of the pure compounds studied were measured in order to calculate the SLE phase diagram. Table 16 displays the values obtained using DSC that were used for the SLE phase diagram calculations. The degradation temperature Td of the DES was obtained using TGA to assess the limit of the heating temperature of the eutectic systems using DSC. The glass transition (T_g) and crystallization temperatures (T_{cr}), and the enthalpy of crystallization (ΔH_{cr}) were obtained for each eutectic solvent system at a molar ratio closest to the eutectic point, as shown in Table 17. Crystallization was affected by the molecular nature of the substances, and the kinetics of the cooling process [17, 438]. For instance, during crystallization at low temperatures, inefficient crystal packing could form and in order to build a crystal lattice, molecules must adapt a proper conformation which could be hindered at low temperatures [438–440]. Hence, an attraction between unlike molecules as well as the inefficient packing in the crystal structure led to the formation of the glassy states. Consequently, in the studied eutectic systems, the formation of the glassy state at a low temperature occurs due to a strong negative deviation from ideality as a result of an interaction between unlike molecules [438].Based on the results obtained using DSC, the thermal transition behavior of the eutectic systems can be described by cooling to a glass state at low temperature. The T_g is obtained for each system and upon heating, crystallization took place and a T_{cr} was recorded above the T_g, as shown in Table 17. Similar behavior was observed in another study when assessing the thermodynamic behavior of eutectic solvent systems [438, 441].

Table 16: Melting temperature (T_f), enthalpy of fusion (ΔH_f) of the pure compounds.

Component	T_f (K)	ΔH_f (kJ/mol)
Menthol	309.72	13.62
Thymol	324.31	18.54
Borneol	481.33	7.23
Camphor	452.41	6.32
Lactic acid	289.90	14.70
Fructose	466.41	22.77
Urea	405.15	10.34

Table 17: Experimental data of the degradation temperature (T_d), the crystallization temperature (T_{cr}), enthalpy of crystallization (ΔH_{cr}) and the glass transition temperature (T_g) of the eutectic systems.

Eutectic system	T_d (K)	T_{cr} (K)	ΔH_{cr} (J/g)	T_g (K)
Men:Bor (7:3)	366.02	254.08	21.17	223.03
Men:Cam (3:2)	358.29	239.92	28.60	196.98
Thy:Bor (7:3)	355.04	284.64	0.098	215.17
Thy:Cam (1:1)	370.74	260.69	0.077	194.23
Lac:Fru (5:1)	339.45	231.98	0.696	189.15
Lac:Ur (4:1)	308.30	223.42	0.164	171.76

3.4. SLE phase diagram simulation

The SLE phase diagrams were obtained based on Eq. 6. The values of T_f and ΔH_f for the pure components that were used to simulate the systems are shown in Table 16. For the real systems, the diagrams were computed using the COSMO-RS and UNIFAC models, as shown in Figure 7 along with results of DSC experiments. As previously mentioned, the SLE phase diagram was not computed for the lactic acid-based DES as the models were not applicable to the compounds involved in these systems. Assuming that the calculations were acceptably accurate [390], from these plots, the eutectic temperatures and molar ratios at the eutectic point can be estimated (Table 18).

For the menthol-based solvent systems, a negative deviation from ideality was also observed in the SLE diagrams obtained using the models and also from the experiments. The UNIFAC and COSMO-RS models estimated the behavior to be comparable to the ideal eutectic. For instance, the activity coefficient ranged from 1 to 1.01 and from 1.02 to 1.16 for Men:Bor based on the UNIFAC and COSMO-RS (TZVPD-FINE) models, respectively. As menthol is a terpene alcohol with the –OH group attached to a cyclic ring and the components are a mixture of terpene alcohols having similar functional groups, the predicted activity coefficient is close to ideality. Thus, the ideal eutectic temperatures of Men:Bor and Men:Cam (289.8 and 284.7 K respectively), were very close to the predicted real eutectic temperatures (289.8 to 290.7 K and 283.4 to 288.1 K for Men:Bor and Men:Cam, respectively). The models did not predict the extent of the negative deviation from ideality observed in the experiment. For Men:Bor, a lower negative deviation was observed in comparison to Men:Cam and the thymol-based systems. Consequently, for the Men:Bor system, it cannot be confirmed that the behavior had such clear negative deviation from ideality as Men:Cam. The results were comparable to those obtained in another study, where a negative deviation is observed between the ideal and the experimental SLE measurements for the DES menthol:ibuprofen [14].

For the thymol-based solvent systems, the eutectic temperatures obtained experimentally and using the models were lower than the ideal ones. For Thy:Bor, the estimated real eutectic temperatures were 274.4, 293.2 and 300.8 K obtained using COSMO-RS (TZVP and TZVPD-FINE levels) and UNIFAC, respectively, which were lower than the ideal one (309.6 K). A similar

behavior was observed for Thy:Cam as a negative deviation was shown from ideality (300.1 K) to the estimated real behavior (from 166.2 to 281.7 K). The experimental SLE measurements displayed a significant negative deviation from ideality, which was also correctly predicted by the models. Thus, these systems could be considered as DES.

By comparing the estimated real SLE using the models, it can be shown that the COSMO RS model predicts eutectic points further away from ideality than the UNIFAC model, and a higher deviation was observed in the COSMO-RS parametrization level TZVP than that of the TZVPD-FINE level. Moreover, the plots of the thymol-based solvent systems showed that the models estimated a deviation of the eutectic concentration. For example for Thy:Bor, the ideal eutectic concentration was 0.72 while the estimated value by the models was 0.65, 0.52 and 0.58 for UNIFAC, COSMO-RS (TZVP and TZVPD-FINE levels), respectively. This showed that the structural interaction was not fully described by the models and that additional effects may be taking place.

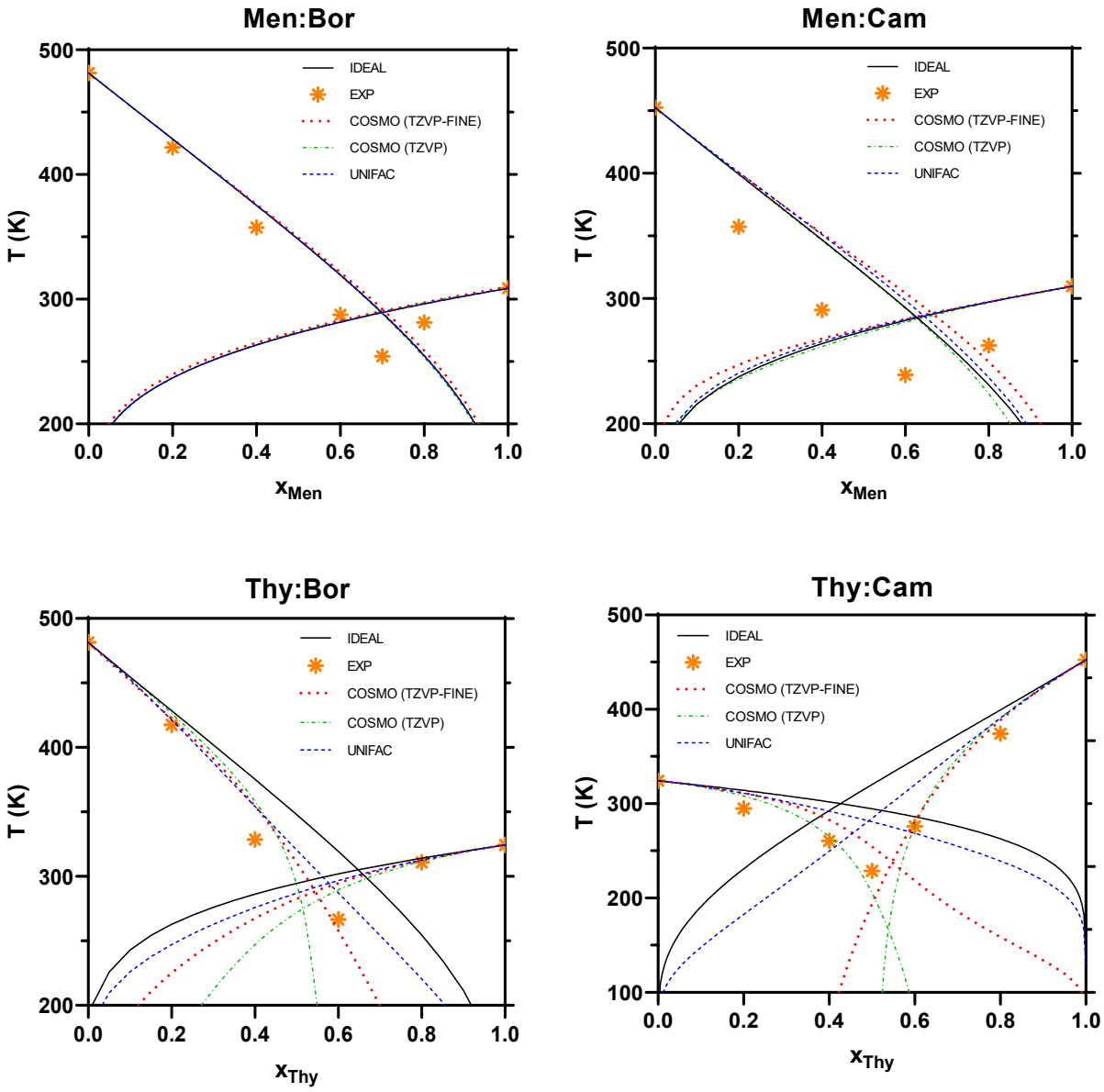

Figure 7: Measured solid-liquid equilibrium phase diagrams of the terpene-based solvent systems.

Table 18: Ideal and predicted real eutectic temperature and molar ratio of the solvent systems.

	Ideal		UNIFAC		COSMO-RS (TZVP)		COSMO-RS (TZVPD-FINE)	
Eutectic systems	$T_{E, ideal}$ **(K)**	$x_{E, ideal}$	$T_{E, UNIFAC}$ **(K)**	$x_{E, UNIFAC}$	$T_{E, TZVP}$ **(K)**	$x_{E, TZVP}$	$T_{E, TZVPD-FINE}$ **(K)**	$x_{E, TZVPD-FINE}$
Men:Bor	155.66	128.07 ± 0.24	0.9152 ± 0.0005	29.04 ± 0.03	1.4670 ± 0.0005	1.1116	25.37	1.4708
Men:Cam	154.65	19.23 ± 0.01	0.9178 ± 0.0001	29.41 ± 0.08	1.4635 ± 0.0008	1.1063	23.25	1.4671
Thy:Bor	151.43	45.63 ± 0.20	0.9716 ± 0.0001	31.75 ± 0.01	1.5105 ± 0.0002	1.1500	29.19	1.4795
Thy:Cam	151.23	21.10 ± 0.02	0.9675 ± 0.0001	30.35 ± 0.06	1.4970 ± 0.0003	1.1350	32.25	1.4731

4. Conclusions

The characterization of the four different terpene-based eutectic solvent systems was done to obtain their physicochemical properties. The density, surface tension and refractive index were computed experimentally and compared to models proposed in the literature for each eutectic system. The accuracy of the models was studied using the RD% for each solvent system, which ranged from 17.3 to 21.5 % for the density, from -21.0 to 6.3 % for the surface tension and from -2.05 to 0.26 % for the refractive index. Furthermore, the chemical structure and interactions were analyzed on the basis of FTIR and ^{1}H-NMR measurements to confirm the presence of the intermolecular hydrogen bonding in the eutectic systems. The thermodynamic properties, such as the enthalpy of crystallization, the degradation, glass transition and crystallization temperatures were measured using TGA and DSC. From these obtained values, the SLE phase diagram of the eutectic mixtures was studied using UNIFAC and COSMO-RS with two different parametrization

levels. From the curves, the eutectic temperature and molar concentration was estimated for each system and the deviation from ideality was studied to assess the behavior of the systems checking if they behave as DES. The UNIFAC and COSMO-RS models predicted comparable but not completely accurate curves in comparison to the experimental data. They showed similar results without any of the models capturing the trends better than the other in all studied cases. However, optimization of the models is needed to improve the prediction of the interaction in the systems. The difference in the chemical interactions between the pure compounds and the eutectic systems, observed experimentally for terpene- and lactic acid-based systems, and analyzed by simulation for terpene-based systems, proved that in fact the systems did not act as an ideal mixture due to the presence of significant hydrogen bonding, which confirmed their behavior as possible DES candidates.

Chapter III:
Extraction of bioactives from marine by-products using deep eutectic solvents

This chapter was published by MDPI as:

Abdallah, M. M., Cardeira, M., Matias, A. A., Bronze, M. D. R., & Fernández, N. (2022). Lactic acid-Based Natural Deep Eutectic Solvents to Extract Bioactives from Marine By-Products. Molecules, 27(14), 4356. DOI: 10.3390/molecules27144356

Abstract

Deep eutectic solvents (DES) were used to extract bioactive compounds from marine by-products: codfish bones (CB), mussel meat (MM) and tuna vitreous humor (TVH). DES were prepared using natural components, including selected terpenes (menthol, thymol, borneol, camphor), lactic acid (Lac), fructose (Fru) and urea (Ur). The yield obtained using lactic acid-based DES was significantly higher than that using terpene-based DES. Hence, the extracts obtained using lactic acid-based DES were characterized to define their composition in hyaluronic acid (HA), chondroitin sulfate (CS), proteins, lipids and ash. Results demonstrated that the extracts composition highly differed, depending not only on the DES used, but also on the structure and composition of the raw material used. Proteins were the main components of these extracts, mostly in extracts obtained from MM. The extracts obtained from all raw materials also contained ash and lipids. HA was mainly extracted from TVH using both Lac:Ur and Lac:Fru. The HA and CS contents in the extracts obtained using the conventional method is shown to be higher than the yield of DES extraction, as this method has a higher capacity in hydrolyzing the tissues to isolate the target compounds

Keywords: marine by-products, natural bioactive ingredients, deep eutectic solvents, alternative solvents, extraction process, chemical characterization.

1. Introduction

The total mass of marine generated by-products was estimated to be approximately 20 million tons globally [442]. These wastes are generally discarded on land or in the sea and they can lead to the contamination of the coastal water [443]. Marine by-products were largely investigated for their valorization and use in industrial applications due to abundance, low-cost and environmental advantages [161]. Therefore, their use as a source for the isolation of bioactive compounds has great advantages as nowadays the integration of natural products in pharmaceutical and cosmetic industries has remarkably increased, as their biological activity and structural properties may differ from the synthetic molecules [164, 444]. Many compounds used

in pharmaceutical applications were originally isolated from natural sources, such as plants and biomass [166]. For example, vitamin C was obtained from citrus, salicylic acid from Willow Bark, taxol from Yew Bark, pilocarpine from *Pilocarpus microphyllus* leaves and quinine from Cinchona Bark, among many others [167]. Natural proteins obtained from plant and animal sources have been used in drug and gene delivery systems, including hydrogels, nanocarriers and nanoparticles [445, 446]. Moreover, natural lipids were also used in cosmetics, pharmaceuticals, and nutritional supplements. They include oils obtained from plants and animals, natural fats, waxes, and phospholipids [447]. For instance, natural retinoids, carotenoids, and tocopherols were employed in medicinal applications due to their antioxidant properties [448–450]. Glycosaminoglycans, including hyaluronic acid (HA) and chondroitin sulfate (CS), are highly employed compounds in pharmaceutical and medical applications. They are natural hydrophilic polysaccharides with valuable therapeutic properties as they play an important role in the hydration and the elastoviscosity of tissues [174, 175]. They display non-immunogenic and biocompatible effects that increase their application in diverse formulations. Their isolation from natural terrestrial and marine sources has been extensively studied, as they present great advantages for their industrial application [165, 174, 451]. These include animal cartilage, fish bones (such as codfish, spiny dogfish, salmon, and tuna), animal eyeballs and invertebrate species, such as squid and mollusc bivalve [165, 220, 234, 240]. Hence, a considerable amount of the inedible parts of fish by-products is discarded globally from processing industries, which includes skin, trimmings, heads, fins, and viscera [160, 442]. Marine by-products are mainly used as a source of several bioactive compounds, such as proteins (collagen and gelatin), fatty acids, minerals (calcium phosphate and hydroxyapatite), enzymes (pepsin, collagenases, trypsin and chymotrypsin) [452].

Deep eutectic solvents (DES) were widely employed as alternative solvents to isolate bioactive compounds [117]. DES are green solvents used in several applications as they present promising advantageous characteristics due to their low-cost, low- to non-toxicity and biodegradability for environmental-friendly processes [7, 8, 13]. They are defined as novel eutectic mixtures having a lower melting point than the pure substances used to prepare them, which is caused by the complexation of the hydrogen bond acceptor and hydrogen bond donor molecules in the system [453]. They present a wide combination of compounds for their preparation at a diverse tunability [131, 434]. This has allowed the optimization of the processes that employ these

solvents to enhance the yield, solubility, and selectivity, among different physicochemical properties of interest, depending on the application [24, 25]. Previous studies have shown the potential uses of versatile DES in various applications [13], including the pre-treatment, purification, extraction, recovery and preparation of materials from natural sources [10, 36, 454]. For instance, they demonstrated to be potential novel solvents in the extraction of bioactive compounds, including proteins, carbohydrate polymers, phenolic compounds, flavonoids, and fatty acids, among others [49, 64, 65, 455].

In this work, the selected by-products as a source of bioactive molecules were codfish bones (CB), mussel meat (MM) and tuna vitreous humor (TVH). These materials are abundantly discarded in fishery processing industries, either because they are not edible, or not safe for human consumption [456–458]. Hence, various methods were developed for the efficient extraction of valuable ingredients from biomass sources [165]. Terpene- and lactic acid-based DES were prepared in order to be used for the isolation of extracts from marine raw material as a potential technique to obtain bioactive natural compounds, including proteins, lipids and minerals. The extraction using these novel solvents is compared to conventional methods used for the extraction of the mentioned compounds, to evaluate their viability as an alternative extraction approach.

2. Materials and methods

2.1. Materials

Codfish bones were kindly donated from Pascoal & Filhos (Nazaré, Portugal), mussels from Testa & Cunhas (Nazaré, Portugal), and tuna eyes from Tunipex (Faro, Portugal). Tuna eyes were kept frozen until cut, to separate the vitreous humor from the eyeball.

The chemical reagents used for the extraction process were the following: DL-lactic acid (aqueous solution, 85.0-90.0 %, CAS: 50-21-5), thymol (CAS [89-83-8], ≥98 %) and L-borneol (CAS [464-45-9], ≥97 %)) from Alfa Aesar, MA, USA. DL-menthol (CAS [89-78-1], ≥95 %), DL-camphor (CAS [76-22-2], ≥96 %)), D-fructose (CAS: 57-48-7), urea (CAS: 57-13-6), chondroitin disaccharide (di-6S) sodium salt (CAS: 136144-56-4), chondroitin disaccharide (di-4S) sodium salt (CAS: 136132-72-4), Chondroitinase ABC from Proteus vulgaris (CAS: 9024-13-9), and Papain from papaya latex (≥10 units/mg protein, CAS: 9001-73-4) were obtained from Sigma-

Aldrich, MA, USA. Hyaluronic acid disaccharide (di-HA, CAS: 149368-06-9) from Santa Cruz Biotechnology, Inc., Dallas, Texas, USA.

The reagents used in NaDES and extracts characterization were the following: 2,2-Dimethyl-2-silapentane-5-sulfonate (DSS, CAS: 2039-96-5), deuterium oxide (D_2O, CAS: 7789-20-0), chloroform (CAS: 67-66-3), hydrochloric acid (≥ 37 %, CAS: 7647-01-0), sodium chloride (CAS: 7647-14-5), disodium hydrogen phosphate (CAS: 7558-79-4), sodium tetraborate (99 %, CAS: 1330-43-4), Trizma® base (≥ 99.9 %, CAS: 77-86-1), glycine (≥ 99 %, CAS: 56-40-6), sodium dodecyl sulfate (≥ 99 %, CAS: 151-121-3), Folin & Ciocalteu's Phenol Reagent (2N, CAS: 12111-13-6) were obtained from Sigma-Aldrich, MA, USA. Methanol (≥ 99.8 %, CAS: 67-56-1) from Carlo Erba Reagents, Val de Reuil, France. Sodium phosphate (96 %, CAS: 7601-54-9) from Aldrich, MA, USA. Sodium hydroxide (98%, pellets, CAS: 1310-73-2) from Acros Organics, Geel, Belgium. The reagents used to prepare the complex-forming reagent of Lowry's method are the following: sodium carbonate (anhydrous, CAS: 497-19-8) from Panreac, Barcelona, Spain. Copper(II) sulfate pentahydrate (> 99 %, CAS: 7758-99-8) from Acros Organics, Geel, Belgium. Potassium sodium tartrate tetrahydrate (≥ 99 %, CAS: 6381-59-5) and bovine serum albumin (≥ 96 %, CAS: 9048-46-8) from Sigma-Aldrich, MA, USA.

2.2. DES preparation

The DES were prepared by mixing and heating (at 80 °C) for 15 minutes to ensure the formation of a homogenous liquid. The compounds were combined at specific molar ratio (Table 19), based on the literature for lactic acid-based DES [75, 406–408], and based on the studies done in Chapter II for the terpene-based DES.

Table 19: Molar ratio of the prepared deep eutectic systems (DES).

DES	Molar ratio
Men:Bor	7:3
Thy:Cam	1:1
Lac:Fru	5:1
Lac:Ur	4:1

2.3. Extraction process

All three raw materials were freeze-dried and codfish bones were ground to a particle size less than 1 mm. The scheme of the extraction process is shown in Figure 8. Briefly, the raw materials were mixed with the DES at a component mass ratio of 1:100 of raw materials:DES and stirred for 24 h at 50 °C. To collect the dissolved extracts in the solvents, the mixture was first centrifuged at 6000 rpm for 15 min at 45 °C to separate the undissolved particles and collect the supernatant. These supernatants represent the samples of the soluble fractions (SF) of the raw materials in Lac:Fru ($SF_{Lac:Fru}$) and in Lac:Ur ($SF_{Lac:Ur}$). Extract precipitation was done by the addition of 3 volumes of ethanol. The precipitate was then collected by centrifugation at 6000 rpm for 15 min at 45 °C and the samples represent the precipitated extracts (PE): $PE_{Lac:Fru}$ and $PE_{Lac:Ur}$.

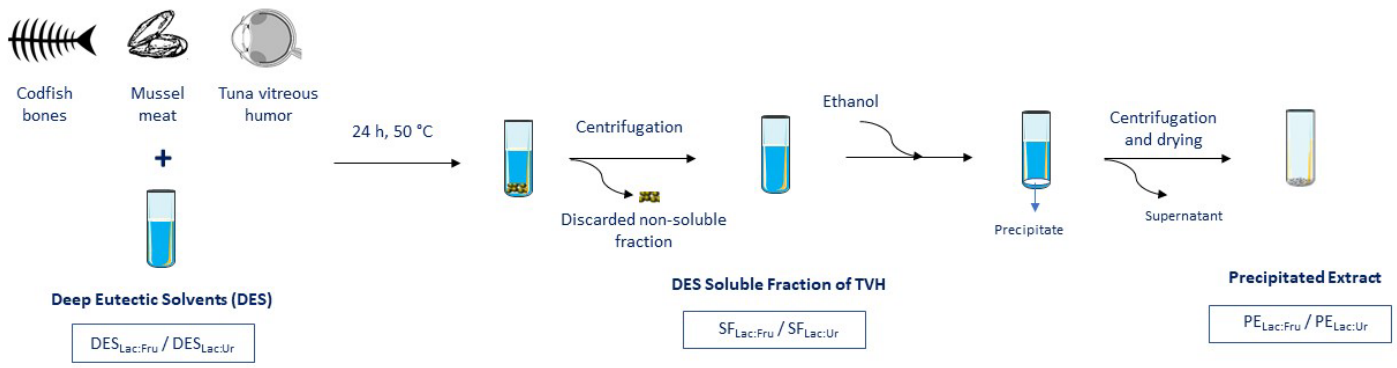

Figure 8: Scheme of the extraction process.

2.4. Biomass characterization

Biomass was characterized in terms of HA, CS, protein, lipids and ash content. The lipids were extracted based on the Bligh & Dyer technique [459], in order to quantify them. The proteins were extracted according to a previously described method with slight modifications [460, 461], briefly 1 g of freeze-dried raw material was suspended in 100 mL of ultrapure Milli-Q water. Ultra-sonication was then done for 2 h, and the sample was stirred at 4 °C overnight using a magnetic stirrer plate. The solution was then centrifuged at 4500 rpm for 30 min and the supernatant was collected and stored at 4 °C. The pellet fraction was re-suspended in 20 mL of Milli-Q water and subjected again to ultrasonication and stirring as described above. The sample was then

centrifuged, and the supernatant was pooled together with the initial supernatant and mixed with 80 % (w/v) of ammonium sulfate saturation and stirred at 4 °C during 1 h. Centrifugation was done to precipitate and collect the protein fraction. Following this, the precipitates were dialyzed at 4 °C for 24 h against Milli-Q water using a 10 kDa molecular weight cut-off dialysis tubing (Snake Skin™ Dialysis Tubing, Fischer Scientific, USA). The total protein content was analyzed according to the Lowry method [462]. It is a biochemical calorimetric assay used to determine the total amount of protein in a solution [462]. In brief, a complex-forming reagent was prepared according to a previously reported procedure [463]. An amount of 0.2 mL of the testing samples was added to 1 mL of freshly prepared complex-forming reagent. They were then vortexed and left at room temperature for 10 min; 0.1 mL of Folin reagent (1 N) was then added and vortexed. The mixture was kept protected from light at room temperature for 30 min and the absorbance was obtained at 750 nm (GENESYS™ 10S UV-Vis Spectrophotometer, Boston, MA, USA). The experiments were done in duplicate.

The ash content of the samples was determined by placing them in crucibles and heating them in a high-temperature muffle furnace (Nabertherm, Germany) type LT 15/13, provided with a C450 Controller. The muffle furnace was run for 4 h at a temperature of 550 ºC.

HA and CS were quantified in the raw materials. For CB and MM, papain was used for the enzymatic hydrolysis of the raw materials [234]. Briefly, 5 g of raw materials were solubilized in 50 mL acetone to ensure the de-fatting of the tissue. They were then centrifuged and dried at 50 ºC for 24 h. Then 1 g of raw material was solubilized in 10 mL of 100 mM sodium acetate buffer (pH 5.5) containing 5 mM EDTA and 5 mM cysteine. 60 mg of the enzyme papain was then added and stirred at 60 °C. After 24 h, the solution was boiled to de-nature the enzyme during 10 min. Centrifugation at 6000 rpm at 30 °C for 15 min was done and ethanol saturated with sodium acetate were added to the supernatant at a volume 3 times the volume of the supernatant. The precipitate was then recovered by centrifugation and dried at 50 ºC for 6 h. To extract HA from the freeze-dried TVH, the raw material was dissolved in distilled water at 25 ºC for 3 h to ensure the dissolution of the aqueous fraction of the vitreous humor, which includes the HA. The samples were then hydrolyzed enzymatically to quantify HA and CS using high-performance liquid chromatography (HPLC, Waters Alliance 2695 HPLC System, Waters Chromatography, Milford, MA) and capillary electrophoresis (CE) (P/ACE MDQ Capillary Electrophoresis System, Beckman

Coulter, CA, USA). The long chain biopolymers were hydrolyzed into their disaccharide unit using the enzyme Chondroitinase ABC. The hydrolysis was done by treating 40 µg of the sample with 25 mU of chondroitinase ABC in a 1 mM sodium phosphate buffer at pH = 7 at 37 °C for 3 h [464]. The sample was then boiled for 1 min to block the enzyme. HA and CS analyzed disaccharide units are shown in Table 20.

As the HA disaccharide di-HA (D-glucuronic acid and N-acetyl-D-glucosamine) and the CS non-sulfated disaccharide di-0s (GlcAβ1-3GalNAc) have a similar chemical structure with a hydroxyl group being axial for di-0s and equatorial di-HA, they were quantified using CE. The CE was equipped with an uncoated fused-silica capillary tube (85 cm, Sciex, ref. 338472) and UV detection was performed at 230 nm. The buffer was prepared using 40 mM disodium hydrogen phosphate, 10 mM sodium tetraborate and 40 mM sodium dodecyl sulfate at a pH of 9 adjusted using 1 M HCl and 1 M NaOH. The detection limit was found to be 3 µg/mL for both di-0s and di-HA.

The two CS disaccharides sulfated at different positions di-4s (GlcAβ1-3GalNAc(4s)) and di-6s (GlcAβ1-3GalNAc(6s)) were quantified using HPLC by the application of an isocratic separation (0.05 M NaCl pH 4) for 5 min. A linear gradient was then applied from 5 to 25 min (0.05 to 1.2 M NaCl pH 4), followed by 10 min of isocratic separation (0.05 M NaCl pH 4). The flow rate was set at 1.2 mL/min. The calibration curve was obtained using the di-4s and di-6s standards at concentrations ranging from 2.5 to 40 µg/mL with two-fold serial dilutions. The HPLC limit of detection was found to be 0.125 µg/mL for di-4s and 0.25 µg/mL for di-6s. Experiments were done in triplicate and the HPLC analysis in duplicate.

Table 20: The chemical structure of hyaluronic acid and chondroitin sulfate disaccharides.

Biopolymer	Disaccharide name	Chemical structure of the disaccharide	Systematic name
Hyaluronic acid	di-HA	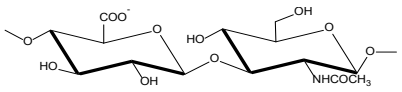	D-GlcA-*β*1-4-D-GalNAc-α1-4
Chondroitin sulfate	di-0s	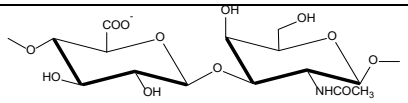	GlcA*β*1-3GalNAc
	di-4s	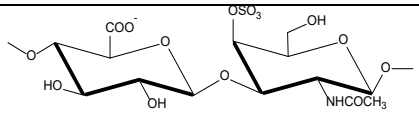	GlcA*β*1-3GalNAc(4s)
	di-6s	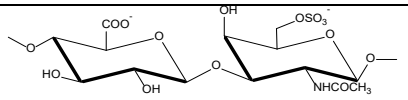	GlcA*β*1-3GalNAc(6s)

2.5. Extracts characterization

The total protein content in the extracts was determined according to Lowry's method [45]. The experiments were done in duplicates. Lipids, ash, HA and CS were quantified according to the method shown in section 2.4. The molecular weight of the proteins in the extracts samples was determined using SDS–PAGE, carried out using 7.5% Mini-PROTEAN ® TGX™ Precast Gels (Bio-Rad). The Laemmli running buffer was prepared using 25 mM Tris, 190 mM glycine and 0.1 % sodium dodecyl sulfate. Coomassie blue (Bio-Rad) was used as the staining material and Precision Plus Protein™ Dual Xtra Prestained Protein Standards (Bio-Rad) as the standard. The run was carried out according to the manufacturer's instructions.

3. Results and Discussion

3.1. Extraction yield

The extraction was done using two different types of DES: lipophilic terpene-based and hydrophilic lactic acid-based DES. The extraction yield using each solvent is shown in Table 21. Based on these results, it can be concluded that the yield of the extracts obtained using the

terpene-based DES ranges from 0.6 to 1.9 % (w/w), while it ranges from 9.1 to 22.5 % (w/w) for extracts obtained using lactic acid-based DES. Hence, the latter were able to extract a higher percentage of bioactive compounds from the raw material and the extracts composition was analyzed. In addition, as the compounds used for the lactic acid-based DES are hydrophilic, they have a higher tendency in isolating target hydrophilic compounds, including HA and CS.

Table 21: Extraction yield % (mg extract/ 100 mg raw material) using terpene- and lactic acid-based DES.

	Terpene-based DES		**Lactic acid-based DES**	
	Men:Bor	**Thy:Cam**	**Lac:Fru**	**Lac:Ur**
Codfish bones	0.6 ± 0.2	1.6 ± 0.7	9.1 ± 1.3	10.7 ± 2.1
Mussels	1.3 ± 0.6	1.5 ± 0.1	19.3 ± 1.8	22.5 ± 1.9
Tuna vitreous humor	1.4 ± 0.4	1.9 ± 1.1	13.1 ± 1.7	15.3 ± 1.6

3.2. Extracts characterization

The chemical composition in HA, CS, lipids, proteins, and ash per 100 mg extract is displayed in Figure 9 and their yield per 100 mg raw material is shown in Table 22. According to the results, proteins present the highest content in the obtained extracts. For CB, proteins percentage is 53.12 and 57.63 % of the extracts (corresponding to 5.07 and 6.70 mg proteins/ 100 mg raw materials) using Lac:Fru and Lac:Ur, respectively. A much higher ash content was determined from this raw material in comparison to lipids. The amount of HA and CS in the extracts obtained using DES were lower than the detection limit. Their content in CB was 0.26 mg HA + CS/ 100 mg raw material. According to the results, Lac:Ur was shown to be most suitable for the extraction of proteins from CB, as it was able to extract around 1/6 of the total proteins from this raw material. Furthermore, when comparing the extracts content with the raw material composition (Table 5), it can be concluded that the bones contain mainly ash (54.35 %), followed by proteins (38.59 %). Previous studies demonstrated that 81.09 to 84.88 % of proteins was present in fish bones [465], and 39.43 and 58.01 % of ash and proteins, respectively [466]. These

results vary depending on different factors that can contribute to the variation in chemical composition of these raw materials, such as the local of capture, season, nutrient intake, among others. In addition, it is generally possible to find leftover of meat and proteins with the bones, as when the meat is separated for commercial use, there could be some meat that remains with the discarded bones.

In the extracts obtained from MM, a higher percentage of proteins was obtained in comparison to the extracts obtained from the other raw materials, with a value of 66.11 and 75.20 mg/ 100 mg extract using Lac:Fru and Lac:Ur, respectively. The characterization of this raw material showed that it was mainly composed of proteins (51.32 %), followed by ash (17.57 %) and lipids (15.41 %). As previously discussed also the chemical composition of this raw material is highly variant based on seasonal and geographical factors [467]. For this raw material, Lac:Ur was also the more suitable DES to extract the highest yield of protein, as it isolated around 1/3 of the total protein present in MM. In addition, the HA and CS content in the isolated extracts was 0.32 and 0.43 µg HA and CS/ 100 mg of mussels using Lac:Fru and Lac:Ur, respectively. The HA and CS content in the extracts obtained using the conventional method is shown to be higher than the yield of DES extraction. Since this method involves the use of an enzyme and more organic solvents, it could lead to a higher capacity in hydrolyzing the tissues to isolate the target compounds [234].

	(A) Extracts obtained using Lac:Fru	(B) Extracts obtained using Lac:Ur
Codfish bones:	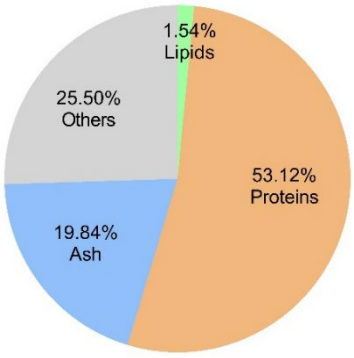	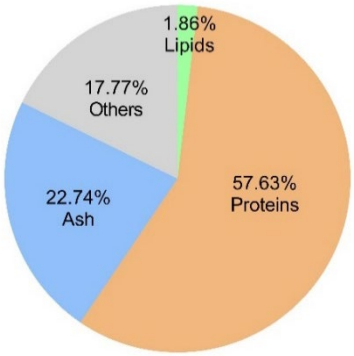
Mussel meat:	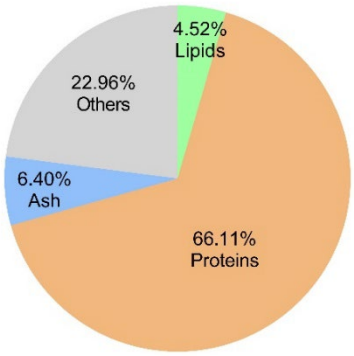	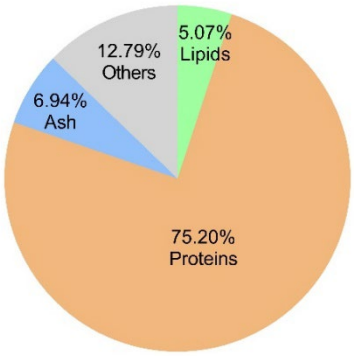
Tuna vitreous humor:	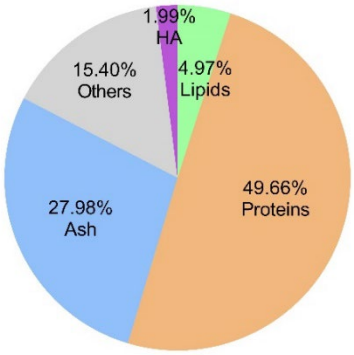	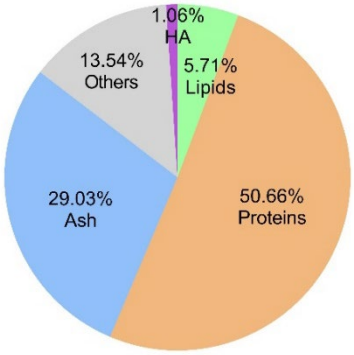

Figure 9: Percentage composition (mg/ 100 mg extract) of lipids, proteins, ash and hyaluronic acid (HA) in the extracts obtained from the raw materials using natural deep eutectic solvents Lactic acid:Fructose (Lac:Fru), Lactic acid:Urea (Lac:Ur).

The extracts obtained from TVH were composed of 50 % proteins in the extracts using both DES, equivalent to 5.16 and 7.43 mg protein/ 100 mg tuna vitreous humor using Lac:Fru and Lac:Ur, respectively. Hence, these DES were able to extract around half of the total proteins present in TVH. Consequently, Lac:Ur had the highest capacity to extract proteins from all raw materials used. In addition, the ash content was shown to be 27.98 and 29.03 % of the extracts using Lac:Fru and Lac:Ur, respectively, which are higher than the amount of lipids isolated in these extracts. The HA content was 1.99 and 1.06 % (3.3 and 2.1 µg HA/ 100 mg of tuna vitreous humor) using Lac:Fru and Lac:Ur, respectively. These values are higher than those of the extracts obtained from the remaining raw materials. The characterization of the TVH showed that it was mainly composed of ash (62.26 %), followed by proteins (14.31 %), lipids (8.06 %), and HA (8.62 %). By comparing these results to previous studies, it can be concluded that the composition varied as the amounts were 50.78, 30.89, 7.32 and 10.99 % of ash, protein, lipids, and HA, respectively [468, 469]. For all raw materials, the extracts isolated using both DES contained other remaining compounds, which could include additional carbohydrate polymers and polysaccharides isolated using DES [8, 10, 64].

Table 22: Concentration (mg/ 100 mg raw material) of HA, CS, lipids, proteins, and ash in the extracts obtained from the raw materials using Lac:Fru and Lac:Ur.

		$PE_{Lac:Fru}$	$PE_{Lac:Ur}$	Raw materials characterization
CB	**Σ (HA+CS)**	< d. l.	< d. l.	0.26 ± 0.04
	Lipids	0.14 ± 0.03	0.18 ± 0.03	2.60 ± 0.95
	Proteins	5.07 ± 0.02	6.70 ± 0.14	38.59 ± 4.17
	Ash	1.87 ± 0.04	2.63 ± 0.27	54.35 ± 0.24
MM	**Σ (HA+CS)**	0.00032 ± 0.00003	0.00043 ± 0.00004	1.33 ± 0.19
	Lipids	0.82 ± 0.15	1.08 ± 0.03	15.41 ± 2.09
	Proteins	13.99 ± 0.43	18.21 ± 0.36	51.32 ± 2.78
	Ash	0.83 ± 0.25	1.17 ± 0.39	17.57 ± 0.50
TVH	**HA**	0.0033 ± 0.0017	0.0021 ± 0.0005	8.62 ± 0.63
	Lipids	0.52 ± 0.06	0.59 ± 0.14	8.06 ± 1.42
	Proteins	5.16 ± 0.15	7.43 ± 0.25	14.31 ± 1.62
	Ash	3.94 ± 0.22	4.77 ± 0.33	62.26 ± 0.46

SDS-PAGE analysis was performed to evaluate the distribution of the molecular weight of the proteins extracted from all raw materials using Lac:Fru and Lac:Ur, as shown in Figure 10. By comparing the results to the reference protein standard, it can be seen that none of the extracts is rich in any particular molecular weight proteins, as all extracts contain a varying and unspecific molecular weight distribution of protein from 2 to 250 kDa. This could be due to their hydrolysis during the extraction process at 50 ˚C during a long period of 24 hours. Hence, as a conclusion, the lactic acid-based DES efficiently extracted bioactive compounds with varying composition, depending on the raw material and DES used, and their bioactivity will be further analyzed to confirm their safety in potential therapeutic applications.

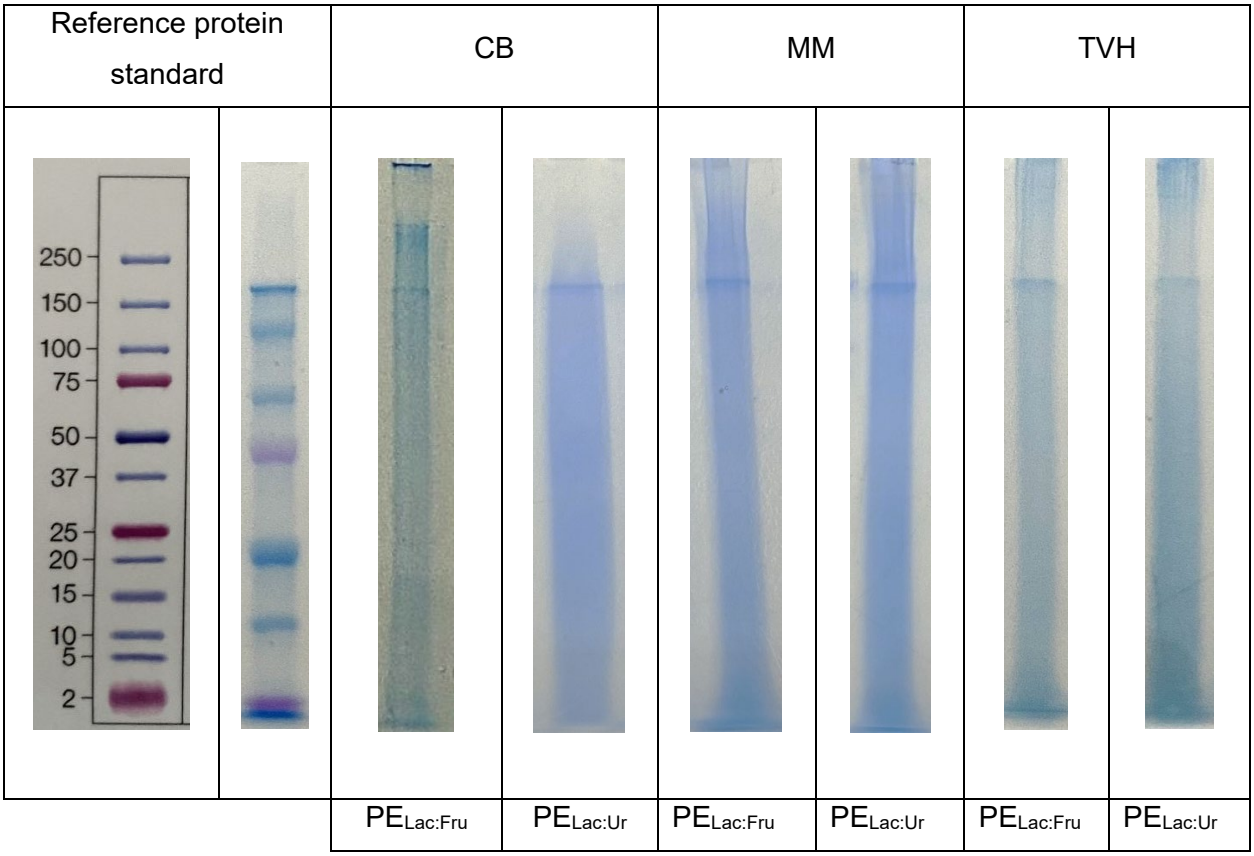

Figure 10: SDS-PAGE analysis of extracts obtained from each raw material using Lac:Fru and Lac:Ur, compared to reference protein standard.

4. Conclusions

DES were prepared for the extraction of bioactive compounds as a novel green technique for marine waste valorization. They were prepared using natural compounds: Men, Thy, Borm, Cam, Lac, Fru, and Ur. The use of DES has different advantages to the use of conventional extraction methods, including the elimination of enzymes and/or organic solvents, decrease of process time and cost. A higher yield was obtained from the extraction process using lactic acid-based DES in comparison to terpene-based DES. Proteins were shown to be the main components of these extracts. In general, lactic acid-based DES have a higher capacity to isolate proteins, as the extracts contained up to half of the total proteins present in all raw materials. The amounts differed based on the raw materials used, as the extraction from bones had the lowest

yields due to their dense structure. Extracts obtained from all raw materials were composed of both ash and lipids. HA was mainly extracted from the tuna vitreous humor using both DES, at a very low concentration yield in comparison to the conventional extraction methods. Furthermore, the extracted ash and lipids amounts using both Lac:Fru and Lac:Ur were low in comparison to the amounts of ash present in the raw materials. As for HA and CS, the isolated amounts are negligeable, as the conventional method extractions demonstrated a higher content in these biopolymers in comparison to the extracts. In addition, the extracts composition highly differs, depending not only on the DES used, but also on the structure and composition of the raw material used. Further biocompatibility studies will be performed to evaluate the use of the compounds obtained from the extraction process in potential therapeutic applications.

Chapter IV:
Bioactivity evaluation of compounds obtained from the extraction process using deep eutectic solvents

This chapter was published by MDPI as:

Abdallah, M. M., Leonardo, I. C., Krstić, L., Enríquez-de-Salamanca, A., Diebold, Y., González-García, M. J., Gaspar, F. G., Matias, A. A., Bronze, M. D. R., & Fernández, N. (2022). Potential Ophthalmological Application of Extracts Obtained from Tuna Vitreous Humor Using Lactic Acid-Based Deep Eutectic Systems. Foods, 11(3), 342.
DOI: 10.3390/foods11030342

Abstract

Deep eutectic solvents (DES) were used to extract bioactive compounds from codfish bones (CB), mussel meat (MM), and tuna vitreous humor (TVH) for its potential application in the management of dry eye disease. The DES, the soluble fraction of the raw material in DES (SF) and the precipitated extracts (PE) were evaluated to assess their biocompatibility. Preliminary studies were done on Caco-2 cell line, and the results showed that TVH soluble fraction in DES was the most viable to the cells. Hence, this raw material was selected for further studies on human corneal epithelial (HCE) cell line. Oxygen radical absorbance capacity (ORAC) assay was done to chemically assess the antioxidant effect of the compounds. In vitro experiments on human corneal epithelial cell line and the effect on dry eye-associated microorganisms were performed. The influence of the samples on the HCE viability, their intracellular reactive oxygen species (ROS) scavenging capacity and inflammatory response, and antimicrobial properties were studied. According to the results, all samples displayed an antioxidant effect using chemical and cell-based studies, which was significantly higher for PE in comparison to SF. Most of the tested samples did not induce an inflammatory response in cells, which confirmed the safety in ophthalmic formulations. In addition, the DES and SF proved to be efficient against the studied bacterial strains, while PE did not show an antimicrobial effect. Hence, both DES, SF at defined concentrations could be used as potential compounds in dry eye disease management.

Keywords: food waste valorization, natural hyaluronic acid, deep eutectic solvents, ocular therapy, antioxidant, anti-inflammatory, antimicrobial.

1. Introduction

Nowadays, the trend of seeking ingredients from natural sources is on the rise as companies are more committed to a sustainable development of green products [1]. The use of marine by-products as a source of natural ingredients has attracted a great attention due to abundance, low-cost, safety and environmental benefit [2]. The total mass of world marine obtained from fisheries and aquaculture was estimated to be 170.9 million tons in 2016 in contrast to 151.2 million tons of human consumption [3]. Thus, a significant amount of marine wastes is

generated annually, which are commonly dis-carded on land or in the sea and they contaminate the coastal water and air [4]. There-fore, their use as a source for the extraction of natural compounds has great advantages in waste valorization and natural ingredients isolation. The Food and Agricultural Organization refers to food waste as the disposal of inedible food fractions along the entire food production and distribution chain [5]. Some of these wastes were classified as avoidable food waste, depending on the causes that lead to its generation and that could be prevented. Hence, the use of the inedible food wastes as a source of bioactive molecules for drug formulation is of high value with environmental and therapeutical benefits.

There have been various techniques for the efficient extraction of materials from biomass sources, including the use of novel deep eutectic solvents (DES) [6]. These solvents are formed by combining hydrogen bond donor and acceptor molecules, and are characterized by having a melting point lower than that of the compounds used to prepare them [7]. They have shown to be promising molecular solvents due to their advantageous tunability, that allows the optimization of their solubilizing capacity, viscosity, among other different physicochemical properties of interest depending on their application [8, 9]. Previous studies and ongoing research have shown various potential use of versatile combinations of DES in pharmaceutical, biochemical and other industrial applications [10]. One of the most important roles of DES is their multifunctional role in solubilization, extraction, purification, and production of valuable products from biomass [11, 12].

In this work, DES were prepared using lactic acid, fructose and urea for the extraction of hyaluronic acid (HA) from the marine raw material codfish bones (CB), mussel meat (MM), and tuna vitreous humor (TVH). The use of DES replaces the time consuming and/or toxic conventional methods to extract natural HA. Various techniques have been applied for the extraction of HA from natural sources, such as terrestrial and marine biomass [6, 13, 14]. Preliminary HA solubility studies were done with different combinations of natural DES previously described in the literature [406, 408, 470]. Lactic acid-based systems were the most promising in dissolving HA. Therefore, DES were prepared by combining lactic acid with fructose and urea as they are natural, low-cost, and non-toxic compounds that have been applied in several drug formulations and therapeutical applications [471–473]. Lactic acid is a carboxylic acid widely employed in formulations due to its biobased and biodegradable features and was already described to enhance the stability and the shelf life of Miconazole eye drops [473–475]. On the

other hand, fructose is a naturally occurring monosaccharide that has been used in the food and pharmaceutical industries. It has been employed as an excipient in drug formulations due to its safety [472, 476]. Also, it was shown to be present in the eye, mainly in the aqueous humor and the stroma, obtained by the sorbitol pathway in the lens [477, 478]. Additionally, urea is an endogenous metabolite used in drug formulations for the treatment of skin and ocular diseases, hyponatremia, malignancy, among others [471, 479–481]. It is a compound formed in ocular tissues and is an important constituent of the tear fluid, as lower urea levels are observed in the tear film of patients with dry eye [482, 483]. Considering the relevance and applicability of these compounds, two distinct DES were prepared in this work combining lactic acid with either fructose or urea (Lac:Fru and Lac:Ur, respectively). DES were used for the extraction of HA from the raw material, a natural marine by-product that is abundantly discarded. This method could not only ensure the use of natural HA for a therapeutic purpose, but also implement the valorization of the discarded raw material in a green and low-cost process using DES. HA is a highly valuable biopolymer that has shown increased use in pharmaceutical formulations, namely in tear formulations for dry eye treatment [364]. It is a hydrophilic molecule with an important role in preserving the hydration and the elastoviscosity of tissues, such as the vitreous humor and the synovial fluid, and in lubricating numerous moving parts, such as the muscles and the joints [15]. Its non-immunogenic and biocompatible effects have significantly increased its application in the pharmaceutical and medical fields, including joint injections, osteoarthritis treatment, ocular therapy, plastic surgeries and skin treatments [16]. In recent years, HA has been increasingly used in formulations for patients suffering from the dry eye disease, as it has shown to improve the corneal epithelial barrier and the tear film stability [17–20]. Dry eye is a highly prevalent inflammatory disease in which ocular surface epithelia and the tear film are altered, leading to visual impairment, discomfort, eye dryness, burning and pain [1–3]. Tear production stimulation and tear replacement agents have been used for symptom's relief, including the HA-based artificial tears, which re-store the homeostasis of the tear film [18, 24]. In this work, DES and HA-containing samples were evaluated on Caco-2 cell line to obtain preliminary results regarding their biocompatibility. Following that, these compounds were tested on human corneal epithelial cells to study their potential use in ophthalmic formulations for the treatment of the dry eye disease. In addition, the antimicrobial effect of the samples was tested using dry eye-associated bacterial species, such as *Staphylococcus aureus* and *Pseudomonas aeruginosa* to assess

whether the samples may also reduce the bacterial growth, which would be helpful in the management of dry eye cases prone to infections.

2. Materials and methods

2.1. Materials

The reagents used in the extraction and chemical characterization processes were the following: ethanol absolute (≥ 99.9 %, CAS: 64-17-5, Carlo Erba Reagents, Val de Reuil, France), hyaluronic acid disaccharide (di-HA, CAS: 149368-06-9, Santa Cruz Bio-technology, Inc., Dallas, Texas, USA), DL-lactic acid (aqueous solution, 85.0 – 90.0 %, CAS: 50-21-5, Alfa Aesar, MA, USA), sodium phosphate (96 %, CAS: 7601-54-9, Aldrich, MA, USA. The reagents D-fructose (CAS: 57-48-7), urea (CAS: 57-13-6), Chondroitinase ABC from Proteus vulgaris (CAS: 9024-13-9) and sodium chloride (≥ 99 %, CAS: 7647-14-5) were obtained from Sigma (MA, USA).

The reagents used in cellular viability, antioxidant and anti-inflammatory studies were the following: non-essential amino acids (NEAA) and penicillin-streptomycin (PenStrep) were purchased from Invitrogen (Gibco, Paisley, UK). PrestoBlue® Cell Viability Reagent (Molecular Probes®) was obtained from Life Technologies (Oregon, USA). penicillin-streptomycin, insulin (CAS: 11061-68-0), epidermal growth factor (EGF, E9644, CAS: 62253-63-8), phosphate buffered saline (PBS), benzalkonium chloride (CAS: 8001-54-5), phenazine methosulfate (PMS, CAS: 299-11-6), fluorescein sodium salt (CAS: 518-47-8), and 2,2′-azobis(2-methylpropionamidine) dihydrochloride (AAPH, CAS: 2997-92-4) were obtained from Sigma (MA, USA). Dulbecco's Modified Eagle Medium (DMEM)/F-12 + GlutaMAX-I, fetal bovine serum (FBS), tetrazolium salt (2,3-bis-(2-methoxy-4-nitro-5-sulfophenyl)-2H-tetrazolium-5-carboxanilide, XTT, CAS: 298-96-4), the BCA protein kit, and DMEM/F12 without phenol red were obtained from Thermo Fischer Scientific (MA, USA). Cell permeant 2',7'-dichlorodihydrofluorescein diacetate (H_2DCF-DA) dye (CAS: 4091-99-0) was obtained from Merck Life Sciences (Germany). Tumor necrosis factor-α (TNF-α, CAS: 94948-59-1) and the IL-6 (REF 950.030.192) and IL-10 (REF 950.060.192) ELISA kits (Diaclone) were obtained from bi-oNOVA cientifica, S. L. (Madrid, Spain). (±)-6-hydroxy-2,5,7,8-tetramethylchromane-2-carboxylic acid (Trolox) was obtained from Fluka (Buchs, Swizterland).

The reagents used in the microbial studies were the following: cation-adjusted Mueller Hinton broth (CAMHB) was obtained from BD (Sparks, USA), trypticase soy agar (TSA) and trypticase soy broth (TSB) were obtained from VWR (PA, USA). Gram-positive bacteria *Staphylococcus aureus* ATCC 6538 and gram-negative bacteria *Pseudomonas aeruginosa* ATCC 9027 were selected for the antimicrobial susceptibility testing assays. Two commercially available eye drops were used: HYABAK®, with 0.15 % HA (Théa Pharmaceuticals, France), and Clorocil eye drop, with 8 mg/mL chloramphenicol (Edol Laboratory, Portugal).

2.2. Samples preparation

The raw material tuna eyes were kindly donated from Tunipex, Faro, Portugal. They were kept frozen and cut to separate the tuna vitreous humor (TVH) part from the eyeball. The frozen vitreous humor was then freeze-dried and kept stored at -20°C until needed.

The DES were prepared by combining the natural components under heating at 80 °C and stirring for 30 min until a homogeneous liquid system was obtained, as explained in Chapter II. The systems prepared were lactic acid:fructose (Lac:Fru) and latic acid:urea (Lac:Ur) at a molar ratio of (5:1) and (4:1), respectively.

The extraction process is then performed as has been described in Chapter III, section 2.3. The PE samples obtained from the extraction using DES were submitted to enzyme hydrolysis before quantification using high-performance liquid chromatography (HPLC) for quantification, as described in Chapter III section 2.5.

2.3. Bioactivity studies

2.3.1. Cellular viability

The two lactic acid-based DES and their corresponding SF and PE testing samples were first evaluated in vitro on non-differentiated and confluent Caco-2 cells. This cell line was employed as it displays characteristics with crypt enterocytes and has been widely implemented as a model to evaluate the effect of compounds on the intestinal function [484, 485]. The cytotoxicity of the samples was analyzed to study the potential use of the compounds in future therapeutic applications. The biocompatibility of the extracts was assessed by comparing the

cellular viability of NaDES with the SF samples, prior to the extract precipitation. The precipitated extracts were not evaluated due to their limited solubility in biocompatible solvents.

The assay was performed as has been previously reported with minor modifications [486]. In brief, the cells were seeded at a density of 2×10^4 cells per well of a 96-well plate. The medium (DMEM + 10% FBS, 1% PenStrep and 1% NEAA) was changed every 3 day and following 7 days of culture, the cells were confluent and were incubated for 24 h with the extracts at different concentrations diluted using the culture medium (DMEM + 0.5% FBS + 1% NEAA). In control wells, the cells were incubated with the culture medium only. After incubation, the medium was discarded, and the cellular viability was assessed using the reagent PrestoBlue® following the manufacturer protocol. The fluorescence was recorded using a FL 800 microplate fluorescence reader (BioTek Instruments, Winooski, VT, USA). Results were computed in terms of the percentage of cellular viability as a function of the control. The half maximal inhibitory concentration (IC_{50}) is a widely employed measure of the potency and efficacy of bioactive ingredients for pharmacological studies. It indicates the concentration required to inhibit by half the cytotoxicity of the compounds. It was assessed using the dose–response curves fit on GraphPad Prism software (Graph-Pad Software, Inc., La Jolla, CA). All the experiments were done in triplicate with at least two independent assays.

Following this preliminary study, the compounds were tested in vitro on HCE cell line [28]. The HCE cell line was cultured in DMEM/F-12 + GlutaMAX-I supplemented with 10 % fetal bovine serum, 10 ng/mL of EGF, 5 µg/mL of insulin, 100 U/mL of penicillin, and 100 µg/mL of streptomycin. The cells were kept in a 5 % CO2 atmosphere at 37 °C. The cellular viability was assessed using the XTT-based colorimetric assay. HCE cells were seeded in 96-well plates, starting with the 38th cell passage, and grown to 90 % of pre-confluence. After 24 h, the cells were maintained in a non-supplemented and serum-free medium for an-other 24 h. A stock solution of each compound was prepared in pure cell culture medium and filtered using sterile 0.2 µm filters. The prepared stock solution concentration was 12 mg/mL for the DES samples and 4 mg/mL for the SF and PE samples. Serial dilutions of the tested compounds were done in the plates. The cells with the treatments were kept for 24 h at 37 °C. Cells that were treated with the culture medium were used as the negative control, and cells treated with benzalkonium chloride (0.005% w/v dissolved in culture medium) were used as the positive control. To perform the XTT

colorimetric assay, 100 µL of DMEM/F12 without phenol red was added to each well, followed by a 25 µL of XTT and PMS mixture prepared prior to its use by adding 10 µL of PMS to the 1 mg/mL XTT solution. Incubation was done at 37 °C for 3 h. The absorbance was then assessed using a UV/Vis microplate multireader at 450 nm and 620 nm (SpectraMax M5; Molecular Devices, Sunnyvale, CA, USA). The experiments were done in triplicate for each condition. The percentage of viable cells in the treated cells in comparison to the control was computed using the following equation:

$$\%\ \text{cell viability} = \frac{\text{Abs}_{450\ \text{nm}}\ \text{sample} - \text{Abs}_{620\ \text{nm}}\ \text{sample}}{\text{Abs}_{450\ \text{nm}}\ \text{control} - \text{Abs}_{620\ \text{nm}}\ \text{control}} \times 100$$

2.3.2. Antioxidant effect

The antioxidant effect of the compounds was analyzed using the H_2DCF-DA dye to measure intracellular reactive oxygen species (ROS) levels in UV-B radiation exposed cells. This non-fluorescent dye diffuses in the cells and is cleaved into H_2DCF that is further oxidized to fluorescent DCF by the ROS. The HCE cells were cultured in 24-well plates and grown to 90 % of pre-confluence. They were then maintained in a medium that is serum- and supplement-free for 24 h at 37 °C. The cells were then pre-treated with the compounds for 1 h at 37 °C at specific concentrations selected based on the results obtained from the results of section 3.5.1. After pre-treatment, the supernatant was discarded and 500 µL of 10 µM dye was added to the cells, which were further incubated for another 30 min at 37 °C. The supernatant was discarded, and the cells were treated with the same treatments as in the pre-treatment step. They were then exposed to 8-W UV-B light for 15 sec, with the lamps located 3 cm below the cells, at 302 nm excitation peak and 7.15 mW/cm2 UV-B radiation power density (Bio-Rad, Inc., Hercules, CA, USA). The cells were then incubated for 1 h at 37 °C. The control cells were kept in incubation without UV-B light stimulation. The fluorescence was obtained using a spectrophotometer at 488 nm/ 522 nm (SpectraMax M5; Molecular Devices, Sunnyvale, CA, USA). The obtained data were normalized to the corresponding total protein content in the adherent cells using the BCA protein assay kit. The experiments were done in triplicate and the sample treatments were performed in duplicate.

Oxygen radical absorbance capacity (ORAC) assay was done to evaluate chemically the antioxidant effect of the samples. It was done based on a procedure previously reported [487]

and modified to adapt to FL 800 microplate fluorescence reader (BioTek Instruments, Winooski, VT, USA) [488]. Through this procedure, the evaluation of the antioxidant species capacity in the protection of the disodium fluorescein (FL) from the oxidation was done. The oxidation was catalyzed by peroxyl radicals that were generated from 2',2'-azobis(2-amidinopropane)dihydrochloride (AAPH). In brief, the samples were diluted in 75 mM PBS at pH = 7, and were mixed with 1.5×10-7 mM of FL in a final volume of 175 µL in total. The mixtures were then placed in a 96-well black microplate at 37 °C. The reaction was initiated by the addition of 25 µL AAPH to each well. The fluorescence that was emitted by the FL reduced form was measured using the microplate fluorescent reader and recorded every 1 min at an excitation wavelength of 485 nm and an emission wavelength of 530 nm during 40 min. The PBS was used as the blank, and the control standards were prepared using 10, 20, 30, 40, and 50 µmol/L of Trolox. Samples were analyzed at least in duplicates. The values of ORAC were expressed as Trolox equivalents antioxidant capacity (µmol TEAC/L) and were calculated by computing a regression equation between the concentration of Trolox and the area under the FL curve.

2.3.3. Evaluation of the potential inflammatory response

The potential inflammatory effect of extracted compounds on corneal epithelial cells was evaluated in vitro measuring cytokine/chemokine secretion after HCE cells stimulation using TNF-α. Similarly to previous studies, HCE cells were cultured in 24-well plates and grown to 90 % of pre-confluence, then maintained in a serum- and supplement-free medium for 24 h at 37 °C. The cells were then pre-treated for 2 h at 37 °C with the compounds at specific concentrations. Following this, TNF-α at a concentration of 25 ng/mL was added to the cells for 24 h. Cell supernatants were collected after 24 h, and interleukins IL-6 and IL-10 production quantified with human interleukins (IL-6 and IL-10) ELISA kits according to manufacturer's instructions. Interleukins' concentration in each well was normalized to total protein content determined by the BCA protein assay kit. The experiments were done in triplicate and the samples were performed in duplicate.

2.3.4. Statistical analysis

The statistical analysis of the biocompatibility studies on the HCE cell line was analyzed using the SPSS software package (SPSS version 15.0 for Windows; SPSS, Inc., Chicago, IL, USA). Results were expressed as mean ± standard error of the mean (SEM). One-way analysis of variance (ANOVA) with Tukey's post hoc test or Games-Howell test was used for intergroup comparisons. P values < 0.05 were considered statistically significant. GraphPad Prism software (GraphPad Software, Inc., La Jolla, CA) was used for the figures plotting.

2.3.5. Antimicrobial activity

The antimicrobial activity studies of the compounds were carried out using *S. aureus* and *P. aeruginosa*. The stock solutions of the DES, SF and PE testing samples were prepared by dissolving the samples at specific concentrations (shown in Table 23) in CAMHB. All samples were filter sterilized using 0.2 µm filters. The antimicrobial activity of the samples was compared to two commercially available eye-drops: an HA-based eye drop (HA-ED) used for ocular hydration and relief, containing 0.15 % HA, and the antibiotic chloramphenicol-based eye drop (CHL-ED) used to combat ocular infection, containing 8 mg/mL chloramphenicol.

The assay was performed based on the broth microdilution method according to the CLSI M07-A10 guidelines [489]. In brief, the bacterial suspensions were diluted using CAMHB and the optical density was standardized at 600 nm using Ultrospec 2100 pro (Biochrom, USA) to obtain a density equivalent to the 0.5 McFarland's standard. Standardized bacterial suspension (50 µL) were used to inoculate a 96-well microtiter plate wells containing 50 µL of a two-fold dilution series range of the testing sample, achieving a final bacterial density per well of 10^6 CFU/mL. The plates were incubated at a temperature of 37 °C for 16 – 20 h. Culture medium without any added compounds was used as a negative control, and bacterial culture without the addition of any agent was used as the positive control. The well having the lowest concentration with no visible bacterial growth observed corresponds to the minimum inhibitory concentration (MIC). In addition, the minimum bactericidal concentration (MBC) was determined by plating 100 µL from the wells with no growth on a TSA medium and incubating for 16 – 24 h at 37 °C. The MBC can be defined as the lowest concentration that killed at least 99.9 % of the bacteria over the period of the assay and is complementary to the MIC. Results of the MIC and MBC were expressed as the median

value obtained for each of the three replicates. A test was performed using a two-fold serial dilution of the samples with the addition of sterile medium to ensure their sterility.

Table 23: Concentration of the compounds in the samples studied for antimicrobial analysis.

	Composition of the stock solution					
Sample [a]	**[Lactic acid] (mg/mL)**	**[Fructose] (mg/mL)**	**[Urea] (mg/mL)**	**[Extract] (mg/mL)**	**[Hyaluronic acid in extract] (µg/mL)**	**[Chloramphenicol] (mg/mL)**
Lac:Fru	22.86	9.14	—	—	—	—
Lac:Ur	27.43	—	4.57	—	—	—
$SF_{Lac:Fru}$	22.80	9.12	—	0.08	10.72	—
$SF_{Lac:Ur}$	27.34	—	4.56	0.10	6.15	—
$PE_{Lac:Fru}$	—	—	—	2.00	0.30	—
$PE_{Lac:Ur}$	—	—	—	2.00	0.15	—
HA-ED [b]	—	—	—	—	1.50	—
CHL-ED [b]	—	—	—	—	—	0.50

3. Results and Discussion

3.1. Cellular viability

The biocompatibility studies of DES and SF samples obtained from CB, MM and TVH were evaluated and compared to study the potential therapeutic effect of the samples. PE were not tested due to limited solubility of the samples in the testing medium. The study was done in

the Caco-2 cell line as it has been shown to be considered an accepted model for biocompatibility evaluation [484, 490, 491]. Previous studies showed that the undifferentiated Caco-2 cell line has a higher sensitivity to the compounds that were tested in comparison to differentiated cells. Hence, this line can be considered as one of the most conservative models for characterization of hazards [491]. The IC_{50} results of the study done using this cell line was evaluated for extracts obtained from codfish bones, mussel meat, and tuna vitreous humor, as shown in Figure 11. Results showed that the IC_{50} value of Lac:Fru (6.39 mg/mL) was significantly lower than that of the $SF_{Lac:Fru}$ for for MM and TVH (8.92 and 12.74 mg/mL, respectively). Therefore, Lac:Fru was shown to be significantly less biocompatible than $SF_{Lac:Fru}$ due to lower IC_{50} values. As for Lac:Ur, the IC_{50} value (5.68 mg/mL) was comparable to that of the $SF_{Lac:Ur}$ of CB and MM (5.61 and 5.90 mg/mL, respectively) and lower than that of $SF_{Lac:Ur}$ of tuna vitreous humor (8.30 mg/mL). Hence, $SF_{Lac:Ur}$ of these raw materials were viable to the cells but did not show any significant increase of the biocompatibility of Lac:Ur. Therefore, the cellular viability differed based on the raw material from which the soluble fraction was dissolved, with TVH being the most viable. Hence, this raw material was selected for further studies on HCE cell line.

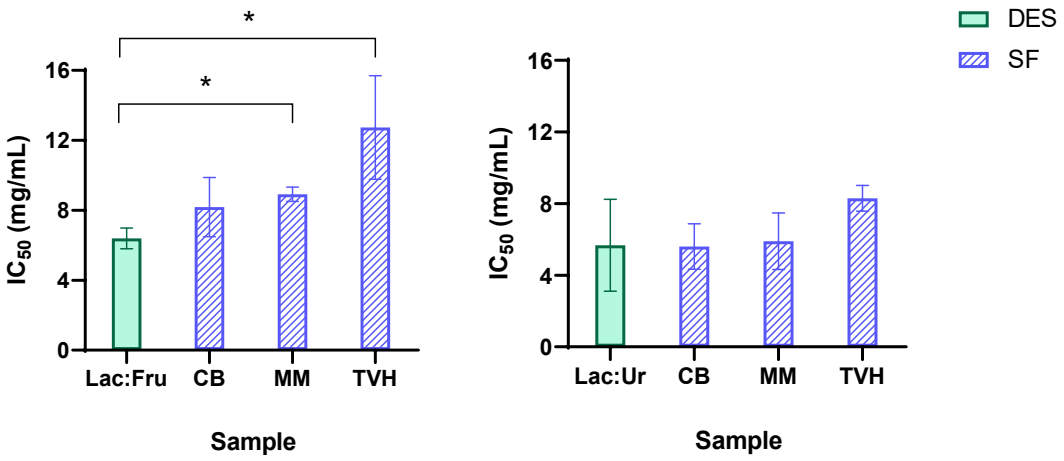

Figure 11: Half inhibitory concentration (IC_{50}) values on Caco-2 cell line of DES and SF testing samples of extracts obtained using the raw materials CB, MM and TVH.

The effect of each testing sample of the extraction process from TVH on cell viability of HCE cells was studied at different concentrations, as shown in Figure 12. Measurement of cell viability enabled the quantification of live cells numbers after treatment with the samples, which was expressed as a percentage relative to the control. The concentrations with 90 % of cell viability or higher (shown in dark grey bars in Figure 12) were considered within an acceptable range [48, 49]. These concentrations with higher or equal to 90 % viability were the ones selected for the antioxidant and inflammatory responses. The highest viable concentration for both DES was shown to be 1 mg/mL, and they displayed a higher value than that of the SF and PE samples. In addition, the SF samples had a higher or same concentration values in comparison to the PE samples. For instance, the highest viable concentration for $SF_{Lac:Fru}$ was 0.75 mg/mL, greater than that of the $PE_{Lac:Fru}$ (0.5 mg/mL). In contrast, $SF_{Lac:Ur}$ and $PE_{Lac:Ur}$ had the same highest viable concentration of 0.5 mg/mL.

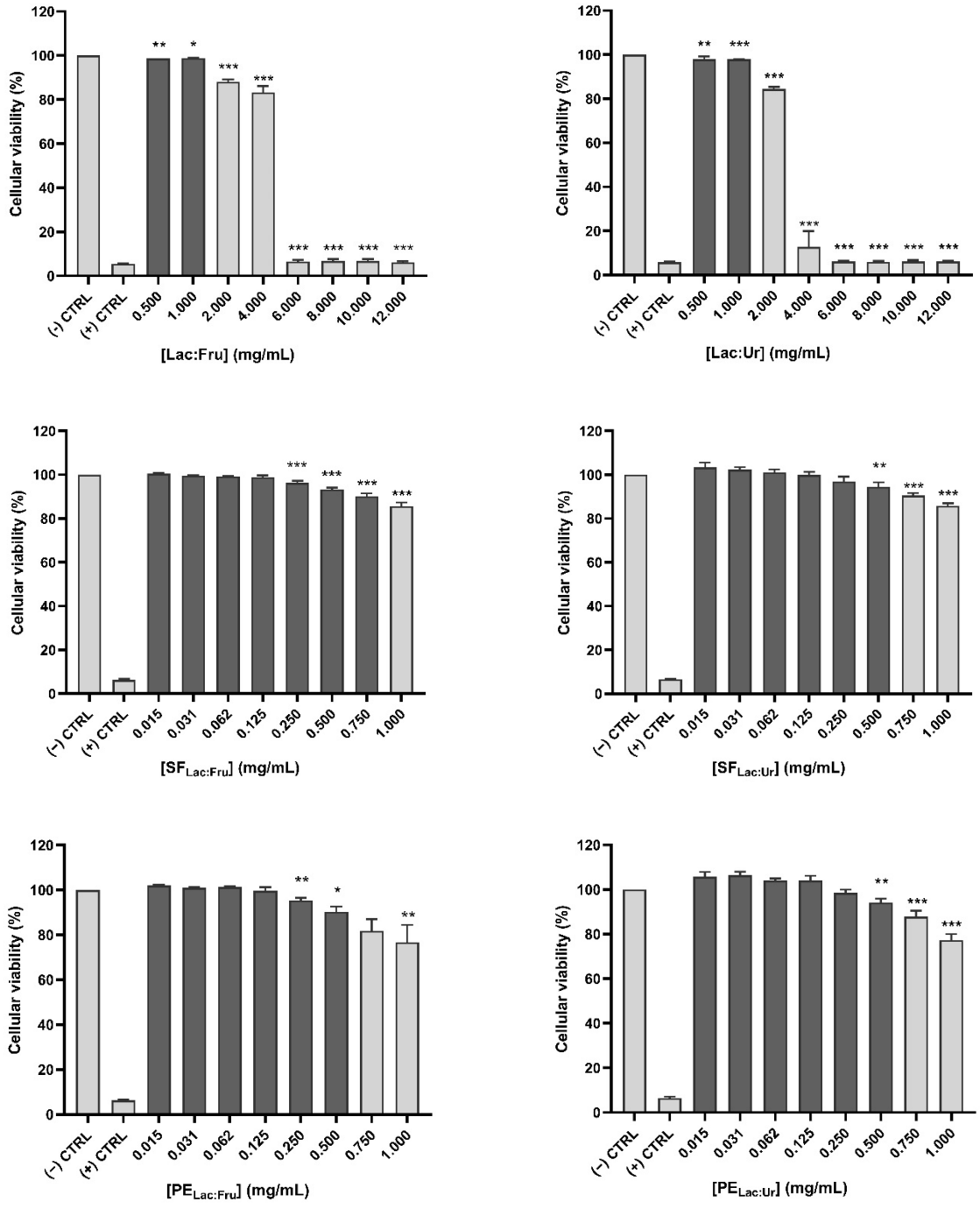

*Figure 12: Cellular viability (%) of HCE cell line after treatment with the testing samples. The concentrations with 90 % of cell viability or higher are shown in dark grey bars (*P < 0.05, **P < 0.01, ***P < 0.001).*

3.2. Antioxidant effect

The antioxidant effect of the samples was evaluated to analyze their potential use in ophthalmic therapy. Previous studies have demonstrated that HA-containing eye drops could decrease oxidative stress and inflammation, which consequently improves dry eye symptoms [50]. DES and SF samples were first analyzed using the ORAC assay to assess their antioxidant effect chemically. PE were not tested due to limited solubility in the testing medium. Based on the results in Table 24, the TEAC concentration of Lac:Fru and Lac:Ur was shown to be 0.47 and 0.30 µmol/mL, respectively. In contrast, the TEAC concentration of $SF_{Lac:Fru}$ and $SF_{Lac:Ur}$ ranged from 0.59 to 1.45 µmol/mL and 1.42 to 2.11 µmol/mL, respectively. Therefore, the dissolved fractions of the raw materials in both Lac:Fru and Lac:Ur enhanced the antioxidant effect of DES. This proves that the SF samples contain bioactive ingredients that enhance the antioxidant effect.

Table 24: The concentration of Trolox equivalents antioxidant capacity (TEAC) of DES and SF samples for extracts obtained using codfish bones, mussel meat and tuna vitreous humor.

Sample		**Concentration TEAC (µmol/mL)**
DES	Lac:Fru	0.47 ± 0.20
	Lac:Ur	0.30 ± 0.16
$SF_{Lac:Fru}$	Codfish bones	1.42 ± 0.37
	Mussels	2.11 ± 0.25
	Tuna vitreous humor	1.54 ± 0.26
$SF_{Lac:Ur}$	Codfish bones	0.59 ± 0.26
	Mussels	1.45 ± 0.35
	Tuna vitreous humor	1.18 ± 0.18

An antioxidant effect is observed when the production of intracellular ROS after an external stimulus (UV-B radiation) decreases in comparison to a control upon treatment with a given sample on HCE cell line. For most tested samples, a positive antioxidant effect was observed as the production of ROS by HCE cells was decreased in their presence. The ROS production in UV stimulated cells was significantly higher than in non-UV stimulated cells ($P < 0.001$) in the testing samples, as shown in Figure 13. For the Lac:Fru, the production of ROS in the highest tested concentration (1 mg/mL) significantly decreased in comparison to the control. No antioxidant effect was observed for the studied doses of Lac:Ur. A significant decrease in ROS production was observed for $SF_{Lac:Fru}$ and $SF_{Lac:Ur}$ in comparison to the control at concentrations of 0.5 and 0.75 mg/mL for $SF_{Lac:Fru}$, and 0.25 and 0.5 mg/mL for $SF_{Lac:Ur}$. Furthermore, $PE_{Lac:Fru}$ and $PE_{Lac:Ur}$ showed antioxidant capacity at different tested concentrations, including low concentrations of 0.062 and 0.125 mg/mL for $PE_{Lac:Fru}$ and $PE_{Lac:Ur}$, respectively. Hence, the precipitation of the bioactive ingredients extracted from TVH display a significant antioxidant property.

To compare the antioxidant effect between the testing samples, the percentage of detected ROS was quantified in comparison to the control (Figure 14). A higher significant decrease was shown for the $PE_{Lac:Fru}$ sample in comparison to $SF_{Lac:Fru}$. Therefore, the $PE_{Lac:Fru}$ samples are most promising compounds having a higher significant antioxidant effect.

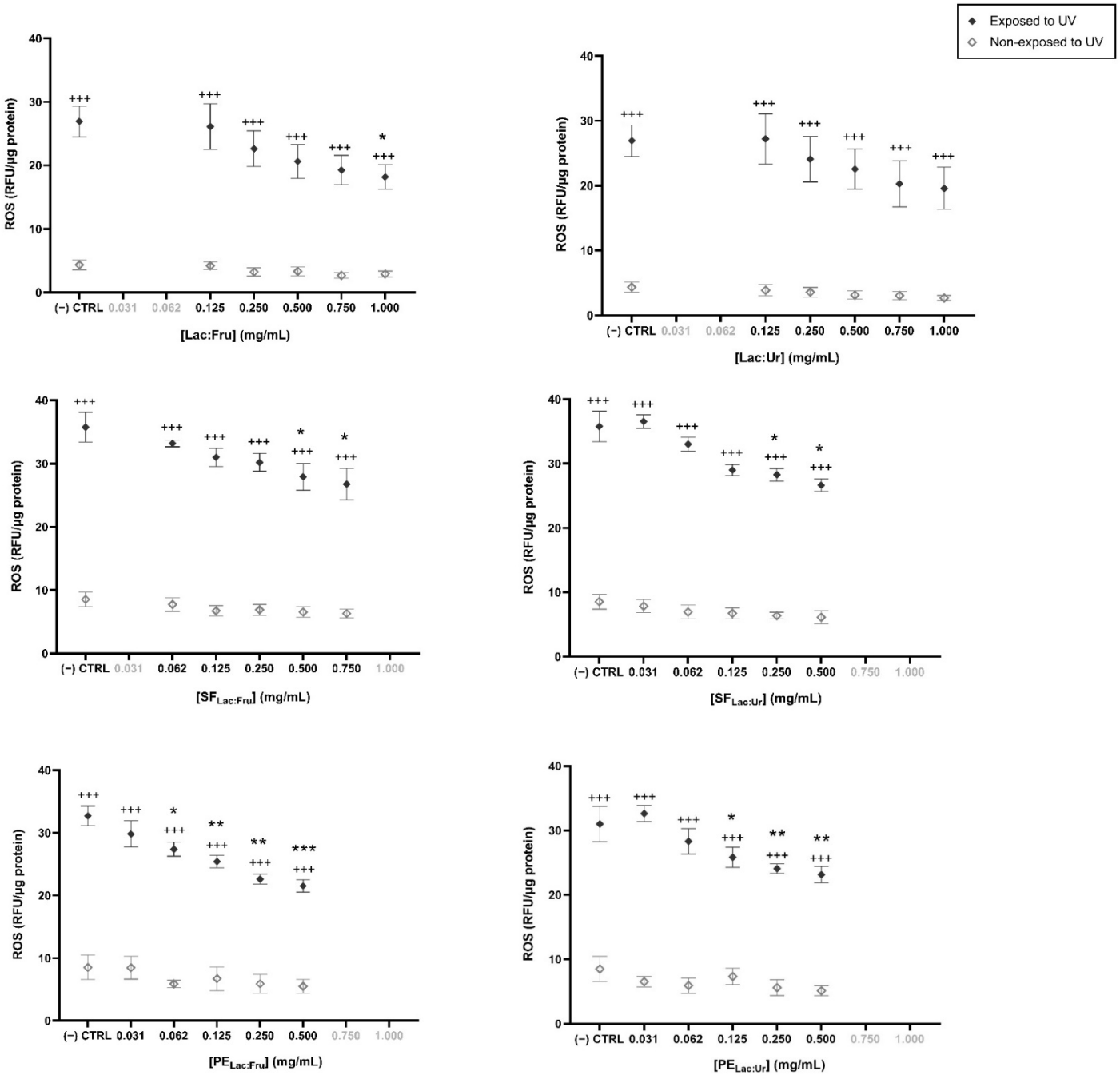

*Figure 13: Antioxidant effect of each sample in the human corneal epithelial cell line. *P < 0.05, **P < 0.01, ***P < 0.001 in comparison to UV-stimulated control cells; +++P < 0.001 in comparison to non-UV-stimulated cells.*

(a)

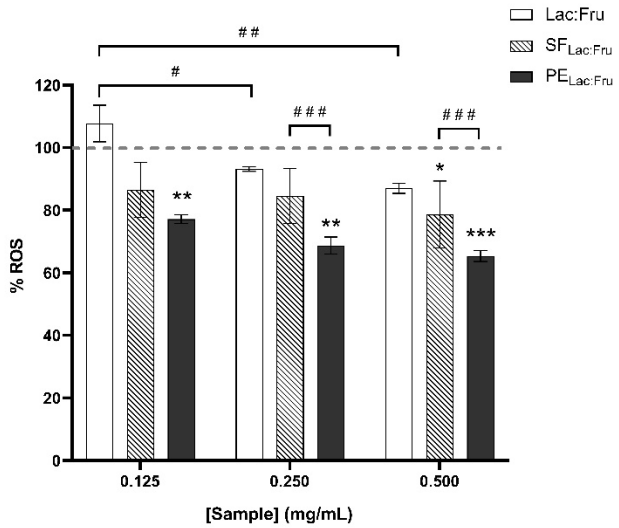

(b)

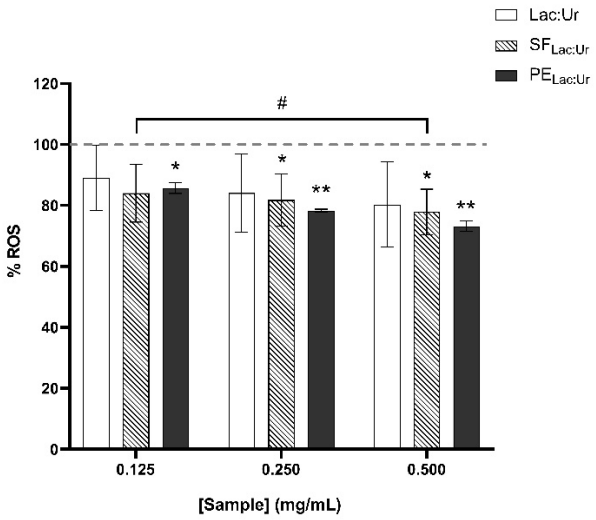

*Figure 14: Percentage of ROS in comparison to the control (represented in the dashed line) for the samples of the extraction process obtained (a) using Lac:Fru, and (b) Lac:Ur. *P < 0.05, **P < 0.01, ***P < 0.001 in comparison to UV-stimulated control cells. # P < 0.05, # # P < 0.01, # # # P < 0.001 in comparison between the compounds and different doses.*

3.3. Evaluation of potential inflammatory response

Previous studies have demonstrated that low molecular weight HA has pro-inflammatory properties [51, 52]. The evaluation of a potential inflammatory response induced by our samples in the corneal cells was done by measuring interleukins IL-6 and IL-10 levels in cell culture supernatants both in basal, unstimulated and stimulated cells following an inflammatory stimulus (TNF-α treatment for 24 h). We selected those interleukins considering their reported level alterations in dry eye [53]. When an inflammatory process takes place, IL-10 is secreted as an anti-inflammatory response. IL-6, a pro-inflammatory cytokine, is detected when cell inflammation occurs. As expected, TNF-α-exposed cells secreted significatively IL-6 levels, but not IL-10 levels compared to that of control unexposed cells. The tested compounds did not influence the IL-10 secretion, as it was not detected in any sample Figure 15. In addition, none of the compounds tested significantly increased basal IL-6 secretion by the cells, except for the case of $SF_{Lac:Fru}$ at 0.5 mg/mL (Figure 16). Therefore, all the other doses and compounds did not exhibit a pro-inflammatory behavior in our experimental conditions. Hence, this could potentially prove that these testing samples are safe ingredients for ocular drug formulations without eliciting a pro-inflammatory response.

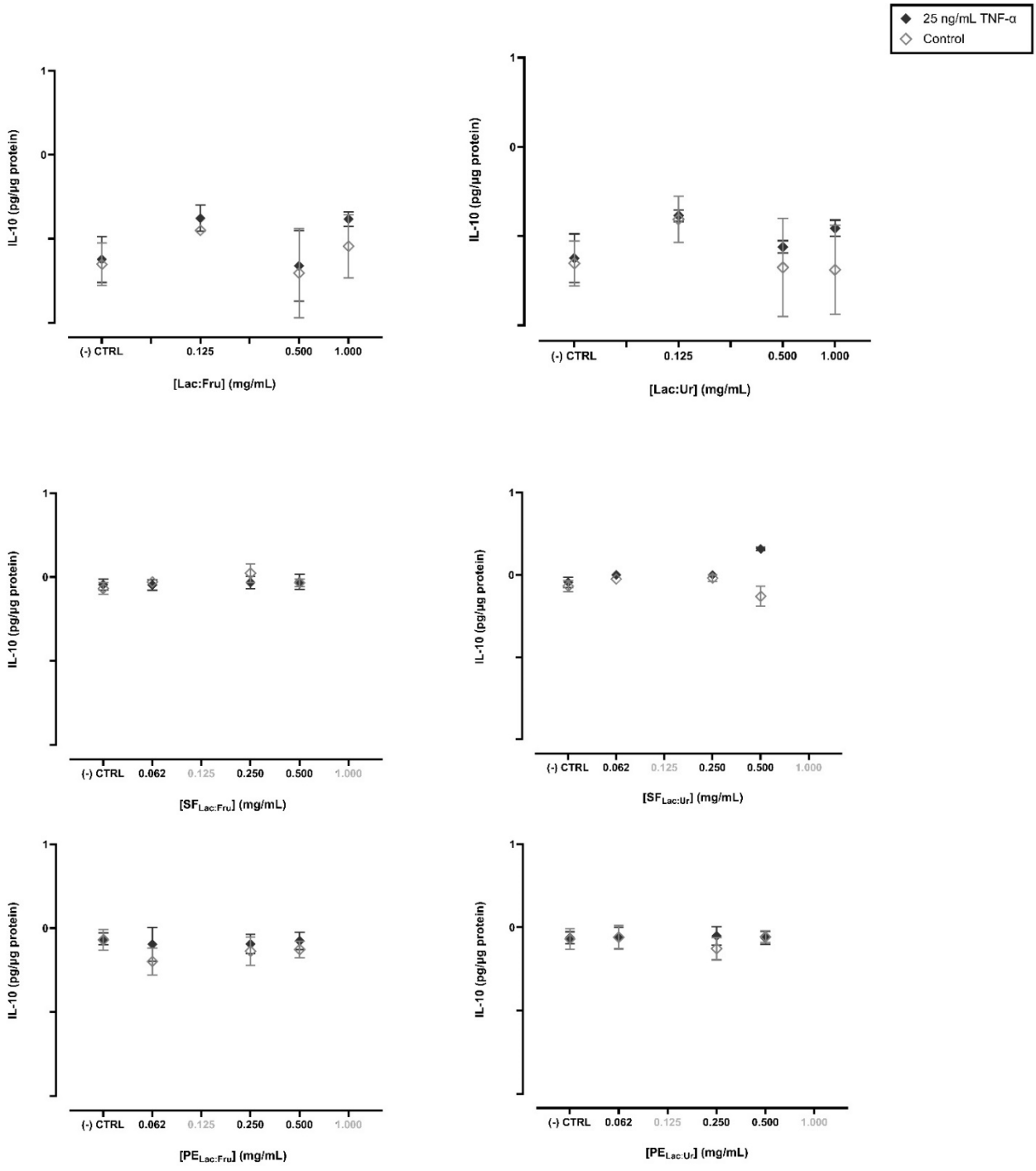

Figure 15: Effect of each compound on TNF-α-induced cells by analyzing IL-10 cytokine release. Negative values of IL-10 concentrations are considered experimental deviations due to equipment variation.

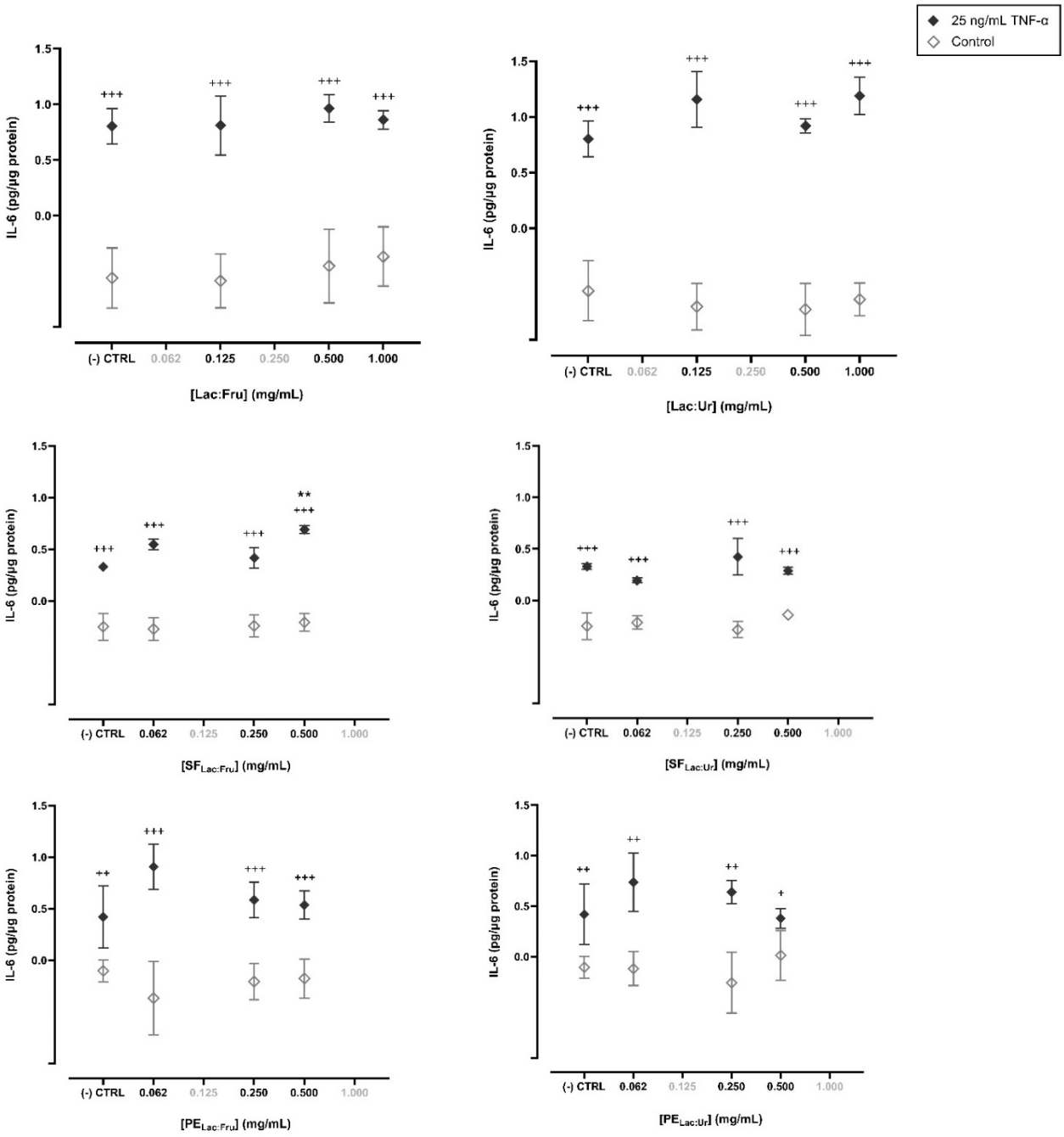

*Figure 16: Effect of each compound on TNF-α-induced cells by analyzing IL-6 cytokine release. Negative values of IL-6 concentrations are considered experimental deviations due to equipment variation. **P < 0.01 in comparison to TNF-α-stimulated control cells; +P < 0.05, ++P < 0.01, +++P < 0.001 in comparison to non-TNF-α-stimulated cells.*

3.4. Antimicrobial activity

Dry eye disease caused by tear deficiency or excessive tear evaporation conditions is often associated with ocular surface conditions, such as meibomian gland dysfunction, anterior blepharitis, keratitis, among others. These conditions lead to modifications in the ocular surface in the type and concentration of bacteria, including *S. aureus* and *P. aeruginosa* [54]. Hence, the antimicrobial potential of the samples was tested against these two bacterial species to assess if the samples inhibit bacterial growth for dry eyes that are prone to infections. In addition, an antimicrobial activity could lead to the use of the samples as preservatives to ensure a safe shelf life increase of the formulation. The concentrations of the testing samples were analyzed with a two-fold dilution series, having a range of 0.03 to 16 mg of sample/mL for DES and SF, and 0.002 to 1 mg of sample/mL for PE. For the PE samples, the highest assessed concentration was lower, due to the limited solubility of the extract in the medium. The testing samples were compared to two commercially available eye drops: HA-ED and CHL-ED. The MIC and MBC median values against *S. aureus* and *P. aeruginosa* are shown in Table 25, including the values for the three replicates.

It was possible to observe that SF samples presented a similar range of MIC and MBC values in comparison to DES. Hence, the presence of the TVH soluble fraction in DES did not improve remarkably its antimicrobial effect. A decreased antimicrobial activity was detected for the PE testing samples towards both bacteria, since MIC and MBC values were higher than those of the DES and SF samples. In that case, these values were above 500 µL for PE sample/mL, the highest concentration tested, corresponding to 148 and 76 µg HA/mL for $PE_{Lac:Fru}$ and $PE_{Lac:Ur}$, respectively. These results suggest that DES testing samples are indeed the most promising compounds to be used for antimicrobial effect against the two selected bacterial strains, as their MIC and MBC values ranged from 4 to 16 mg/mL. Previous studies demonstrated that lactic acid, fructose, and urea were shown to have an antimicrobial effect. For instance, lactic acid was proven to be an effective compound for the treatment of both *S. aureus* and *P. aeruginosa* [55]. Similarly, fructose was proven to enhance the efficiency of antibiotics in the treatment S. aureus, and its administration in an adjunctive therapy treated *P. aeruginosa* infection [56, 57]. Urea also displayed an antibacterial effect mainly on *S. aureus* growth [58]. Furthermore, the DES combinations used in this study could be used as potential preservatives in the formulation as the lactic acid has shown to increase the shelf life of the eye drop [39]. This would eliminate the need

for single use formulations without artificial preservatives. Moreover, the presence of urea could contribute to improvements for dry eye patients, as it was proven to promote the formation of the lipid layer in the tear film [46, 47]. Fructose is a natural non-toxic compound present in the corneal epithelium, at a concentration gradient to the aqueous humor and to the stroma and could be used for ocular applications when used within safe concentrations [41, 42, 59]. Furthermore, based on the results, DES seem to be pleiotropic, as they affect several processes at once and not just one single target in the cells [492]. Hence, it is more difficult for bacteria to mutate with the presence of DES and to have resistance to that antimicrobial compound.

Regarding the tested commercial eye drops, it was observed that the HA-based commercial eye drops did not show an antimicrobial activity against the microorganisms studied. This result is expected since the function of this product is not anti-infective, as HA does not act as antimicrobial agent and is mainly efficient to maintain ocular hydration and comfort [18, 60]. On the other hand, the ophthalmic anti-infective commercial product composed by chloramphenicol had shown to be more efficient against the microorganisms identified in dry eye patients as it is a well-known antimicrobial agent that validates the assays performed.

Table 25: Determination of the minimum inhibitory concentration (MIC) and the minimum bactericidal concentration (MBC) for the testing samples against dry eye-associated bacteria S. aureus *and* P. aeruginosa [a].

Target Bacteria	Sample	MIC (µL of testing sample/mL)	Sample composition at MIC value			MBC (µL of testing sample/mL)	Sample composition at MBC value		
			[DES] (mg/mL)	[HA] (ng/mL)	[CHL] (mg/mL)		[DES] (mg/mL)	[HA] (ng/mL)	[CHL] (mg/mL)
S. aureus	Lac:Fru	125 (125/ 125/ 125)	4 (4 / 4 / 4)	—	—	250 (500/ 250/ 250)	8 (16 / 8 / 8)	—	—
	Lac:Ur	250 (250/ 250/ 250)	8 (8 / 8 / 8)	—	—	500 (250/ 500/ 500)	16 (8 / 16 / 16)	—	—
	$SF_{Lac:Fru}$	250 (250/ 250/ 250)	8 (8 / 8 / 8)	2.30 (22.7/ 22.7/ 22.7)	—	250 (250/ 500/ 250)	8 (8 / 16 / 8)	2.30 (2.30/ 2.30/ 2.30)	—
	$SF_{Lac:Ur}$	250 (250/ 250/ 250)	4 (4 / 4 / 4)	0.67 (0.67/ 0.67/ 0.67)	—	500 (250/ 500/ 500)	16 (8 / 16 / 16)	2.70 (2.70/ 2.70/ 2.70)	—
	$PE_{Lac:Fru}$	> 500 (>500/ >500/ >500)	—	> 148000 (>148000/ >148000/ >148000)	—	> 500 (>500/ >500/ >500)	—	> 148000 (>148000/ >148000/ >148000)	—
	$PE_{Lac:Ur}$	> 500	—	> 76000	—	> 500	—	> 76000	—

		(>500/ >500/ >500)		(>76000/ >76000/ >76000)		(>500/ >500/ >500)		(>76000/ >76000/ >76000)	
	HA-ED	> 500 (>500/ >500/ >500)	—	> 0.75 (0.75/ 0.75/ 0.75)	—	> 500 (>500/ >500/ >500)	—	> 0.75 (0.75/ 0.75/ 0.75)	—
	CHL-ED	0.98	—	—	7.8 (7.8/ 15.6/ 7.8)	31.25 (62.5/ 31.25/ 31.25)	—	—	250 (313/ 250/ 250)
P. aeruginosa	Lac:Fru	125 (125/ 125/ 125)	4 (4 / 4 / 4)	—	—	125	4 (4 / 8 / 4)	—	—
	Lac:Ur	125 (125/ 125/ 125)	4 (4 / 4 / 4)	—	—	125	4 (4 / 4 / 4)	—	—
	$SF_{Lac:Fru}$	250 (125/ 250/ 250)	8 (4 / 8 / 8)	2.70 (2.70/ 2.70/ 2.70)	—	250	8 (8 / 8 / 8)	2.70 (2.70/ 2.70/ 2.70)	—
	$SF_{Lac:Ur}$	125 (125/ 125/ 125)	4 (4 / 4 / 4)	0.67 (0.67/ 0.67/ 0.67)	—	250	8 (4 / 8 / 8)	1.30 (0.67/ 1.30/ 1.30)	—
	$PE_{Lac:Fru}$	> 500 (>500/ >500/ >500)	—	> 148000 (>148000/ >148000/ >148000)	—	> 500 (>500/ >500/ >500)	—	> 148000 (>148000/ >148000/ >148000)	—

	$PE_{Lac:Ur}$	> 500 (>500/ >500/ >500)	—	> 76000 (>76000/ >76000/ >76000)	—	> 500 (>500/ >500/ >500)	—	> 76000 (>76000/ >76000/ >76000)	—
	HA-ED	> 500 (>500/ >500/ >500)	—	> 0.75 (0.75/ 0.75/ 0.75)	—	> 500 (>500/ >500/ >500)	—	> 0.75 (0.75/ 0.75/ 0.75)	—
	CHL-ED	15.63 (7.8/ 15.63/ 15.63)	—	—	125 (62.5/ 125/ 125)	15.63 (15.63/ 31.25/ 15.63)	—	—	125 (125/ 250/ 125)

[a] Cells shaded in grey present the concentration with three different runs shown between parentheses of the DES, HA and CHL in the testing samples, corresponding to the MIC and MBC values obtained.

4. Conclusions

The current work presents a process that contributes to the valorization of the inedible food waste. A green technique was applied to obtain a HA from the raw materials using lactic acid-based DES for the valorization of industrial by-products. The DES, SF and PE testing samples were tested in vitro to evaluate their biocompatibility. Preliminary studies were done on Caco-2 cell line, and the results differed based on the raw material from which the soluble fraction was dissolved, with TVH being the most viable. Hence, this raw material was selected for further studies on HCE cell line. A range of concentrations of the samples were studied to analyze the antioxidant and anti-inflammatory response on HCE cell line. Antioxidant effect was observed chemically and in cell-based assays for all tested samples. A higher antioxidant effect was observed for the $PE_{Lac:Fru}$ sample in comparison to the $SF_{Lac:Fru}$ sample, showing a significant decrease of the ROS in comparison to the control. All testing samples did not display a pro- nor anti-inflammatory response, based on the studied IL-10 and IL-6 levels, except for $SF_{Lac:Fru}$ testing

sample at 0.5 mg/mL that significantly increased IL-6 secretion. Furthermore, DES and SF samples showed antimicrobial activity against dry eye-associated bacteria *S. aureus* and *P. aeruginosa*. In conclusion, DES and SF samples seem to be the most promising samples and they could be used in ophthalmic therapeutic applications due to their antioxidant and antimicrobial activities. Consequently, the precipitation of the extracts from DES would not be necessary in order to obtain bioactive ingredients, which could reduce processing cost and time for future applications.

Chapter V:
Conclusions and Future Perspective

Deep eutectic solvents (DES) have been investigated as novel alternatives to conventional solvents. In this work, they were used to extract bioactive compounds from marine biomass (codfish bones -CB-, mussel meat -MM-, and tuna vitreous humor -TVH-) for their potential application in dry eye disease (DED) treatment.

- DES were prepared using a hydrogen bond donor and acceptor, including lactic acid, fructose, urea and terpenes (menthol, thymol, camphor, and borneol). Their thermodynamic behavior was evaluated, as it should demonstrate that the solvents are strongly non-ideal to define them as “deep” eutectic mixtures. Hence, the simulation of the solid-liquid equilibrium (SLE) phase diagram was done using the UNIFAC function and the COSMO-RS software, which were compared to the real SLE phase diagram of the systems obtained using Differential scanning calorimetry (DSC). The simulation was done for each combination of systems and was not applicable to lactic acid-based solvent. Simulation results for terpene-based solvent systems confirmed negative deviation from ideality experimentally and theoretically for most systems, which showed that they could be defined as DES. In addition, the physicochemical properties were obtained experimentally and theoretically to assess the structure and confirm the presence of hydrogen bonding. These properties were compared to those of the pure components used for their preparation, which further confirmed their behavior as a non-ideal mixture. Error parameters were computed to confirm the accuracy of the proposed models. According to the results, these models need further optimization to minimize the error and ensure their reliable use for the theoretical characterization of different combinations of DES.

- The extraction process was then implemented using terpene- and lactic acid-based systems for the isolation of bioactive ingredients from marine by-products: CB, MM and TVH. When the DES were mixed with each marine biomass, a soluble fraction (SF) of the raw materials in the DES was obtained. An anti-solvent was then used to obtain precipitated extracts (PE) from the samples, and the extraction yield was calculated to define the more suitable DES for a higher yield of bioactive ingredients. Lactic acid-based DES had a significantly higher yield in comparison to the terpene-based DES, which were selected for further characterization and bio-assay studies. The obtained extracts were

analyzed to identify their composition in proteins, lipids, ash, hyaluronic acid (HA) and chondroitin sulfate (CS). Proteins and lipids were mainly present in extracts obtained from MM, while ash content was the highest in the extracts obtained from CD. HA was mostly obtained from the TVH. As proteins were shown to be the main constituent of all isolated extracts, deeper analysis of the protein quality must be done, including the amino acid profile. Moreover, other isolated compounds in the extracts remained undefined. Further analysis must be done to evaluate the compounds that could be isolated in these samples, in order to ensure complete characterization of these extracts. The analysis of the molecular weight of hyaluronic acid must be done for its use in industrial applications. In addition, the optimization of the extraction process is essential to evaluate the most suitable extraction conditions, process time and components ratios.

- Bioactivity studies were performed to evaluate the potential application of selected compounds in therapeutic formulations for the DED treatment. The testing samples include DES, SF and PE samples to compare their biocompatibility. Preliminary cytotoxicity studies on Caco-2 cell line shown that the presence of the SF of the raw materials in DES decreased the toxicity of DES. Therefore, the soluble ingredients improved the biocompatibility of DES on this cell line. Further studies on HCE cell line and dry eye-associated microorganisms were performed. The influence of the testing samples on the viability of the cells, their intracellular ROS scavenging capacity and potential inflammatory response were studied in UV and TNF-α stimulated cells, respectively. Additionally, antimicrobial properties of the samples against dry eye-associated gram-positive bacteria (*Staphylococcus aureus*) and gram-negative bacteria (*Pseudomonas aeruginosa*) were evaluated to furtherly study the use of the samples as preservatives that ensure a safe shelf life increase in ophthalmic formulation. According to the results, all samples displayed an antioxidant effect within the tested concentrations, which was significantly higher for PE in comparison to SF. Most of the tested samples did not induce an inflammatory response in cells, which confirms the safety in ophthalmic formulations. In addition, the DES and SF proved to be efficient against the studied bacterial strains, while PE did not show an antimicrobial effect. Hence, both DES, SF at defined concentrations could be potentially used in DED management. However, further studies

must be done for their application in this ophthalmic therapy. These include in vivo and preclinical studies, prior to their evaluation in clinical studies, such as small animal models to assess the immunogenicity and for safety and risk assessment.

The preliminary extract characterization and bio-assay studies of the compounds obtained from the extraction process defined their composition and confirmed their safety for potential use in DED management. However, further analyses must be conducted to determine their detailed composition, characteristics and therapeutic effect, to be able to potentially commercialize these bioactive compounds. These additional studies should also focus on the verification if SF and PE samples have a significantly higher therapeutic effect for DED treatment in comparison to DES samples. If DES display a higher viability in comparison to the other samples, this would mean that the extracted bioactive ingredients are not as strongly beneficial as the DES. In addition, as these DES have been studied in diverse cosmetic and pharmaceutical applications, it could be expected that they have a significant bioactivity. In such cases, the DES could be prepared and studied for this application, without the need for the bioactive compounds extraction. Moreover, it is highly important to note that the studies will differ depending on the target application. For instance, the isolated bioactive compounds could be tested for their use in pharmaceutical and biomedical applications due to their potential healing effects. Hence, these compounds are not only limited to DED treatment and could also be analyzed for additional therapeutical applications.

Reference List

1. Anastas, P., Eghbali, N., Green Chemistry: Principles and Practice. *Chem. Soc. Rev.* **2009**, *39*, 1, 301–312. doi: 10.1039/B918763B.

2. Chen, T. L., Kim, H., Pan, S. Y., Tseng, P. C., Lin, Y. P., Chiang, P. C., Implementation of green chemistry principles in circular economy system towards sustainable development goals: Challenges and perspectives. *Sci. Total Environ.* **2020**, *716*136998. doi: 10.1016/J.SCITOTENV.2020.136998.

3. Abdussalam-Mohammed, W., Qasem Ali, A., O. Errayes, A., Green Chemistry: Principles, Applications, and Disadvantages. *Chem. Methodol.* **2020**, *4*, 4, 408–423. doi: 10.33945/SAMI/CHEMM.2020.4.4.

4. Häkkinen, R., Abbott, A. P., Deep eutectic solvents—Teaching nature lessons that it knew already. , in *Advances in Botanical Research*, *97*, Academic Press Inc., 2021, 1–16. doi: 10.1016/bs.abr.2020.09.013.

5. Abbott, A. P., Boothby, D., Capper, G., Davies, D. L., Rasheed, R. K., Deep Eutectic Solvents formed between choline chloride and carboxylic acids: Versatile alternatives to ionic liquids. *J. Am. Chem. Soc.* **2004**, *126*, 29, 9142–9147. doi: 10.1021/ja048266j.

6. Makoś, P., Słupek, E., Gębicki, J., Hydrophobic deep eutectic solvents in microextraction techniques–A review. *Microchem. J.* **2020**, *152*104384–104400. doi: 10.1016/J.MICROC.2019.104384.

7. Zhang, Q., De Oliveira Vigier, K., Royer, S., Jérôme, F., Deep eutectic solvents: syntheses, properties and applications. *Chem. Soc. Rev.* **2012**, *41*, 21, 7108. doi: 10.1039/c2cs35178a.

8. Kalhor, P., Ghandi, K., Deep eutectic solvents for pretreatment, extraction, and catalysis of biomass and food waste. *Molecules* **2019**, *24*, 22, 4012. doi: 10.3390/molecules24224012.

9. Alañón, M. E., Ivanovic, M., Gómez-Caravaca, A. M., Arráez-Román, D., Segura-Carretero, A., Choline chloride derivative-based deep eutectic liquids as novel green alternative solvents for extraction of phenolic compounds from olive leaf. *Arab. J. Chem.* **2020**, *13*, 1, 1685–1701. doi: 10.1016/j.arabjc.2018.01.003.

10. Zdanowicz, M., Wilpiszewska, K., Spychaj, T., Deep eutectic solvents for polysaccharides processing. A review. *Carbohydr. Polym.* **2018**, *200*, March, 361–380. doi: 10.1016/j.carbpol.2018.07.078.

11. Płotka-Wasylka, J., de la Guardia, M., Andruch, V., Vilková, M., Deep eutectic solvents vs ionic liquids: Similarities and differences. , *Microchemical Journal*, *159*. Elsevier Inc., 105539, Dec. 01, 2020. doi: 10.1016/j.microc.2020.105539.

12. Jablonsky, M., Skulcova, A., Haz, A., Sima, J., Majova, V., Long-term Isothermal Stability of Deep Eutectic Solvents. *BioResources* **2018**, *13*, 4, . doi: 10.15376/biores.13.4.7545-7559.

13. Hansen, B. B. *et al.*, Deep Eutectic Solvents: A Review of Fundamentals and Applications. , *Chemical Reviews*. American Chemical Society, 2021. doi: 10.1021/acs.chemrev.0c00385.

14. Martins, M. A. R. *et al.*, Tunable Hydrophobic Eutectic Solvents Based on Terpenes and Monocarboxylic Acids. *ACS Sustain. Chem. Eng.* **2018**, *6*, 7, 8836–8846. doi: 10.1021/acssuschemeng.8b01203.

15. Hammond, O. S., Bowron, D. T., Edler, K. J., Liquid structure of the choline chloride-urea deep eutectic solvent (reline) from neutron diffraction and atomistic modelling. *Green Chem.* **2016**, *18*, 9, 2736–2744. doi: 10.1039/c5gc02914g.

16. Wagle, D. V., Adhikari, L., Baker, G. A., Computational perspectives on structure, dynamics, gas sorption, and bio-interactions in deep eutectic solvents. *Fluid Phase Equilib.* **2017**, *448*50–58. doi: 10.1016/j.fluid.2017.04.018.

17. Kollau, L. J. B. M., Vis, M., Van Den Bruinhorst, A., De With, G., Tuinier, R., Activity modelling of the solid-liquid equilibrium of deep eutectic solvents. , in *Pure and Applied Chemistry*, Aug. 2019, *91*, 8, , 1341–1349. doi: 10.1515/pac-2018-1014.

18. Abdallah, M. M. *et al.*, Physicochemical Characterization and Simulation of the Solid–Liquid Equilibrium Phase Diagram of Terpene-Based Eutectic Solvent Systems. *Molecules* **2021**, *26*, 6, 1801. doi: 10.3390/molecules26061801.

19. Zahn, S., Kirchner, B., Mollenhauer, D., Charge Spreading in Deep Eutectic Solvents. *ChemPhysChem* **2016**, *17*, 21, 3354–3358. doi: 10.1002/cphc.201600348.

20. Francisco, M., van den Bruinhorst, A., Kroon, M. C., Low-Transition-Temperature Mixtures (LTTMs): A New Generation of Designer Solvents. *Angew. Chemie Int. Ed.* **2013**, *52*, 11, 3074–3085. doi: 10.1002/anie.201207548.

21. Chen, Z., Greaves, T. L., Warr, G. G., Atkin, R., Mixing cations with different alkyl chain lengths markedly depresses the melting point in deep eutectic solvents formed from alkylammonium bromide salts and urea. *Chem. Commun.* **2017**, *53*, 15, 2375–2377. doi: 10.1039/c7cc00201g.

22. Makoś, P., Boczkaj, G., Deep eutectic solvents based highly efficient extractive desulfurization of fuels – Eco-friendly approach. *J. Mol. Liq.* **2019**, *296*111916. doi: 10.1016/j.molliq.2019.111916.

23. Mjalli, F. S., Ahmed, O. U., Characteristics and intermolecular interaction of eutectic binary mixtures: Reline and Glyceline. *Korean J. Chem. Eng.* **2016**, *33*, 1, 337–343. doi: 10.1007/s11814-015-0134-7.

24. Shahbaz, K., Bagh, F. S. G., Mjalli, F. S., AlNashef, I. M., Hashim, M. A., Prediction of refractive index and density of deep eutectic solvents using atomic contributions. *Fluid Phase Equilib.* **2013**, *354*304–311. doi: 10.1016/j.fluid.2013.06.050.

25. Abbott, A. P., Capper, G., Gray, S., Design of Improved Deep Eutectic Solvents Using Hole Theory. *ChemPhysChem* **2006**, *7*, 4, 803–806. doi: 10.1002/cphc.200500489.

26. Procentese, A., Raganati, F., Olivieri, G., Russo, M. E., Rehmann, L., Marzocchella, A., Deep Eutectic Solvents pretreatment of agro-industrial food waste. *Biotechnol. Biofuels* **2018**, *11*, 1, 37. doi: 10.1186/s13068-018-1034-y.

27. Roy, R., Rahman, M. S., Raynie, D. E., Recent advances of greener pretreatment

technologies of lignocellulose. *Curr. Res. Green Sustain. Chem.* **2020**, *3*100035. doi: 10.1016/j.crgsc.2020.100035.

28. Xia, S., Baker, G. A., Li, H., Ravula, S., Zhao, H., Aqueous ionic liquids and deep eutectic solvents for cellulosic biomass pretreatment and saccharification. *RSC Adv.* **2014**, *4*, 21, 10586–10596. doi: 10.1039/c3ra46149a.

29. Loow, Y. L. *et al.*, Deep eutectic solvent and inorganic salt pretreatment of lignocellulosic biomass for improving xylose recovery. *Bioresour. Technol.* **2018**, *249*818–825. doi: 10.1016/j.biortech.2017.07.165.

30. Procentese, A. *et al.*, Deep eutectic solvent pretreatment and subsequent saccharification of corncob. *Bioresour. Technol.* **2015**, *192*31–36. doi: 10.1016/j.biortech.2015.05.053.

31. Loow, Y. L., New, E. K., Yang, G. H., Ang, L. Y., Foo, L. Y. W., Wu, T. Y., Potential use of deep eutectic solvents to facilitate lignocellulosic biomass utilization and conversion. , *Cellulose*, *24*, 9, . Springer Netherlands, 3591–3618, Sep. 01, 2017. doi: 10.1007/s10570-017-1358-y.

32. Jablonský, M., Škulcová, A., Kamenská, L., Vrška, M., Šíma, J., Deep Eutectic Solvents: Fractionation of Wheat Straw. *BioResources* **2015**, *10*, 4, . doi: 10.15376/biores.10.4.8039-8047.

33. Wahlström, R., Hiltunen, J., Pitaluga De Souza Nascente Sirkka, M., Vuoti, S., Kruus, K., Comparison of three deep eutectic solvents and 1-ethyl-3-methylimidazolium acetate in the pretreatment of lignocellulose: Effect on enzyme stability, lignocellulose digestibility and one-pot hydrolysis. *RSC Adv.* **2016**, *6*, 72, 68100–68110. doi: 10.1039/c6ra11719h.

34. Zhang, C. W., Xia, S. Q., Ma, P. S., Facile pretreatment of lignocellulosic biomass using deep eutectic solvents. *Bioresour. Technol.* **2016**, *219*1–5. doi: 10.1016/j.biortech.2016.07.026.

35. Kim, K. H., Dutta, T., Sun, J., Simmons, B., Singh, S., Biomass pretreatment using deep eutectic solvents from lignin derived phenols. *Green Chem.* **2018**, *20*, 4, 809–815. doi: 10.1039/c7gc03029k.

36. Sumiati, T., Suryadi, H., Potency of Deep Euteutic Solvent as an Alternative Solvent on Pretreatment Process of Lignocellulosic Biomass: Review. , in *Journal of Physics: Conference Series*, Feb. 2021, *1764*, 1, , 012014. doi: 10.1088/1742-6596/1764/1/012014.

37. Gupta, R., Sadaf, A., Grewal, J., Khare, K., Deep eutectic solvents compatible Aspergillus niger cellulase and its utility for in situ pre-treatment and saccharification of wheat straw. , **2017**, . Accessed: Mar. 21, 2021. [Online]. Available: www.jees.in

38. Hou, X. D., Feng, G. J., Ye, M., Huang, C. M., Zhang, Y., Significantly enhanced enzymatic hydrolysis of rice straw via a high-performance two-stage deep eutectic solvents synergistic pretreatment. *Bioresour. Technol.* **2017**, *238*139–146. doi: 10.1016/j.biortech.2017.04.027.

39. Zulkefli, S., Abdulmalek, E., Abdul Rahman, M. B., Pretreatment of oil palm trunk in deep eutectic solvent and optimization of enzymatic hydrolysis of pretreated oil palm trunk. *Renew. Energy* **2017**, *107*36–41. doi: 10.1016/j.renene.2017.01.037.

40. Zhang, H., Lang, J., Lan, P., Yang, H., Lu, J., Wang, Z., Study on the dissolution mechanism of cellulose by ChCl-based deep eutectic solvents. *Materials (Basel).* **2020**, *13*, 2, . doi: 10.3390/ma13020278.

41. Lynam, J. G., Kumar, N., Wong, M. J., Deep eutectic solvents' ability to solubilize lignin, cellulose, and hemicellulose; thermal stability; and density. *Bioresour. Technol.* **2017**, *238*684–689. doi: 10.1016/j.biortech.2017.04.079.

42. Ren, H., Chen, C., Wang, Q., Zhao, D., Guo, S., The properties of choline chloride-based deep eutectic solvents and their performance in the dissolution of cellulose. *BioResources* **2016**, *11*, 2, 5435–5451. doi: 10.15376/biores.11.2.5435-5451.

43. Nam, M. W., Zhao, J., Lee, M. S., Jeong, J. H., Lee, J., Enhanced extraction of bioactive natural products using tailor-made deep eutectic solvents: Application to flavonoid extraction from Flos sophorae. *Green Chem.* **2015**, *17*, 3, 1718–1727. doi: 10.1039/c4gc01556h.

44. Skarpalezos, D., Detsi, A., Deep Eutectic Solvents as Extraction Media for Valuable

Flavonoids from Natural Sources. *Appl. Sci.* **2019**, *9*, 19, 4169. doi: 10.3390/app9194169.

45. Xia, G. H., Li, X. H., Jiang, Y. hang, Deep eutectic solvents as green media for flavonoids extraction from the rhizomes of Polygonatum odoratum. *Alexandria Eng. J.* **2021**, *60*, 2, 1991–2000. doi: 10.1016/j.aej.2020.12.008.

46. Hao, C., Chen, L., Dong, H., Xing, W., Xue, F., Cheng, Y., Extraction of flavonoids from scutellariae radix using ultrasound-assisted deep eutectic solvents and evaluation of their anti-inflammatory activities. *ACS Omega* **2020**, *5*, 36, 23140–23147. doi: 10.1021/acsomega.0c02898.

47. Dai, Y., Witkamp, G. J., Verpoorte, R., Choi, Y. H., Natural deep eutectic solvents as a new extraction media for phenolic metabolites in carthamus tinctorius L. *Anal. Chem.* **2013**, *85*, 13, 6272–6278. doi: 10.1021/ac400432p.

48. Bajkacz, S., Adamek, J., Development of a Method Based on Natural Deep Eutectic Solvents for Extraction of Flavonoids from Food Samples. *Food Anal. Methods* **2018**, *11*, 5, 1330–1344. doi: 10.1007/s12161-017-1118-5.

49. Lu, W., Liu, S., Choline chloride–based deep eutectic solvents (Ch-DESs) as promising green solvents for phenolic compounds extraction from bioresources: state-of-the-art, prospects, and challenges. , *Biomass Conversion and Biorefinery*. Springer, 1–14, May 21, 2020. doi: 10.1007/s13399-020-00753-7.

50. Oomen, W. W., Begines, P., Mustafa, N. R., Wilson, E. G., Verpoorte, R., Choi, Y. H., Natural Deep Eutectic Solvent Extraction of Flavonoids of Scutellaria baicalensis as a Replacement for Conventional Organic Solvents. *Molecules* **2020**, *25*, 3, . doi: 10.3390/molecules25030617.

51. Chen, L. *et al.*, Extraction of Phenolic Acids and Polysaccharides from Lilium lancifolium Thunb. Using Deep Eutectic Solvent. *Anal. Methods* **2021**, *13*, 10, 1226–1231. doi: 10.1039/d0ay02352c.

52. Wang, D., Yang, X.-H., Tang, R.-C., Yao, F., Extraction of Keratin from Rabbit Hair by a Deep Eutectic Solvent and Its Characterization. *Polymers (Basel).* **2018**, *10*, 9, 993. doi: 10.3390/polym10090993.

53. Pang, J. *et al.*, Green aqueous biphasic systems containing deep eutectic solvents and sodium salts for the extraction of protein. *RSC Adv.* **2017**, *7*, 78, 49361–49367. doi: 10.1039/c7ra07315a.

54. Grudniewska, A., De Melo, E. M., Chan, A., Gniłka, R., Boratyński, F., Matharu, A. S., Enhanced Protein Extraction from Oilseed Cakes Using Glycerol-Choline Chloride Deep Eutectic Solvents: A Biorefinery Approach. *ACS Sustain. Chem. Eng.* **2018**, *6*, 11, 15791–15800. doi: 10.1021/acssuschemeng.8b04359.

55. Lin, Z., Jiao, G., Zhang, J., Celli, G. B., Brooks, M. S. L., Optimization of protein extraction from bamboo shoots and processing wastes using deep eutectic solvents in a biorefinery approach. *Biomass Convers. Biorefinery* **2020**, 1–12. doi: 10.1007/s13399-020-00614-3.

56. Wahlström, R. *et al.*, High Yield Protein Extraction from Brewer's Spent Grain with Novel Carboxylate Salt - Urea Aqueous Deep Eutectic Solvents. *ChemistrySelect* **2017**, *2*, 29, 9355–9363. doi: 10.1002/slct.201701492.

57. Sequeira, R. A., Bhatt, J., Prasad, K., Recent Trends in Processing of Proteins and DNA in Alternative Solvents: A Sustainable Approach. *Sustain. Chem.* **2020**, *1*, 2, 116–137. doi: 10.3390/suschem1020010.

58. Florindo, C., Branco, L. C., Marrucho, I. M., Development of hydrophobic deep eutectic solvents for extraction of pesticides from aqueous environments. *Fluid Phase Equilib.* **2017**, *448*135–142. doi: 10.1016/j.fluid.2017.04.002.

59. Musarurwa, H., Tavengwa, N. T., Deep eutectic solvent-based dispersive liquid-liquid micro-extraction of pesticides in food samples. , *Food Chemistry*, *342*. Elsevier Ltd, 127943, Apr. 16, 2021. doi: 10.1016/j.foodchem.2020.127943.

60. Farajzadeh, M. A., Abbaspour, M., Kazemian, R., Afshar Mogaddam, M. R., Preparation of a new three-component deep eutectic solvent and its use as an extraction solvent in dispersive liquid–liquid microextraction of pesticides in green tea and herbal distillates. *J. Sci. Food Agric.* **2020**, *100*, 5, 1904–1912. doi: 10.1002/jsfa.10200.

61. Liu, X. *et al.*, Extraction of benzoylurea pesticides from tea and fruit juices using deep

eutectic solvents. *J. Chromatogr. B* **2020**, *1140*121995. doi: 10.1016/j.jchromb.2020.121995.

62. Zhang, W. *et al.*, Green and Efficient Extraction of Polysaccharides From *Poria cocos* F.A. Wolf by Deep Eutectic Solvent. *Nat. Prod. Commun.* **2020**, *15*, 2, 1934578X1990070. doi: 10.1177/1934578X19900708.

63. Morais, E. S., Da Costa Lopes, A. M., Freire, M. G., Freire, C. S. R., Coutinho, J. A. P., Silvestre, A. J. D., Use of ionic liquids and deep eutectic solvents in polysaccharides dissolution and extraction processes towards sustainable biomass valorization. , *Molecules*, *25*, 16, . MDPI AG, Aug. 01, 2020. doi: 10.3390/molecules25163652.

64. Zainal-Abidin, M. H., Hayyan, M., Hayyan, A., Jayakumar, N. S., New horizons in the extraction of bioactive compounds using deep eutectic solvents: A review. , *Analytica Chimica Acta*, *979*. Elsevier B.V., 1–23, Aug. 01, 2017. doi: 10.1016/j.aca.2017.05.012.

65. Wang, M. *et al.*, Ecofriendly Mechanochemical Extraction of Bioactive Compounds from Plants with Deep Eutectic Solvents. *ACS Sustain. Chem. Eng.* **2017**, *5*, 7, 6297–6303. doi: 10.1021/acssuschemeng.7b01378.

66. Ivanović, M., Islamčević Razboršek, M., Kolar, M., Innovative Extraction Techniques Using Deep Eutectic Solvents and Analytical Methods for the Isolation and Characterization of Natural Bioactive Compounds from Plant Material. *Plants* **2020**, *9*, 11, 1428. doi: 10.3390/plants9111428.

67. Duan, L., Dou, L. L., Guo, L., Li, P., Liu, E. H., Comprehensive Evaluation of Deep Eutectic Solvents in Extraction of Bioactive Natural Products. *ACS Sustain. Chem. Eng.* **2016**, *4*, 4, 2405–2411. doi: 10.1021/acssuschemeng.6b00091.

68. Ma, W., Row, K. H., Optimized extraction of bioactive compounds from Herba Artemisiae Scopariae with ionic liquids and deep eutectic solvents. *J. Liq. Chromatogr. Relat. Technol.* **2017**, *40*, 9, 459–466. doi: 10.1080/10826076.2017.1322522.

69. Grozdanova, T. *et al.*, Extracts of medicinal plants with natural deep eutectic solvents: enhanced antimicrobial activity and low genotoxicity. *BMC Chem.* **2020**, *14*, 1, 73. doi: 10.1186/s13065-020-00726-x.

70. Vieira, V., Prieto, M. A., Barros, L., Coutinho, J. A. P., Ferreira, I. C. F. R., Ferreira, O., Enhanced extraction of phenolic compounds using choline chloride based deep eutectic solvents from Juglans regia L. *Ind. Crop. Prod.* **2018**, *115*261–271. doi: 10.1016/j.indcrop.2018.02.029.

71. Bradić, B., Novak, U., Likozar, B., Crustacean shell bio-refining to chitin by natural deep eutectic solvents. *Green Process. Synth.* **2020**, *9*, 1, 13–25. doi: 10.1515/GPS-2020-0002/DOWNLOADASSET/SUPPL/GPS-2020-0002_SM.PDF.

72. Zhuang, B., Dou, L. L., Li, P., Liu, E. H., Deep eutectic solvents as green media for extraction of flavonoid glycosides and aglycones from Platycladi Cacumen. *J. Pharm. Biomed. Anal.* **2017**, *134*214–219. doi: 10.1016/J.JPBA.2016.11.049.

73. Wang, X. *et al.*, Ultrasound-assisted deep eutectic solvent extraction of echinacoside and oleuropein from Syringa pubescens Turcz. *Ind. Crops Prod.* **2020**, *151*112442. doi: 10.1016/j.indcrop.2020.112442.

74. Bosiljkov, T. *et al.*, Natural deep eutectic solvents and ultrasound-assisted extraction: Green approaches for extraction of wine lees anthocyanins. *Food Bioprod. Process.* **2017**, *102*195–203. doi: 10.1016/j.fbp.2016.12.005.

75. Jakovljević, M., Jokić, S., Molnar, M., Jerković, I., Application of Deep Eutectic Solvents for the Extraction of Carnosic Acid and Carnosol from Sage (Salvia officinalis L.) with Response Surface Methodology Optimization. *Plants* **2021**, *10*, 1, 80. doi: 10.3390/plants10010080.

76. Sharma, M., Mukesh, C., Mondal, D., Prasad, K., Dissolution of α-chitin in deep eutectic solvents. *RSC Adv.* **2013**, *3*, 39, 18149–18155. doi: 10.1039/c3ra43404d.

77. Chen, J., Li, Y., Wang, X., Liu, W., Application of deep eutectic solvents in food analysis: A review. , *Molecules*, *24*, 24, . MDPI AG, Dec. 16, 2019. doi: 10.3390/molecules24244594.

78. Leron, R. B., Li, M. H., Solubility of carbon dioxide in a choline chloride-ethylene glycol based deep eutectic solvent. *Thermochim. Acta* **2013**, *551*14–19. doi: 10.1016/j.tca.2012.09.041.

79. Li, X., Hou, M., Han, B., Wang, X., Zou, L., Solubility of CO2 in a choline chloride + urea eutectic mixture. *J. Chem. Eng. Data* **2008**, *53*, 2, 548–550. doi: 10.1021/je700638u.

80. Zubeir, L. F., Van Osch, D. J. G. P., Rocha, M. A. A., Banat, F., Kroon, M. C., Carbon Dioxide Solubilities in Decanoic Acid-Based Hydrophobic Deep Eutectic Solvents. *J. Chem. Eng. Data* **2018**, *63*, 4, 913–919. doi: 10.1021/acs.jced.7b00534.

81. Sze, L. L. *et al.*, Ternary deep eutectic solvents tasked for carbon dioxide capture. *ACS Sustain. Chem. Eng.* **2014**, *2*, 9, 2117–2123. doi: 10.1021/sc5001594.

82. Xie, Y., Dong, H., Zhang, S., Lu, X., Ji, X., Solubilities of CO2, CH4, H2, CO and N2 in choline chloride/urea. *Green Energy Environ.* **2016**, *1*, 3, 195–200. doi: 10.1016/j.gee.2016.09.001.

83. Bhawna, Pandey, A., Pandey, S., Superbase-Added Choline Chloride-Based Deep Eutectic Solvents for CO_2 Capture and Sequestration. *ChemistrySelect* **2017**, *2*, 35, 11422–11430. doi: 10.1002/slct.201702259.

84. Lu, M., Han, G., Jiang, Y., Zhang, X., Deng, D., Ai, N., Solubilities of carbon dioxide in the eutectic mixture of levulinic acid (or furfuryl alcohol) and choline chloride. *J. Chem. Thermodyn.* **2015**, *887*2–77. doi: 10.1016/j.jct.2015.04.021.

85. Ma, C., Sarmad, S., Mikkola, J. P., Ji, X., Development of Low-Cost Deep Eutectic Solvents for CO2 Capture. , in *Energy Procedia*, Dec. 2017, *142*, 3320–3325. doi: 10.1016/j.egypro.2017.12.464.

86. Sun, S., Niu, Y., Xu, Q., Sun, Z., Wei, X., Efficient SO2 absorptions by four kinds of deep eutectic solvents based on choline chloride. *Ind. Eng. Chem. Res.* **2015**, *54*, 33, 8019–8024. doi: 10.1021/ACS.IECR.5B01789.

87. Pelaquim, F. P., Barbosa Neto, A. M., Dalmolin, I. A. L., Costa, M. C. da, Gas Solubility Using Deep Eutectic Solvents: Review and Analysis. *Ind. Eng. Chem. Res.* **2021**, *60*, 24, 8607–8620. doi: 10.1021/ACS.IECR.1C00947/SUPPL_FILE/IE1C00947_SI_001.PDF.

88. Li, C. *et al.*, Extraction desulfurization process of fuels with ammonium-based deep eutectic solvents. *Green Chem.* **2013**, *15*, 10, 2793–2799. doi: 10.1039/c3gc41067f.

89. Chandran, D. *et al.*, Deep eutectic solvents for extraction-desulphurization: A review. , *Journal of Molecular Liquids*, *275*. Elsevier B.V., 312–322, Feb. 01, 2019. doi: 10.1016/j.molliq.2018.11.051.

90. Li, C. *et al.*, Extraction desulfurization of fuels with “metal ions” based deep eutectic solvents (MDESs). *Green Chem.* **2016**, *18*, 13, 3789–3795. doi: 10.1039/c6gc00366d.

91. Wang, B. *et al.*, Study on the Desulfurization and Regeneration Performance of Functional Deep Eutectic Solvents. *ACS Omega* **2020**, *5*, 25, 15353–15361. doi: 10.1021/acsomega.0c01467.

92. Schaeffer, N., Martins, M. A. R., Neves, C. M. S. S., Pinho, S. P., Coutinho, J. A. P., Sustainable hydrophobic terpene-based eutectic solvents for the extraction and separation of metals. *Chem. Commun.* **2018**, *54*, 58, 8104–8107. doi: 10.1039/c8cc04152k.

93. Riaño, S. *et al.*, Separation of rare earths and other valuable metals from deep-eutectic solvents: A new alternative for the recycling of used NdFeB magnets. *RSC Adv.* **2017**, *7*, 51, 32100–32113. doi: 10.1039/c7ra06540j.

94. Cen, P., Spahiu, K., Tyumentsev, M. S., Foreman, M. R. S. J., Metal extraction from a deep eutectic solvent, an insight into activities. *Phys. Chem. Chem. Phys.* **2020**, *22*, 19, 11012–11024. doi: 10.1039/c9cp05982b.

95. Zante, G., Boltoeva, M., Review on Hydrometallurgical Recovery of Metals with Deep Eutectic Solvents. *Sustain. Chem.* **2020**, *1*, 3, 238–255. doi: 10.3390/suschem1030016.

96. García, G., Aparicio, S., Ullah, R., Atilhan, M., Deep eutectic solvents: Physicochemical properties and gas separation applications. *Energy and Fuels* **2015**, *29*, 4, 2616–2644. doi: 10.1021/ef5028873.

97. Wang, G. N. *et al.*, Novel ionic liquid analogs formed by triethylbutylammonium carboxylate-water mixtures for CO 2 absorption. *J. Mol. Liq.* **2012**, *168*, 168, 17–20. doi: 10.1016/j.molliq.2011.12.006.

98. Duarte, A. R. C., Ferreira, A. S. D., Barreiros, S., Cabrita, E., Reis, R. L., Paiva, A., A

comparison between pure active pharmaceutical ingredients and therapeutic deep eutectic solvents: Solubility and permeability studies. *Eur. J. Pharm. Biopharm.* **2017**, *114*296–304. doi: 10.1016/j.ejpb.2017.02.003.

99. Lu, C., Cao, J., Wang, N., Su, E., Significantly improving the solubility of non-steroidal anti-inflammatory drugs in deep eutectic solvents for potential non-aqueous liquid administration. *Medchemcomm* **2016**, *7*, 5, 955–959. doi: 10.1039/c5md00551e.

100. Li, Z., Lee, P. I., Investigation on drug solubility enhancement using deep eutectic solvents and their derivatives. *Int. J. Pharm.* **2016**, *505*, 1–2, 283–288. doi: 10.1016/j.ijpharm.2016.04.018.

101. Jangir, A. K., Lad, B., Dani, U., Shah, N., Kuperkar, K., In vitro toxicity assessment and enhanced drug solubility profile of green deep eutectic solvent derivatives (DESDs) combined with theoretical validation. *RSC Adv.* **2020**, *10*, 40, 24063–24072. doi: 10.1039/c9ra10320a.

102. Gállego, I., Grover, M. A., Hud, N. V., Folding and Imaging of DNA Nanostructures in Anhydrous and Hydrated Deep-Eutectic Solvents. *Angew. Chemie Int. Ed.* **2015**, *54*, 23, 6765–6769. doi: 10.1002/anie.201412354.

103. Núñez-Pertíñez, S., Wilks, T. R., Deep Eutectic Solvents as Media for the Prebiotic DNA-Templated Synthesis of Peptides. *Front. Chem.* **2020**, *8*41. doi: 10.3389/fchem.2020.00041.

104. Mamajanov, I., Engelhart, A. E., Bean, H. D., Hud, N. V., DNA and RNA in Anhydrous Media: Duplex, Triplex, and G-Quadruplex Secondary Structures in a Deep Eutectic Solvent. *Angew. Chemie Int. Ed.* **2010**, *49*, 36, 6310–6314. doi: 10.1002/anie.201001561.

105. Mondal, D., Sharma, M., Mukesh, C., Gupta, V., Prasad, K., Improved solubility of DNA in recyclable and reusable bio-based deep eutectic solvents with long-term structural and chemical stability. *Chem. Commun.* **2013**, *49*, 83, 9606–9608. doi: 10.1039/c3cc45849k.

106. Zhao, C., Ren, J., Qu, X., G-quadruplexes form ultrastable parallel structures in deep eutectic solvent. *Langmuir* **2013**, *29*, 4, 1183–1191. doi: 10.1021/la3043186.

107. Lannan, F. M., Mamajanov, I., Hud, N. V., Human telomere sequence DNA in water-free and high-viscosity solvents: G-quadruplex folding governed by Kramers rate theory. *J. Am. Chem. Soc.* **2012**, *134*, 37, 15324–15330. doi: 10.1021/ja303499m.

108. Zhang, Y., De La Harpe, K., Hariharan, M., Kohler, B., Excited-state dynamics of mononucleotides and DNA strands in a deep eutectic solvent. *Faraday Discuss.* **2018**, *207*, 0, 267–282. doi: 10.1039/c7fd00205j.

109. Tortora, M. *et al.*, Effect of Hydrated Deep Eutectic Solvents on the Thermal Stability of DNA. *Crystals* **2021**, *11*, 9, 1057–1069. doi: 10.3390/CRYST11091057.

110. Hayyan, M., Looi, C. Y., Hayyan, A., Wong, W. F., Hashim, M. A., In Vitro and In Vivo Toxicity Profiling of Ammonium-Based Deep Eutectic Solvents. *PLoS One* **2015**, *10*, 2, e0117934. doi: 10.1371/journal.pone.0117934.

111. Radošević, K., Železnjak, J., Cvjetko Bubalo, M., Radojčić Redovniković, I., Slivac, I., Gaurina Srček, V., Comparative in vitro study of cholinium-based ionic liquids and deep eutectic solvents toward fish cell line. *Ecotoxicol. Environ. Saf.* **2016**, *131*30–36. doi: 10.1016/j.ecoenv.2016.05.005.

112. Mbous, Y. P., Hayyan, M., Wong, W. F., Looi, C. Y., Hashim, M. A., Unraveling the cytotoxicity and metabolic pathways of binary natural deep eutectic solvent systems. *Sci. Rep.* **2017**, *7*, 1, 1–14. doi: 10.1038/srep41257.

113. Macário, I. P. E. *et al.*, Cytotoxicity profiling of deep eutectic solvents to human skin cells. *Sci. Rep.* **2019**, *9*, 1, 1–9. doi: 10.1038/s41598-019-39910-y.

114. Nie, J., Chen, D., Lu, Y., Deep eutectic solvents based ultrasonic extraction of polysaccharides from edible brown Seaweed Sargassum horneri. *J. Mar. Sci. Eng.* **2020**, *8*, 6, . doi: 10.3390/JMSE8060440.

115. Dai, Y. *et al.*, Natural deep eutectic solvents in plants and plant cells: In vitro evidence for their possible functions. , in *Advances in Botanical Research*, *97*, Academic Press Inc., 2021, 159–184. doi: 10.1016/bs.abr.2020.09.012.

116. Choi, Y. H. *et al.*, Are natural deep eutectic solvents the missing link in understanding

cellular metabolism and physiology?. *Plant Physiol.* **2011**, *156*, 4, 1701–1705. doi: 10.1104/pp.111.178426.

117. Smith, E. L., Abbott, A. P., Ryder, K. S., Deep Eutectic Solvents (DESs) and Their Applications. *Chem. Rev.* **2014**, *114*, 21, 11060–11082. doi: 10.1021/cr300162p.

118. Van Osch, D. J. G. P. *et al.*, A Search for Natural Hydrophobic Deep Eutectic Solvents Based on Natural Components. *ACS Sustain. Chem. Eng.* **2019**, *7*, 3, 2933–2942. doi: 10.1021/acssuschemeng.8b03520.

119. Nahar, Y., Thickett, S. C., Greener, Faster, Stronger: The Benefits of Deep Eutectic Solvents in Polymer and Materials Science. *Polymers (Basel).* **2021**, *13*, 3, 471. doi: 10.3390/POLYM13030447.

120. Mokhtary, M., Deep Eutectic Solvents in The Synthesis of Polymers. *Acad. J. Polym. Sci.* **2019**, *2*, 3, 55–60. doi: 10.19080/AJOP.2019.02.555586.

121. Mota-Morales, J. D., Sánchez-Leija, R. J., Carranza, A., Pojman, J. A., del Monte, F., Luna-Bárcenas, G., Free-radical polymerizations of and in deep eutectic solvents: Green synthesis of functional materials. *Prog. Polym. Sci.* **2018**, *78*139–153. doi: 10.1016/J.PROGPOLYMSCI.2017.09.005.

122. Fernandes, P. M. V., Campiña, J. M., Pereira, C. M., Silva, F., Electrosynthesis of Polyaniline from Choline-Based Deep Eutectic Solvents: Morphology, Stability and Electrochromism. *J. Electrochem. Soc.* **2012**, *159*, 9, G97–G105. doi: 10.1149/2.059209JES.

123. Golgovici, F., Anicai, L., Florea, A., Visan, T., Electrochemical Synthesis of Conducting Polymers Involving Deep Eutectic Solvents. *Curr. Nanosci.* **2019**, *16*, 4, 478–494. doi: 10.2174/1573413715666190206145036.

124. García-Argüelles, S., García, C., Serrano, M. C., Gutiérrez, M. C., Ferrer, M. L., Del Monte, F., Near-to-eutectic mixtures as bifunctional catalysts in the low-temperature-ring-opening-polymerization of ε-caprolactone. *Green Chem.* **2015**, *17*, 6, 3632–3643. doi: 10.1039/C5GC00348B.

125. García-Argüelles, S. *et al.*, Deep eutectic solvent-assisted synthesis of biodegradable polyesters with antibacterial properties. *Langmuir* **2013**, *29*, 30, 9525–9534. doi: 10.1021/LA401353R/SUPPL_FILE/LA401353R_SI_001.PDF.

126. Bednarz, S., Fluder, M., Galica, M., Bogdal, D., Maciejaszek, I., Synthesis of hydrogels by polymerization of itaconic acid–choline chloride deep eutectic solvent. *J. Appl. Polym. Sci.* **2014**, *131*, 16, . doi: 10.1002/APP.40608.

127. Abo-Hamad, A., Hayyan, M., AlSaadi, M. A. H., Hashim, M. A., Potential applications of deep eutectic solvents in nanotechnology. , *Chemical Engineering Journal*, *273*. Elsevier B.V., 551–567, Aug. 01, 2015. doi: 10.1016/j.cej.2015.03.091.

128. Huang, Y. *et al.*, Synthesis and characterization of CuCl nanoparticles in deep eutectic solvents. *Part. Sci. Technol.* **2013**, *31*, 1, 81–84. doi: 10.1080/02726351.2011.648823.

129. Azizi, N., Edrisi, M., Manochehri, Z., Greener synthesis of magnetic nanoparticles in an aqueous deep eutectic solvent. *Sci. Iran.* **2016**, *23*, 6, 2750–2755. Accessed: Mar. 25, 2021. [Online]. Available: www.scientiairanica.com

130. Raghuwanshi, V. S., Ochmann, M., Hoell, A., Polzer, F., Rademann, K., Deep eutectic solvents for the self-assembly of gold nanoparticles: A SAXS, UV-Vis, and TEM investigation. *Langmuir* **2014**, *30*, 21, 6038–6046. doi: 10.1021/la500979p.

131. Lee, J. S., Deep eutectic solvents as versatile media for the synthesis of noble metal nanomaterials. *Nanotechnol. Rev.* **2017**, *6*, 3, 271–278. doi: 10.1515/ntrev-2016-0106.

132. Tohidi, M., Mahyari, F. A., Safavi, A., A seed-less method for synthesis of ultra-thin gold nanosheets by using a deep eutectic solvent and gum arabic and their electrocatalytic application. *RSC Adv.* **2015**, *5*, 41, 32744–32754. doi: 10.1039/c4ra17053a.

133. Shahidi, S. *et al.*, A new X-ray contrast agent based on highly stable gum arabic-gold nanoparticles synthesised in deep eutectic solvent. *J. Exp. Nanosci.* **2015**, *10*, 12, 911–924. doi: 10.1080/17458080.2014.933493.

134. Abbott, A. P., Ttaib, K. El, Frisch, G., Ryder, K. S., Weston, D., The electrodeposition of silver composites using deep eutectic solvents. *Phys. Chem. Chem. Phys.* **2012**, *14*, 7,

2443–2449. doi: 10.1039/c2cp23712a.

135. Malaquias, J. C., Steichen, M., Thomassey, M., Dale, P. J., Electrodeposition of Cu-In alloys from a choline chloride based deep eutectic solvent for photovoltaic applications. *Electrochim. Acta* **2013**, *103*15–22. doi: 10.1016/j.electacta.2013.04.068.

136. Gómez, E., Cojocaru, P., Magagnin, L., Valles, E., Electrodeposition of Co, Sm and SmCo from a Deep Eutectic Solvent. *J. Electroanal. Chem.* **2011**, *658*, 1–2, 18–24. doi: 10.1016/j.jelechem.2011.04.015.

137. Jenkin, G. R. T. *et al.*, The application of deep eutectic solvent ionic liquids for environmentally-friendly dissolution and recovery of precious metals. *Miner. Eng.* **2016**, *87*18–24. doi: 10.1016/j.mineng.2015.09.026.

138. You, Y. H., Gu, C. D., Wang, X. L., Tu, J. P., Electrodeposition of Ni-Co alloys from a deep eutectic solvent. *Surf. Coatings Technol.* **2012**, *206*, 17, 3632–3638. doi: 10.1016/j.surfcoat.2012.03.001.

139. Abbott, A. P., Capper, G., McKenzie, K. J., Ryder, K. S., Electrodeposition of zinc-tin alloys from deep eutectic solvents based on choline chloride. *J. Electroanal. Chem.* **2007**, *599*, 2, 288–294. doi: 10.1016/j.jelechem.2006.04.024.

140. Abbott, A. P., Capper, G., Davies, D. L., McKenzie, K. J., Obi, S. U., Solubility of metal oxides in deep eutectic solvents based on choline chloride. *J. Chem. Eng. Data* **2006**, *51*, 4, 1280–1282. doi: 10.1021/je060038c.

141. Gamburg, Y. D., Zangari, G., *Theory and Practice of Metal Electrodeposition*. Springer Science & Business Media, 2011. doi: 10.1007/978-1-4419-9669-5.

142. Lloyd, D., Vainikka, T., Kontturi, K., The development of an all copper hybrid redox flow battery using deep eutectic solvents. *Electrochim. Acta* **2013**, *100*18–23. doi: 10.1016/j.electacta.2013.03.130.

143. Yang, H., Guo, X., Birbilis, N., Wu, G., Ding, W., Tailoring nickel coatings via electrodeposition from a eutectic-based ionic liquid doped with nicotinic acid. *Appl. Surf. Sci.* **2011**, *257*, 21, 9094–9102. doi: 10.1016/J.APSUSC.2011.05.106.

144. Bernasconi, R., Panzeri, G., Accogli, A., Liberale, F., Nobili, L., L.Magagnin, Electrodeposition from Deep Eutectic Solvents. , in *Progress and Developments in Ionic Liquids*, IntechOpen, 2017, 235–261. doi: 10.5772/64935.

145. Wu, Z. *et al.*, Deep Eutectic Solvent Synthesis of LiMnPO4/C Nanorods as a Cathode Material for Lithium Ion Batteries. *Materials (Basel).* **2017**, *10*, 2, 134. doi: 10.3390/ma10020134.

146. Wang, Y. *et al.*, Zn-based eutectic mixture as anolyte for hybrid redox flow batteries. *Sci. Rep.* **2018**, *8*, 1, 1–8. doi: 10.1038/s41598-018-24059-x.

147. Chakrabarti, B. *et al.*, Evaluation of a non-aqueous vanadium redox flow battery using a deep eutectic solvent and graphene-modified carbon electrodes via electrophoretic deposition. *Batteries* **2020**, *6*, 3, 1–20. doi: 10.3390/batteries6030038.

148. Chakrabarti, M. H. *et al.*, Prospects of applying ionic liquids and deep eutectic solvents for renewable energy storage by means of redox flow batteries. , *Renewable and Sustainable Energy Reviews*, *30*. Elsevier Ltd, 254–270, Feb. 01, 2014. doi: 10.1016/j.rser.2013.10.004.

149. Boldrini, C. L., Manfredi, N., Perna, F. M., Trifiletti, V., Capriati, V., Abbotto, A., Dye-Sensitized Solar Cells that use an Aqueous Choline Chloride-Based Deep Eutectic Solvent as Effective Electrolyte Solution. *Energy Technol.* **2017**, *5*, 2, 345–353. doi: 10.1002/ente.201600420.

150. Jhong, H. R., Wong, D. S. H., Wan, C. C., Wang, Y. Y., Wei, T. C., A novel deep eutectic solvent-based ionic liquid used as electrolyte for dye-sensitized solar cells. *Electrochem. commun.* **2009**, *11*, 1, 209–211. doi: 10.1016/j.elecom.2008.11.001.

151. Yang, Y., Zhang, Z., Gao, J., Lin, Z. H., Yan, J. Y., Guo, X. Y., Deep eutectic solvent based polymer electrolyte for dye-sensitized solar cells. *Wuji Cailiao Xuebao/Journal Inorg. Mater.* **2017**, *32*, 1, 25–32. doi: 10.15541/jim20160184.

152. Boldrini, C. L., Manfredi, N., Perna, F. M., Capriati, V., Abbotto, A., Eco-Friendly Sugar-Based Natural Deep Eutectic Solvents as Effective Electrolyte Solutions for Dye-Sensitized Solar Cells. *ChemElectroChem* **2020**, *7*, 7, 1707–1712. doi:

10.1002/celc.202000376.

153. Zhang, Y., Han, J., Liao, C., Insights into the Properties of Deep Eutectic Solvent Based on Reline for Ga-Controllable CIGS Solar Cell in One-Step Electrodeposition. *J. Electrochem. Soc.* **2016**, *163*, 13, D689–D693. doi: 10.1149/2.0611613jes.

154. Sato, T., Masuda, G., Takagi, K., Electrochemical properties of novel ionic liquids for electric double layer capacitor applications. *Electrochim. Acta* **2004**, *49*, 21, 3603–3611. doi: 10.1016/J.ELECTACTA.2004.03.030.

155. Nguyen, D. *et al.*, Choline chloride-based deep eutectic solvents as effective electrolytes for dye-sensitized solar cells. *RSC Adv.* **2021**, *11*, 35, 21560–21566. doi: 10.1039/D1RA03273A.

156. Rudovica, V. *et al.*, Valorization of Marine Waste: Use of Industrial By-Products and Beach Wrack Towards the Production of High Added-Value Products. *Front. Mar. Sci.* **2021**, *8*1350. doi: 10.3389/FMARS.2021.723333/BIBTEX.

157. Mirabella, N., Castellani, V., Sala, S., Current options for the valorization of food manufacturing waste: a review. *J. Clean. Prod.* **2014**, *65*28–41. doi: 10.1016/J.JCLEPRO.2013.10.051.

158. Corrado, S. *et al.*, Food waste accounting methodologies: Challenges, opportunities, and further advancements. *Glob. Food Sec.* **2019**, *20*93–100. doi: 10.1016/J.GFS.2019.01.002.

159. Ma, Y., Liu, Y., Turning food waste to energy and resources towards a great environmental and economic sustainability: An innovative integrated biological approach. *Biotechnol. Adv.* **2019**, *37*, 7, 107425. doi: 10.1016/J.BIOTECHADV.2019.06.013.

160. Food and Agriculture Organization (FAO), *The State of World Fisheries and Aquaculture 2020. In brief*. FAO, 2020. doi: 10.4060/CA9231EN.

161. Jiménez, C., Marine Natural Products in Medicinal Chemistry. *ACS Med. Chem. Lett.* **2018**, *9*, 10, 959–961. doi: 10.1021/ACSMEDCHEMLETT.8B00368.

162. Korhonen, J., Honkasalo, A., Seppälä, J., Circular Economy: The Concept and its

Limitations. *Ecol. Econ.* **2018**, *143*37–46. doi: 10.1016/J.ECOLECON.2017.06.041.

163. Ricciardi, P., Cillari, G., Carnevale Miino, M., Collivignarelli, M. C., Valorization of agro-industry residues in the building and environmental sector: A review. *Waste Manag. Res.* **2020**, *38*, 5, 487–513. doi: 10.1177/0734242X20904426.

164. Amberg, N., Fogarassy, C., Green Consumer Behavior in the Cosmetics Market. *Resources* **2019**, *8*, 3, 137. doi: 10.3390/RESOURCES8030137.

165. Abdallah, M. M., Fernández, N., Matias, A. A., Bronze, M. do R., Hyaluronic acid and Chondroitin sulfate from marine and terrestrial sources: Extraction and purification methods. *Carbohydr. Polym.* **2020**, *243*, April, 116441. doi: 10.1016/j.carbpol.2020.116441.

166. Atanasov, A. G., Zotchev, S. B., Dirsch, V. M., Supuran, C. T., Natural products in drug discovery: advances and opportunities. *Nat. Rev. Drug Discov. 2021 203* **2021**, *20*, 3, 200–216. doi: 10.1038/s41573-020-00114-z.

167. Saxena, P., *Development of Plant-Based Medicines: Conservation, Efficacy and Safety*. Dordrecht, The Netherlands: Kluwer Academic Publishers,., 2001. doi: 10.1007/978-94-015-9779-1.

168. Vázquez, J., Rodríguez-Amado, I., Montemayor, M., Fraguas, J., González, M., Murado, M., Chondroitin Sulfate, Hyaluronic Acid and Chitin/Chitosan Production Using Marine Waste Sources: Characteristics, Applications and Eco-Friendly Processes: A Review. *Mar. Drugs* **2013**, *11*, 12, 747–774. doi: 10.3390/md11030747.

169. Esko, J. D., Kimata, K., Lindahl, U., *Proteoglycans and Sulfated Glycosaminoglycans*, 2nd Editio. Cold Spring Harbor Laboratory Press, 2009.

170. Langer, M. R., Biosynthesis of glycosaminoglycans in foraminifera: A review. *Mar. Micropaleontol.* **1992**, *19*, 3, 245–255. doi: 10.1016/0377-8398(92)90031-E.

171. Severin, I. C. *et al.*, Glycosaminoglycan analogs as a novel anti-inflammatory strategy. *Front. Immunol.* **2012**, *3*, OCT, . doi: 10.3389/fimmu.2012.00293.

172. Morla, S., Glycosaminoglycans and glycosaminoglycan mimetics in cancer and

inflammation. , *International Journal of Molecular Sciences*, *20*, 8, . 1963, 2019. doi: 10.3390/ijms20081963.

173. Kovensky, J., Grand, E., Uhrig, M. L., Applications of Glycosaminoglycans in the Medical, Veterinary, Pharmaceutical, and Cosmetic Fields. , in *Industrial Applications of Renewable Biomass Products*, Cham: Springer International Publishing, 2017, 135–164. doi: 10.1007/978-3-319-61288-1_5.

174. Volpi, N., Therapeutic Applications of Glycosaminoglycans. *Curr. Med. Chem.* **2006**, *13*, 15, 1799–1810. doi: 10.2174/092986706777452470.

175. Köwitsch, A., Zhou, G., Groth, T., Medical application of glycosaminoglycans: a review. *J. Tissue Eng. Regen. Med.* **2018**, *12*, 1, e23–e41. doi: 10.1002/term.2398.

176. Goh, J. C. H., Sahoo, S., Scaffolds for tendon and ligament tissue engineering. , in *Regenerative Medicine and Biomaterials for the Repair of Connective Tissues*, Elsevier, 2010, 452–468. doi: 10.1533/9781845697792.2.452.

177. Nakano, T., Sim, J. S., Glycosaminoglycans from the Rooster Comb and Wattle. *Poult. Sci.* **1989**, *68*, 9, 1303–1306. doi: 10.3382/ps.0681303.

178. Fermor, H. L. *et al.*, Biological, biochemical and biomechanical characterisation of articular cartilage from the porcine, bovine and ovine hip and knee. *Biomed. Mater. Eng.* **2015**, *25*, 4, 381–395. doi: 10.3233/BME-151533.

179. Romanowicz, L., Bańkowski, E., Jaworski, S., Chyczewski, L., Glycosaminoglycans of umbilical cord arteries and their alterations in EPH-gestosis. *Folia Histochem. Cytobiol.* **1994**, *32*, 3, 199–204.

180. Zainudin, N. H., Sirajudeen, K. N. S., Ghazali, F. C., Marine Sourced Glycosaminoglycans “GAGs.” *J. Adv. Lab. Res. Biol.* **2014**, *5*, 3, 46–53.

181. Oliveira, G. B. de *et al.*, Composition and significance of glycosaminoglycans in the uterus and placenta of mammals. *Brazilian Arch. Biol. Technol.* **2015**, *58*, 4, 512–520. doi: 10.1590/S1516-8913201500281.

182. Nam Chang, H., Kim, N.-J., Kang, J., Moon Jeong, C., Biomass-derived Volatile Fatty

Acid Platform for Fuels and Chemicals. *Biotechnol. Bioprocess Eng.* **2010**, *15*1–10. doi: 10.1007/s12257-009-3070-8.

183. Trivedi, N. *et al.*, An integrated process for the extraction of fuel and chemicals from marine macroalgal biomass. *Nat. Publ. Gr.* **2016**, . doi: 10.1038/srep30728.

184. Caruso, G., Fishery Wastes and By-products: A Resource to Be Valorised. *J. Fish. Sci.* **2015**, *9*, 4, 80–83. Accessed: Mar. 17, 2020. [Online]. Available: https://www.researchgate.net/publication/284625083_Fishery_Wastes_and_By-products_A_Resource_to_Be_Valorised

185. Gandhi, N. S., Mancera, R. L., The Structure of Glycosaminoglycans and their Interactions with Proteins. *Chem. Biol. Drug Des.* **2008**, *72*, 6, 455–482. doi: 10.1111/j.1747-0285.2008.00741.x.

186. Rudd, T. R., Yates, E. A., Conformational degeneracy restricts the effective information content of heparan sulfate. *Mol. Biosyst.* **2010**, *6*, 5, 902. doi: 10.1039/b923519a.

187. Sampaio, L. O. *et al.*, Heparins and heparan sulfates. Structure, distribution and protein interactions. , in *Insights into carbohydrate structure and biological function*, *37*, 2, , 2006, 1–24.

188. Pudełko, A., Wisowski, G., Olczyk, K., Koźma, E. M., The dual role of the glycosaminoglycan chondroitin-6-sulfate in the development, progression and metastasis of cancer. , *FEBS Journal*, *286*, 10, . Blackwell Publishing Ltd, 1815–1837, May 01, 2019. doi: 10.1111/febs.14748.

189. Myron, P., Siddiquee, S., Al Azad, S., Fucosylated chondroitin sulfate diversity in sea cucumbers: A review. , *Carbohydrate Polymers*, *112*. Elsevier Ltd, 173–178, Nov. 04, 2014. doi: 10.1016/j.carbpol.2014.05.091.

190. Lamberg, S. I., Stoolmiller, A. C., Glycosaminoglycans. A biochemical and clinical review. *J. Invest. Dermatol.* **1974**, *63*, 6, 433–449. doi: 10.1111/1523-1747.ep12680346.

191. Lindahl, U., Couchman, J., Kimata, K., Esko, J. D., *Proteoglycans and Sulfated Glycosaminoglycans*. Cold Spring Harbor Laboratory Press, 2015. doi:

10.1101/GLYCOBIOLOGY.3E.017.

192. Laurent, T. C., Fraser, J. R., Hyaluronan. *FASEB J.* **1992**, *6*, 7, 2397–404. Accessed: Nov. 27, 2018. [Online]. Available: http://www.ncbi.nlm.nih.gov/pubmed/1563592

193. Sadhasivam, G., Muthuvel, A., Isolation and characterization of hyaluronic acid from marine organisms. *Adv. Food Nutr. Res.* **2014**, *72*61–77. doi: 10.1016/B978-0-12-800269-8.00004-X.

194. Fakhari, A., Berkland, C., Applications and emerging trends of hyaluronic acid in tissue engineering, as a dermal filler and in osteoarthritis treatment. *Acta Biomater.* **2013**, *9*, 7, 7081–92. doi: 10.1016/j.actbio.2013.03.005.

195. Garg, H. G., Hales, C. A., *Chemistry and biology of hyaluronan*. Elsevier, 2004.

196. Barrie, F. C., Lars M, B., Richard, M., Lars K, N., Microbial hyaluronic acid production. *Appl. Microbiol. Biotechnol.* **2005**, *66*, 4, 341–351.

197. Kogan, G., Šoltés, L., Stern, R., Gemeiner, P., Hyaluronic acid: a natural biopolymer with a broad range of biomedical and industrial applications. *Biotechnol. Lett.* **2006**, *29*, 1, 17–25. doi: 10.1007/s10529-006-9219-z.

198. Collins, M. N., Birkinshaw, C., Hyaluronic acid based scaffolds for tissue engineering—A review. *Carbohydr. Polym.* **2013**, *92*, 2, 1262–1279. doi: 10.1016/J.CARBPOL.2012.10.028.

199. Abdelrahman, R. M. *et al.*, Hyaluronan biofilms reinforced with partially deacetylated chitin nanowhiskers: Extraction, fabrication, in-vitro and antibacterial properties of advanced nanocomposites. *Carbohydr. Polym.* **2020**, *235*115951. doi: 10.1016/j.carbpol.2020.115951.

200. Abdel-Rahman, R. M. *et al.*, Wound dressing based on chitosan/hyaluronan/nonwoven fabrics: Preparation, characterization and medical applications. *Int. J. Biol. Macromol.* **2016**, *89*725–736. doi: 10.1016/j.ijbiomac.2016.04.087.

201. Abdel-Mohsen, A. M. *et al.*, A novel in situ silver/hyaluronan bio-nanocomposite fabrics for wound and chronic ulcer dressing: In vitro and in vivo evaluations. *Int. J. Pharm.* **2017**,

520, 1–2, 241–253. doi: 10.1016/j.ijpharm.2017.02.003.

202. Abdel-Mohsen, A. M. *et al.*, Antibacterial activity and cell viability of hyaluronan fiber with silver nanoparticles. *Carbohydr. Polym.* **2013**, *92*, 2, 1177–1187. doi: 10.1016/j.carbpol.2012.08.098.

203. Toole, B. P., Wight, T. N., Tammi, M. I., Hyaluronan-cell interactions in cancer and vascular disease. *J. Biol. Chem.* **2002**, *277*, 7, 4593–6. doi: 10.1074/jbc.R100039200.

204. Zakeri, A., Rasaee, M. J., Pourzardosht, N., Enhanced hyluronic acid production in Streptococcus zooepidemicus by over expressing HasA and molecular weight control with Niscin and glucose. **2017**, . doi: 10.1016/j.btre.2017.02.007.

205. Blatter, G., Jacquinet, J. C., The use of 2-deoxy-2-trichloroacetamido-D-glucopyranose derivatives in syntheses of hyaluronic acid-related tetra-, hexa-, and octa-saccharides having a methyl beta-D-glucopyranosiduronic acid at the reducing end. *Carbohydr. Res.* **1996**, *288*109–25. doi: https://doi.org/10.1016/s0008-6215(96)90785-5.

206. Huang, L., Huang, X., Highly Efficient Syntheses of Hyaluronic Acid Oligosaccharides. *Chem. - A Eur. J.* **2007**, *13*, 2, 529–540. doi: 10.1002/chem.200601090.

207. Dinkelaar, J., Gold, H., Overkleeft, H. S., Codée, J. D. C., van der Marel, G. A., Synthesis of Hyaluronic Acid Oligomers using Chemoselective and One-Pot Strategies. *J. Org. Chem.* **2009**, *74*, 11, 4208–4216. doi: 10.1021/jo9003713.

208. Lu, X., Kamat, M. N., Huang, L., Huang, X., Chemical Synthesis of a Hyaluronic Acid Decasaccharide. *Jounral Org. Chem.* **2009**, *74*, 20, 7608–7617. doi: 10.1021/jo9016925.

209. Abdel-Mohsen, A. M. *et al.*, Green synthesis of hyaluronan fibers with silver nanoparticles. *Carbohydr. Polym.* **2012**, *89*, 2, 411–422. doi: 10.1016/j.carbpol.2012.03.022.

210. Abdel-Mohsen, A. M., Pavliňák, D., Čileková, M., Lepcio, P., Abdel-Rahman, R. M., Jančář, J., Electrospinning of hyaluronan/polyvinyl alcohol in presence of in-situ silver nanoparticles: Preparation and characterization. *Int. J. Biol. Macromol.* **2019**, *139*730–739. doi: 10.1016/j.ijbiomac.2019.07.205.

211. Mathews, M. B., Macromolecular evolution of connective tissue. *Biol. Rev.* **1967**, *42*, 4, 499–551. doi: 10.1111/j.1469-185X.1967.tb01528.x.

212. Haylock-Jacobs, S., Keough, M. B., Lau, L., Yong, V. W., Chondroitin sulphate proteoglycans: Extracellular matrix proteins that regulate immunity of the central nervous system. *Autoimmun. Rev.* **2011**, *10*, 12, 766–772. doi: 10.1016/J.AUTREV.2011.05.019.

213. Malavaki, C., Mizumoto, S., Karamanos, N., Sugahara, K., Recent Advances in the Structural Study of Functional Chondroitin Sulfate and Dermatan Sulfate in Health and Disease. *Connect. Tissue Res.* **2008**, *49*, 3–4, 133–139. doi: 10.1080/03008200802148546.

214. Sugahara, K., Shigeno, K., Masuda, M., Fujii, N., Kurosaka, A., Takeda, K., Structural studies on the chondroitinase ABC-resistant sulfated tetrasaccharides isolated from various chondroitin sulfate isomers. *Carbohydr. Res.* **1994**, *255*145–163. doi: 10.1016/S0008-6215(00)90976-5.

215. Robinsons, H. C., Dorfman, A., The Sulfation of Chondroitin Sulfate in Embryonic Chick Cartilage Epiphyses. *J. Biol. Chem.* **1969**, *244*, 2, 348–352.

216. Hjertquist, S. O., Wasteson, Å., The molecular weight of chondroitin sulphate from human articular cartilage - Effect of age and of osteoarthritis. *Calcif. Tissue Res.* **1972**, *10*, 1, 31–37. doi: 10.1007/BF02012533.

217. Schiraldi, C., Cimini, D., De Rosa, M., Production of chondroitin sulfate and chondroitin. *Appl. Microbiol. Biotechnol.* **2010**, *87*, 4, 1209–1220. doi: 10.1007/s00253-010-2677-1.

218. Henrotin, Y., Mathy, M., Sanchez, C., Lambert, C., Chondroitin sulfate in the treatment of osteoarthritis: from in vitro studies to clinical recommendations. *Ther. Adv. Musculoskelet. Dis.* **2010**, *2*, 6, 335–48. doi: 10.1177/1759720X10383076.

219. Gilbert, M. E. *et al.*, Chondroitin Sulfate Hydrogel and Wound Healing in Rabbit Maxillary Sinus Mucosa. *Laryngoscope* **2004**, *114*, 8, 1406–1409. doi: 10.1097/00005537-200408000-00017.

220. Volpi, N., Maccari, F., Purification and characterization of hyaluronic acid from the

mollusc bivalve Mytilus galloprovincialis. *Biochimie* **2003**, *85*, 6, 619–625. doi: 10.1016/S0300-9084(03)00083-X.

221. Mucci, A., Schenetti, L., Volpi, N., 1H and 13C nuclear magnetic resonance identification and characterization of components of chondroitin sulfates of various origin. *Carbohydr. Polym.* **2000**, *41*, 1, 37–45. doi: 10.1016/S0144-8617(99)00075-2.

222. Volpi, N., Disaccharide mapping of chondroitin sulfate of different origins by high-performance capillary electrophoresis and high-performance liquid chromatography. *Carbohydr. Polym.* **2004**, *55*, 3, 273–281. doi: 10.1016/J.CARBPOL.2003.09.010.

223. Volpi, N., Analytical aspects of pharmaceutical grade chondroitin sulfates. *J. Pharm. Sci.* **2007**, *96*, 12, 3168–3180. doi: 10.1002/jps.20997.

224. Silbert, J. E., Sugumaran, G., Biosynthesis of Chondroitin/Dermatan Sulfate. *IUBMB Life (International Union Biochem. Mol. Biol. Life)* **2002**, *54*, 4, 177–186. doi: 10.1080/15216540214923.

225. Poh, Z. W., Gan, C. H., Lee, E. J., Guo, S., Yip, G. W., Lam, Y., Divergent Synthesis of Chondroitin Sulfate Disaccharides and Identification of Sulfate Motifs that Inhibit Triple Negative Breast Cancer. *Nat. Publ. Gr.* **2015**, . doi: 10.1038/srep14355.

226. Chen, S., Xue, C., Yin, L., Tang, Q., Yu, G., Chai, W., Comparison of structures and anticoagulant activities of fucosylated chondroitin sulfates from different sea cucumbers. *Carbohydr. Polym.* **2011**, *83*, 2, 688–696. doi: 10.1016/j.carbpol.2010.08.040.

227. Liu, H., Zhang, X., Wu, M., Li, Z., Synthesis and anticoagulation studies of “short-armed” fucosylated chondroitin sulfate glycoclusters. *Carbohydr. Res.* **2018**, *467*45–51. doi: 10.1016/j.carres.2018.07.008.

228. Vieira, R. P., Mulloy, B., Mourao, P. A. S., Structure of a Fucose-branched Chondroitin Sulfate from Sea Cucumber. *J. Biol. Chem.* **1991**, *266*, 21, 13530–13536.

229. He, W., Fu, L., Li, G., Andrew Jones, J., Linhardt, R. J., Koffas, M., Production of chondroitin in metabolically engineered E. coli. *Metab. Eng.* **2015**, *27*92–100. doi: 10.1016/J.YMBEN.2014.11.003.

230. Jin, P., Zhang, L., Yuan, P., Kang, Z., Du, G., Chen, J., Efficient biosynthesis of polysaccharides chondroitin and heparosan by metabolically engineered Bacillus subtilis. *Carbohydr. Polym.* **2016**, *140*424–432. doi: 10.1016/J.CARBPOL.2015.12.065.

231. Shi, Y., Meng, Y., Li, J., Chen, J., Liu, Y., Bai, X., Chondroitin sulfate: extraction, purification, microbial and chemical synthesis. *J. Chem. Technol. Biotechnol.* **2014**, *89*, 10, 1445–1465. doi: 10.1002/jctb.4454.

232. Senni, K. *et al.*, Marine polysaccharides: a source of bioactive molecules for cell therapy and tissue engineering. *Mar. Drugs* **2011**, *9*, 9, 1664–81. doi: 10.3390/md9091664.

233. Garnjanagoonchorn, W., Wongekalak, L., Engkagul, A., Determination of Chondroitin Sulfate from different sources of cartilage. *Chem. Eng. Process. Process Intensif.* **2007**, *46*, 5, 465–471. doi: 10.1016/J.CEP.2006.05.019.

234. Maccari, F., Galeotti, F., Volpi, N., Isolation and structural characterization of chondroitin sulfate from bony fishes. *Carbohydr. Polym.* **2015**, *129*143–147. doi: 10.1016/j.carbpol.2015.04.059.

235. Higashi, K. *et al.*, Functional Chondroitin sulfate from Enteroctopus dofleini containing a 3- O -sulfo glucuronic acid residue. *Carbohydr. Polym.* **2015**, *134*557–565. doi: 10.1016/j.carbpol.2015.07.082.

236. Xie, J., Ye, J., Luo, H. Y., An efficient preparation of chondroitin sulfate and collagen peptides from shark cartilage. *Int. Food Res. J.* **2014**, *21*, 3, 1171–1175.

237. Higashi, K. *et al.*, Composition of Glycosaminoglycans in Elasmobranchs including Several Deep-Sea Sharks: Identification of Chondroitin/Dermatan Sulfate from the Dried Fins of Isurus oxyrinchus and Prionace glauca. *PLoS One* **2015**, *10*, 3, e0120860. doi: 10.1371/journal.pone.0120860.

238. Lamari, F. N., Karamanos, N. K., Structure of chondroitin sulfate. *Adv. Pharmacol.* **2006**, *53*33–48. doi: 10.1016/S1054-3589(05)53003-5.

239. Blanco, M., Fraguas, J., Sotelo, C. G., Pérez-Martín, R. I., Vázquez, J. A., Production of chondroitin sulphate from head, skeleton and fins of Scyliorhinus canicula by-products by

combination of enzymatic, chemical precipitation and ultrafiltration methodologies. *Mar. Drugs* **2015**, *13*, 6, 3287–3308. doi: 10.3390/md13063287.

240. Vázquez, J. *et al.*, Isolation and Chemical Characterization of Chondroitin Sulfate from Cartilage By-Products of Blackmouth Catshark (Galeus melastomus). *Mar. Drugs* **2018**, *16*, 10, 344. doi: 10.3390/md16100344.

241. Vasconcelos Oliveira, A. P. *et al.*, Characteristics of Chondroitin Sulfate Extracted of Tilapia (Oreochromis niloticus) Processing. *Procedia Eng.* **2017**, *200*193–199. doi: 10.1016/j.proeng.2017.07.028.

242. Souza, A. R. C., Kozlowski, E. O., Cerqueira, V. R., Castelo-Branco, M. T. L., Costa, M. L., Pavão, M. S. G., Chondroitin sulfate and keratan sulfate are the major glycosaminoglycans present in the adult zebrafish Danio rerio (Chordata-Cyprinidae). *Glycoconj. J.* **2007**, *24*, 9, 521–530. doi: 10.1007/s10719-007-9046-z.

243. Novoa-Carballal, R. *et al.*, By-products of Scyliorhinus canicula, Prionace glauca and Raja clavata: A valuable source of predominantly 6S sulfated chondroitin sulfate. *Carbohydr. Polym.* **2017**, *157*31–37. doi: 10.1016/J.CARBPOL.2016.09.050.

244. Vázquez, J. A., Blanco, M., Fraguas, J., Pastrana, L., Pérez-Martín, R., Optimisation of the extraction and purification of Chondroitin sulphate from head by-products of Prionace glauca by environmental friendly processes. *Food Chem.* **2016**, *198*28–35. doi: 10.1016/j.foodchem.2015.10.087.

245. Zhao, T. *et al.*, Extraction, purification and characterisation of chondroitin sulfate in Chinese sturgeon cartilage. *J. Sci. Food Agric.* **2013**, *93*, 7, 1633–1640. doi: 10.1002/jsfa.5937.

246. Kim, S.-B. *et al.*, Simplified purification of chondroitin sulphate from scapular cartilage of shortfin mako shark (Isurus oxyrinchus). *Int. J. Food Sci. Technol.* **2012**, *47*, 1, 91–99. doi: 10.1111/j.1365-2621.2011.02811.x.

247. Murado, M. A., Fraguas, J., Montemayor, M. I., Vázquez, J. A., González, P., Preparation of highly purified chondroitin sulphate from skate (Raja clavata) cartilage by-products. Process optimization including a new procedure of alkaline hydroalcoholic hydrolysis.

Biochem. Eng. J. **2010**, *49*, 1, 126–132. doi: 10.1016/j.bej.2009.12.006.

248. Song, Y. O. *et al.*, Chondroitin sulfate-rich extract of skate cartilage attenuates lipopolysaccharide-induced liver damage in mice. *Mar. Drugs* **2017**, *15*, 6, 1–14. doi: 10.3390/md15060178.

249. Jeong, K.-S., Development of High Purity Purification Method of Chondroitin Sulfate Extracted from Skate Cartilage. *J. Korea Acad. Coop. Soc.* **2016**, *17*, 6, 9–17. doi: 10.5762/KAIS.2016.17.6.9.

250. Lignot, B., Lahogue, V., Bourseau, P., Enzymatic extraction of chondroitin sulfate from skate cartilage and concentration-desalting by ultrafiltration. *J. Biotechnol.* **2003**, *103*, 3, 281–284. doi: 10.1016/S0168-1656(03)00139-1.

251. Gargiulo, V., Lanzetta, R., Parrilli, M., De Castro, C., Structural analysis of chondroitin sulfate from Scyliorhinus canicula: A useful source of this polysaccharide. *Glycobiology* **2009**, *19*, 12, 1485–1491. doi: 10.1093/glycob/cwp123.

252. Takai, M., Kono, H., Salmon-origin chondroitin sulfate. , 2003

253. Tamura, J. *et al.*, Sulfation Patterns and the Amounts of Chondroitin Sulfate in the Diamond Squid, Thysanoteuthis rhombus. *Biosci. Biotechnol. Biochem.* **2009**, *73*, 6, 1387–1391. doi: 10.1271/bbb.90037.

254. Karamanos, N. K., Manouras, A., Tsegenidis, T., Antonopoulos, C. A., Isolation and chemical study of the glycosaminoglycans from squid cornea. *Int. J. Biochem.* **1991**, *23*, 1, 67–72.

255. Sumi, T. *et al.*, Method for the preparation of chondroitin sulfate compounds. , Jan. 29, 2002

256. Bai, M., Han, W., Zhao, X., Wang, Q., Gao, Y., Deng, S., Glycosaminoglycans from a Sea Snake (Lapemis curtus): Extraction, Structural Characterization and Antioxidant Activity. *Mar. Drugs* **2018**, *16*, 5, . doi: 10.3390/md16050170.

257. Murado, M. A., Montemayor, M. I., Cabo, M. L., Vázquez, J. A., González, M. P., Optimization of extraction and purification process of hyaluronic acid from fish eyeball.

Food Bioprod. Process. **2012**, *90*, 3, 491–498. doi: 10.1016/J.FBP.2011.11.002.

258. Kanchana, S., Arumugam, M., Giji, S., Balasubramanian, T., Isolation, characterization and antioxidant activity of hyaluronic acid from marine bivalve mollusc Amussium pleuronectus (Linnaeus, 1758). *Bioact. Carbohydrates Diet. Fibre* **2013**, *2*, 1, 1–7. doi: 10.1016/J.BCDF.2013.06.001.

259. Sadhasivam, G., Muthuvel, A., Pachaiyappan, A., Thangavel, B., Isolation and characterization of hyaluronic acid from the liver of marine stingray Aetobatus narinari. *Int. J. Biol. Macromol.* **2013**, *54*84–89. doi: 10.1016/J.IJBIOMAC.2012.11.028.

260. Mizuno, H., Iso, N., Saito, T., Ogawa, H., Sawairi, H., Saito, M., Characterization of hyaluronic acid of yellowfin tuna eyeball. *Nippon SUISAN GAKKAISHI* **1991**, *57*, 3, 517–519. doi: 10.2331/suisan.57.517.

261. Amagai, I., Tashiro, Y., Ogawa, H., Improvement of the extraction procedure for hyaluronan from fish eyeball and the molecular characterization. *Fish. Sci.* **2009**, *75*, 3, 805–810. doi: 10.1007/s12562-009-0092-2.

262. Jayathilakan, K., Sultana, K., Radhakrishna, K., Bawa, A. S., Utilization of byproducts and waste materials from meat, poultry and fish processing industries: a review. *J. Food Sci. Technol.* **2012**, *49*, 3, 278–93. doi: 10.1007/s13197-011-0290-7.

263. Sakar, S., Yetilmezsoy, K., Kocak, E., Anaerobic digestion technology in poultry and livestock waste treatment — a literature review. *Waste Manag. Res.* **2009**, *27*, 1, 3–18. doi: 10.1177/0734242X07079060.

264. Nakano, T., Nakano, K., Sim, J. S., A Simple Rapid Method To Estimate Hyaluronic Acid Concentrations in Rooster Comb and Wattle Using Cellulose Acetate Electrophoresis. *J. Agric. Food Chem.* **1994**, *42*, 12, 2766–2768. doi: 10.1021/jf00048a022.

265. Cullis-Hill, D., Preparation of hyaluronic acid from synovial fluid. *U.S. Pat. No. 4,879,375* **1989**, . Accessed: Mar. 05, 2019. [Online]. Available: https://patents.google.com/patent/US4879375

266. Gherezghiher, T., Koss, M. C., Nordquist, R. E., Wilkinson, C. P., Analysis of vitreous and

aqueous levels of hyaluronic acid: Application of high-performance liquid chromatography. *Exp. Eye Res.* **1987**, *45*, 2, 347–349. doi: 10.1016/S0014-4835(87)80156-2.

267. Balazs, E. A., Ultrapure hyaluronic acid and the use thereof. , Oct. 25, 1977 Accessed: Jun. 28, 2019. [Online]. Available: https://patents.google.com/patent/US4141973A/en

268. Swann, D. A., Studies on hyaluronic acid: I. The preparation and properties of rooster comb hyaluronic acid. *Biochim. Biophys. Acta - Gen. Subj.* **1968**, *156*, 1, 17–30. doi: 10.1016/0304-4165(68)90099-8.

269. Kang, D. Y., Kim, W.-S., Heo, I. S., Park, Y. H., Lee, S., Extraction of hyaluronic acid (HA) from rooster comb and characterization using flow field-flow fractionation (FlFFF) coupled with multiangle light scattering (MALS). *J. Sep. Sci.* **2010**, *33*, 22, 3530–3536. doi: 10.1002/jssc.201000478.

270. Kulkarni, S. S., Patil, S. D., Chavan, D. G., Extraction , purification and characterization of hyaluronic acid from Rooster comb. *J. Appl. Nat. Sci.* **2018**, *10*, 1, 313–315. doi: 10.31018/jans.v10i1.1623.

271. Boas, F. N., Isolation of hyaluronic acid from the cock's comb. *J. Biol. Chem.* **1949**, *181*573–575.

272. Sundaresan, G., Abraham, J. J. R., Appa Rao, V., Narendra Babu, R., Govind, V., Meti, M. F., Established method of chondroitin sulphate extraction from buffalo (Bubalus bubalis) cartilages and its identification by FTIR. *J. Food Sci. Technol.* **2018**, *55*, 9, 3439–3445. doi: 10.1007/s13197-018-3253-4.

273. Nakano, T., Lkawa, N., Ozimek, L., An economical method to extract chondroitin sulphate-peptide from bovine nasal cartilage. *Can. Agric. Eng.* **2000**, *42*, 4, 205–208.

274. Kim, C.-T., Gujral, N., Ganguly, A., Suh, J.-W., Sunwoo, H. H., Chondroitin sulphate extracted from antler cartilage using high hydrostatic pressure and enzymatic hydrolysis. *Biotechnol. Reports* **2014**, *4*14–20. doi: 10.1016/j.btre.2014.07.004.

275. Zhujun, Z., Guolei, Z., Fengmei, S., Extraction of the chondroitin sulfate from cartilage of

sheep. *J. Agric. Univ. Hebei* **2008**, *31*, 4, 98–101.

276. Dewanti Widyaningsih, T. *et al.*, Extraction of Glycosaminoglycans Containing Glucosamine and Chondroitin Sulfate from Chicken Claw Cartilage. *Res. J. Life Sci.* **2016**, *3*, 3, 181–189. doi: 10.21776/ub.rjls.2016.003.03.7.

277. Shin, S. C., You, S. J., An, B. K., Kang, C. W., Study on Extraction of Mucopolysaccharide-protein Containing Chondroitin Sulfate from Chicken Keel Cartilage Electrophoresis. *Asian-Australasian J. Anim. Sci.* **2006**, *19*, 4, 601–604. doi: 10.5713/ajas.2006.601.

278. Li, A., Xiong, S., Preparation and Structure Analysis of Chondroitin Sulfate from Pig Laryngeal Cartilage. , in *2010 4th International Conference on Bioinformatics and Biomedical Engineering*, Jun. 2010, 1–5. doi: 10.1109/ICBBE.2010.5515812.

279. Rosa, C. S. da, Tovar, A. F., Mourão, P., Pereira, R., Barreto, P., Beirão, L. H., Purification and characterization of hyaluronic acid from chicken combs. *Ciência Rural* **2012**, *42*, 9, 1682–1687. doi: 10.1590/S0103-84782012005000056.

280. Matsumura, G., De Salegui, M., Herp, A., Pigman, W., The preparation of hyaluronic acid from bovine synovial fluid. *Biochim. Biophys. Acta* **1963**, *69*574–576. doi: 10.1016/0006-3002(63)91314-3.

281. Ürgeová, E., Vulganová, K., Comparison of Enzymatic Hydrolysis of Polysaccharides from Eggshells Membranes. *Nov. Biotechnol. Chim.* **2016**, *15*, 2, 133–141. doi: 10.1515/nbec-2016-0014.

282. Khanmohammadi, M., Khoshfetrat, A. B., Eskandarnezhad, S., Sani, N. F., Ebrahimi, S., Sequential optimization strategy for hyaluronic acid extraction from eggshell and its partial characterization. *J. Ind. Eng. Chem.* **2014**, *20*, 6, 4371–4376. doi: 10.1016/j.jiec.2014.02.001.

283. Michelacci, Y. M., Horton, D. S. P. Q., Proteoglycans from the cartilage of young hammerhead shark Sphyrna lewini. *Comp. Biochem. Physiol. Part B Comp. Biochem.* **1989**, *92*, 4, 651–658. doi: 10.1016/0305-0491(89)90245-9.

284. Dao, D. T. A., Extraction of chondroitin sulfate from chicken kneel cartilage by combining of ultrasound treatment and alcalase hydrolysis. *Vietnam J. Sci. Technol.* **2018**, *56*, 4A, 137. doi: 10.15625/2525-2518/56/4A/12757.

285. Cheng, C., Duan, W., Duan, Z., Hai, Y., Lei, X., Chang, H., Extraction of Chondroitin Sulfate from Tilapia Byproducts with Ultrasonic-Microwave Synergistic. *Adv. Mater. Researc* **2013**, *726–731*4381–4385. doi: 10.4028/www.scientific.net/AMR.726-731.4381.

286. Barker, S. A., Young, N. M., Isolation of hyaluronic acid from human synovial fluid by pronase digestion and gel filtration. *Carbohydr. Res.* **1966**, *2*, 1, 49–55. doi: 10.1016/S0008-6215(00)81776-0.

287. Heinegård, D., Hascall, V. C., Characterization of chondroitin sulfate isolated from trypsin-chymotrypsin digests of cartilage proteoglycans. *Arch. Biochem. Biophys.* **1974**, *165*, 1, 427–441. doi: 10.1016/0003-9861(74)90182-9.

288. Bychkov, S. M., Kolesnikova, M. F., Investigation of highly purified preparations of hyaluronic acid. *Biokhimiia* **1969**, *34*, 1, 204–8. Accessed: Jun. 22, 2019. [Online]. Available: http://www.ncbi.nlm.nih.gov/pubmed/4240709

289. Chascall, V., Calabro, A., Midura, R. J., Yanagishita, M., Isolation and characterization of proteoglycans. *Methods Enzymol.* **1994**, *230*390–417. doi: 10.1016/0076-6879(94)30026-7.

290. Scott, J. E., Aliphatic ammonium salts in the assay of acidic polysaccharides from tissues. *Methods Biochem. Anal.* **1960**, 145–97. doi: 10.1002/9780470110249.ch4.

291. Opdensteinen, P., Clodt, J. I., Müschen, C. R., Filiz, V., Buyel, J. F., A Combined Ultrafiltration/Diafiltration Step Facilitates the Purification of Cyanovirin-N From Transgenic Tobacco Extracts. *Front. Bioeng. Biotechnol.* **2019**, *6*. doi: 10.3389/fbioe.2018.00206.

292. Choi, S., Choi, W., Kim, S., Lee, S.-Y., Noh, I., Kim, C.-W., Purification and biocompatibility of fermented hyaluronic acid for its applications to biomaterials. *Biomater. Res.* **2014**, *18*6. doi: 10.1186/2055-7124-18-6.

293. Khare, A. B., Houliston, S. A., Black, T. J., Isolating chondroitin sulfate. *U.S. Pat. Appl. 10/704,866* **2004**, .

294. Liu, L., Du, G., Chen, J., Wang, M., Sun, J., Enhanced hyaluronic acid production by a two-stage culture strategy based on the modeling of batch and fed-batch cultivation of Streptococcus zooepidemicus. *Bioresour. Technol.* **2008**, *99*, 17, 8532–8536. doi: 10.1016/j.biortech.2008.02.035.

295. Ogrodowski, C. S., Hokka, C. O., Santana, M. H. A., Production of hyaluronic acid by Streptococcus: The effects of the addition of lysozyme and aeration on the formation and the rheological properties of the product. , in *Applied Biochemistry and Biotechnology - Part A Enzyme Engineering and Biotechnology*, Mar. 2005, *122*, 1–3, , 753–761. doi: 10.1385/abab:122:1-3:0753.

296. Johns, M. R., Goh, L. T., Oeggerli, A., Effect of pH, agitation and aeration on hyaluronic acid production by Streptococcus zooepidemicus. *Biotechnol. Lett.* **1994**, *16*, 5, 507–512. doi: 10.1007/BF01023334.

297. Zhang, J., Ding, X., Yang, L., Kong, Z., A serum-free medium for colony growth and hyaluronic acid production by Streptococcus zooepidemicus NJUST01. *Appl. Microbiol. Biotechnol.* **2006**, *72*, 1, 168–172. doi: 10.1007/s00253-005-0253-x.

298. Volpi, N., Chondroitin sulfate safety and quality. *Molecules* **2019**, *24*, 8, . doi: 10.3390/molecules24081447.

299. Volpi, N., Quality of different chondroitin sulfate preparations in relation to their therapeutic activity. *J. Pharm. Pharmacol.* **2009**, *61*, 10, 1271–1280. doi: 10.1211/jpp/61.10.0002.

300. Markoulli, M., Hui, A., Emerging targets of inflammation and tear secretion in dry eye disease. *Drug Discov. Today* **2019**, *24*, 8, 1427–1432. doi: 10.1016/J.DRUDIS.2019.02.006.

301. Craig, J. P. *et al.*, TFOS DEWS II Definition and Classification Report. *Ocul. Surf.* **2017**, *15*, 3, 276–283. doi: 10.1016/J.JTOS.2017.05.008.

302. Fong, P. Y., Shih, K. C., Lam, P. Y., Chan, T. C. Y., Jhanji, V., Tong, L., Role of tear film biomarkers in the diagnosis and management of dry eye disease. *Taiwan J. Ophthalmol.* **2019**, *9*, 3, 150. doi: 10.4103/TJO.TJO_56_19.

303. Periman, L. M., Perez, V. L., Saban, D. R., Lin, M. C., Neri, P., The Immunological Basis of Dry Eye Disease and Current Topical Treatment Options. *https://home.liebertpub.com/jop* **2020**, *36*, 3, 137–146. doi: 10.1089/JOP.2019.0060.

304. Labbé, A., Wang, Y. X., Jie, Y., Baudouin, C., Jonas, J. B., Xu, L., Dry eye disease, dry eye symptoms and depression: the Beijing Eye Study. *Br. J. Ophthalmol.* **2013**, *97*, 11, 1399–1403. doi: 10.1136/BJOPHTHALMOL-2013-303838.

305. Wang, M. T. M. *et al.*, Ageing and the natural history of dry eye disease: A prospective registry-based cross-sectional study. *Ocul. Surf.* **2020**, *18*, 4, 736–741. doi: 10.1016/J.JTOS.2020.07.003.

306. Chhadva, P., Goldhardt, R., Galor, A., Meibomian Gland Disease: The Role of Gland Dysfunction in Dry Eye Disease. *Ophthalmology* **2017**, *124*, 11, S20–S26. doi: 10.1016/J.OPHTHA.2017.05.031.

307. Deng, R. *et al.*, Oxidative stress markers induced by hyperosmolarity in primary human corneal epithelial cells. *PLoS One* **2015**, *10*, 5, . doi: 10.1371/JOURNAL.PONE.0126561.

308. Seen, S., Tong, T., Dry eye disease and oxidative stress. *Acta Ophthalmol.* **2018**, *96*, 4, e412–e420. doi: 10.1111/AOS.13526.

309. Yamaguchi, T., Inflammatory Response in Dry Eye. *Invest. Ophthalmol. Vis. Sci.* **2018**, *59*, 14, DES192–DES199. doi: 10.1167/IOVS.17-23651.

310. Nguyen, C. Q., Peck, A. B., Unraveling the pathophysiology of Sjogren syndrome-associated dry eye disease. *Ocul. Surf.* **2009**, *7*, 1, 11–27. doi: 10.1016/S1542-0124(12)70289-6.

311. Ulbricht, K. U., Schmidt, R. E., Witte, T., Antibodies against alpha-fodrin in Sjögren's syndrome. *Autoimmun. Rev.* **2003**, *2*, 2, 109–113. doi: 10.1016/S1568-9972(03)00002-8.

312. Al-Saedi, Z. *et al.*, Dry Eye Disease: Present Challenges in the Management and Future

Trends. *Curr. Pharm. Des.* **2016**, *22*, 28, 4470–4490. doi: 10.2174/1381612822666160614012634.

313. Donthineni, P. R., Kammari, P., Shanbhag, S. S., Singh, V., Das, A. V., Basu, S., Incidence, demographics, types and risk factors of dry eye disease in India: Electronic medical records driven big data analytics report I. *Ocul. Surf.* **2019**, *17*, 2, 250–256. doi: 10.1016/J.JTOS.2019.02.007.

314. Gayton, J. L., Etiology, prevalence, and treatment of dry eye disease. , *Clinical Ophthalmology*, *3*, 1, . 405–412, 2009. doi: 10.2147/opth.s5555.

315. Favero, G., Moretti, E., Krajčíková, K., Tomečková, V., Rezzani, R., Evidence of Polyphenols Efficacy against Dry Eye Disease. *Antioxidants 2021, Vol. 10, Page 190* **2021**, *10*, 2, 190. doi: 10.3390/ANTIOX10020190.

316. Paulsen, A. K. *et al.*, Dry eye in the beaver dam offspring study: prevalence, risk factors, and health-related quality of life. *Am. J. Ophthalmol.* **2014**, *157*, 4, 799–806. doi: 10.1016/J.AJO.2013.12.023.

317. Li, W., Lin, M. C., Sex Disparity in How Pain Sensitivity Influences Dry Eye Symptoms. *Cornea* **2019**, *38*, 10, 1291–1298. doi: 10.1097/ICO.0000000000002050.

318. Calonge, M. *et al.*, Effects of the External Environment on Dry Eye Disease. *Int. Ophthalmol. Clin.* **2017**, *57*, 2, 23–40. doi: 10.1097/IIO.0000000000000168.

319. Elhusseiny, A. M., Khalil, A. A., Sheikh, R. H. El, Bakr, M. A., Eissa, M. G., Sayed, Y. M. El, New approaches for diagnosis of dry eye disease. *Int. J. Ophthalmol.* **2019**, *12*, 10, 1618. doi: 10.18240/IJO.2019.10.15.

320. Golden, M. I., Meyer, J. J., Patel, B. C., *Dry Eye Syndrome*. StatPearls Publishing, 2017. Accessed: Dec. 12, 2021. [Online]. Available: https://www.ncbi.nlm.nih.gov/books/NBK470411/

321. Schein, O. D., Muñoz, B., Tielsch, J. M., Bandeen-Roche, K., West, S., Prevalence of dry eye among the elderly. *Am. J. Ophthalmol.* **1997**, *124*, 6, 723–728. doi: 10.1016/S0002-9394(14)71688-5.

322. Wolffsohn, J. S. *et al.*, TFOS DEWS II Diagnostic Methodology report. *Ocul. Surf.* **2017**, *15*, 3, 539–574. doi: 10.1016/J.JTOS.2017.05.001.

323. Jones, L. *et al.*, TFOS DEWS II Management and Therapy Report. *Ocul. Surf.* **2017**, *15*, 3, 575–628. doi: 10.1016/J.JTOS.2017.05.006.

324. McCann, L. C., Tomlinson, A., Pearce, E. I., Papa, V., Effectiveness of artificial tears in the management of evaporative dry eye. *Cornea* **2012**, *31*, 1, 1–5. doi: 10.1097/ICO.0B013E31821B71E6.

325. O'brien, P. D., Collum, L. M. T., Dry Eye: Diagnosis and Current Treatment Strategies. *Curr. Allergy Asthma Rep.* **2004**, *4*314–319.

326. Yang, Y. J., Lee, W. Y., Kim, Y. J., Hong, Y. P., A meta-analysis of the efficacy of hyaluronic acid eye drops for the treatment of dry eye syndrome. *Int. J. Environ. Res. Public Health* **2021**, *18*, 5, 1–14. doi: 10.3390/ijerph18052383.

327. Belalcázar-Rey, S. *et al.*, Efficacy and Safety of Sodium Hyaluronate/chondroitin Sulfate Preservative-free Ophthalmic Solution in the Treatment of Dry Eye: A Clinical Trial. *Curr. Eye Res.* **2021**, *46*, 7, 919–929. doi: 10.1080/02713683.2020.1849733/FORMAT/EPUB.

328. Tananuvat, N. *et al.*, Controlled study of the use of autologous serum in dry eye patients. *Cornea* **2001**, *20*, 8, 802–806. doi: 10.1097/00003226-200111000-00005.

329. Na, K.-S., Kim, M. S., Allogeneic Serum Eye Drops for the Treatment of Dry Eye Patients with Chronic Graft-Versus-Host Disease. *J. Ocul. Pharmacol. Ther.* **2012**, *28*, 5, 479–483. doi: 10.1089/JOP.2012.0002.

330. Bereiter, D. A., Rahman, M., Thompson, R., Stephenson, P., Saito, H., TRPV1 and TRPM8 Channels and Nocifensive Behavior in a Rat Model for Dry Eye. *Invest. Ophthalmol. Vis. Sci.* **2018**, *59*, 8, 3739–3746. doi: 10.1167/IOVS.18-24304.

331. Ervin, A., Law, A., Pucker, A. D., Punctal occlusion for dry eye syndrome. *Cochrane Database Syst. Rev.* **2017**, *2017*, 6, . doi: 10.1002/14651858.CD006775.PUB3.

332. Tang, T. B., Noor, N. H. M., Towards wearable active humidifier for dry eyes. *Proceeding - 2015 IEEE Int. Circuits Syst. Symp. ICSyS 2015* **2016**, 116–119. doi:

10.1109/CIRCUITSANDSYSTEMS.2015.7394076.

333. Shen, G., Qi, Q., Ma, X., Effect of Moisture Chamber Spectacles on Tear Functions in Dry Eye Disease. *Optom. Vis. Sci.* **2016**, *93*, 2, 158–164. doi: 10.1097/OPX.0000000000000778.

334. Dogru, M., Nakamura, M., Shimazaki, J., Tsubota, K., Changing trends in the treatment of dry-eye disease. *Expert Opin. Investig. Drugs* **2013**, *22*, 12, 1581–1601. doi: 10.1517/13543784.2013.838557.

335. Ridder III, W. H., Karsolia, A., New drugs for the treatment of dry eye disease. *Clin. Optom.* **2015**, *7*91–102. doi: 10.2147/OPTO.S68271.

336. Ono, M. *et al.*, Therapeutic effect of cevimeline on dry eye in patients with Sjögren's syndrome: a randomized, double-blind clinical study. *Am. J. Ophthalmol.* **2004**, *138*, 1, 6–17. doi: 10.1016/J.AJO.2004.02.010.

337. Kawakita, T., Shimmura, S., Tsubota, K., Effect of Oral Pilocarpine in Treating Severe Dry Eye in Patients With Sjögren Syndrome. *Asia-Pacific J. Ophthalmol. (Philadelphia, Pa.)* **2015**, *4*, 2, 101–105. doi: 10.1097/APO.0000000000000040.

338. Ding, J., Sullivan, D. A., The Effects of Insulin-like Growth Factor 1 and Growth Hormone on Human Meibomian Gland Epithelial Cells. *JAMA Ophthalmol.* **2014**, *132*, 5, 593–599. doi: 10.1001/JAMAOPHTHALMOL.2013.8295.

339. Gumus, K., Pflugfelder, S. C., Intranasal tear neurostimulation: An emerging concept in the treatment of dry eye. *Int. Ophthalmol. Clin.* **2017**, *57*, 2, 101–108. doi: 10.1097/IIO.0000000000000163.

340. Craig, J. P., Chen, Y.-H., Turnbull, P. R. K., Prospective Trial of Intense Pulsed Light for the Treatment of Meibomian Gland Dysfunction. *Invest. Ophthalmol. Vis. Sci.* **2015**, *56*, 3, 1965–1970. doi: 10.1167/IOVS.14-15764.

341. Korb, D. R., Blackie, C. A., Debridement-scaling: A new procedure that increases meibomian gland function and reduces dry eye symptoms. *Cornea* **2013**, *32*, 12, 1554–1557. doi: 10.1097/ICO.0B013E3182A73843.

342. Nakayama, N., Kawashima, M., Kaido, M., Arita, R., Tsubota, K., Analysis of Meibum before and after Intraductal Meibomian Gland Probing in Eyes with Obstructive Meibomian Gland Dysfunction. *Cornea* **2015**, *34*, 10, 1206–1208. doi: 10.1097/ICO.0000000000000558.

343. Lane, S. S. *et al.*, A new system, the LipiFlow, for the treatment of meibomian gland dysfunction. *Cornea* **2012**, *31*, 4, 396–404. doi: 10.1097/ICO.0B013E318239AAEA.

344. Arita, R. *et al.*, Effects of a warm compress containing menthol on the tear film in healthy subjects and dry eye patients. *Sci. Rep.* **2017**, *7*, November 2016, 1–6. doi: 10.1038/srep45848.

345. Zheng, X., Goto, T., Ohashi, Y., Comparison of In Vivo Efficacy of Different Ocular Lubricants in Dry Eye Animal Models. *Invest. Ophthalmol. Vis. Sci.* **2014**, *55*, 6, 3454–3460. doi: 10.1167/IOVS.13-13730.

346. Cutolo, C. A., Barabino, S., Bonzano, C., Traverso, C. E., The Use of Topical Corticosteroids for Treatment of Dry Eye Syndrome. *Ocul. Immunol. Inflamm.* **2017**, *27*, 2, 266–275. doi: 10.1080/09273948.2017.1341988.

347. De Paiva, C. S. *et al.*, Corticosteroid and doxycycline suppress MMP-9 and inflammatory cytokine expression, MAPK activation in the corneal epithelium in experimental dry eye. *Exp. Eye Res.* **2006**, *83*, 3, 526–535. doi: 10.1016/J.EXER.2006.02.004.

348. Sullivan, D. A. *et al.*, TFOS DEWS II Sex, Gender, and Hormones Report. *Ocul. Surf.* **2017**, *15*, 3, 284–333. doi: 10.1016/J.JTOS.2017.04.001.

349. Marsh, P., Pflugfelder, S. C., Topical nonpreserved methylprednisolone therapy for keratoconjunctivitis sicca in Sjögren syndrome1. *Ophthalmology* **1999**, *106*, 4, 811–816. doi: 10.1016/S0161-6420(99)90171-9.

350. Perry, H. D. *et al.*, Evaluation of Topical Cyclosporine for the Treatment of Dry Eye Disease. *Arch. Ophthalmol.* **2008**, *126*, 8, 1046–1050. doi: 10.1001/ARCHOPHT.126.8.1046.

351. Rolando, M., Barabino, S., Alongi, S., Calabria, G., Topical Non-Preserved Diclofenac

Therapy for Keratoconjunctivitis Sicca. *Adv. Exp. Med. Biol.* **2002**, *506 B*1237–1240. doi: 10.1007/978-1-4615-0717-8_177.

352. Liu, X., Wang, S., Kao, A. A., Long, Q., The effect of topical pranoprofen 0.1% on the clinical evaluation and conjunctival HLA-DR expression in dry eyes. *Cornea* **2012**, *31*, 11, 1235–1239. doi: 10.1097/ICO.0B013E31824988E5.

353. Aragona, P., Stilo, A., Ferreri, F., Mobrici, M., Effects of the topical treatment with NSAIDs on corneal sensitivity and ocular surface of Sjögren's syndrome patients. *Eye* **2005**, *19*, 5, 535–539. doi: 10.1038/sj.eye.6701537.

354. Lambiase, A. *et al.*, A Two-Week, Randomized, Double-masked Study to Evaluate Safety and Efficacy of Lubricin (150 µg/mL) Eye Drops Versus Sodium Hyaluronate (HA) 0.18% Eye Drops (Vismed®) in Patients with Moderate Dry Eye Disease. *Ocul. Surf.* **2017**, *15*, 1, 77–87. doi: 10.1016/J.JTOS.2016.08.004.

355. Pflugfelder, S. C., Stern, M., Zhang, S., Shojaei, A., LFA-1/ICAM-1 Interaction as a Therapeutic Target in Dry Eye Disease. *J. Ocul. Pharmacol. Ther.* **2017**, *33*, 1, 5–12. doi: 10.1089/JOP.2016.0105.

356. Zhong, M. *et al.*, Discovery and Development of Potent LFA-1/ICAM-1 Antagonist SAR 1118 as an Ophthalmic Solution for Treating Dry Eye. *ACS Med. Chem. Lett.* **2012**, *3*, 3, 203–206. doi: 10.1021/ML2002482.

357. Abidi, A., Shukla, P., Ahmad, A., Lifitegrast: A novel drug for treatment of dry eye disease. *J. Pharmacol. Pharmacother.* **2016**, *7*, 4, 194. doi: 10.4103/0976-500X.195920.

358. Sun, Y., Zhang, R., Gadek, T. R., O'Neill, C. A., Pearlman, E., Corneal Inflammation Is Inhibited by the LFA-1 Antagonist, Lifitegrast (SAR 1118). *J. Ocul. Pharmacol. Ther.* **2013**, *29*, 4, 395–402. doi: 10.1089/JOP.2012.0102.

359. Cosar, C. B. *et al.*, Tarsorrhaphy: Clinical experience from a cornea practice. *Cornea* **2001**, *20*, 8, 787–791. doi: 10.1097/00003226-200111000-00002.

360. Galor, A., Gardener, H., Pouyeh, B., Feuer, W., Florez, H., Effect of a Mediterranean dietary pattern and Vitamin D levels on dry eye syndrome. *Cornea* **2014**, *33*, 5, 441. doi:

10.1097/ICO.0000000000000089.

361. Rand, A. L., Asbell, P. A., Nutritional supplements for dry eye syndrome. *Curr. Opin. Ophthalmol.* **2011**, *22*, 4, 279–282. doi: 10.1097/ICU.0B013E3283477D23.

362. Ousler, G. W., Michaelson, C., Christensen, M. T., An evaluation of tear film breakup time extension and ocular protection index scores among three marketed lubricant eye drops. *Cornea* **2007**, *26*, 8, 949–952. doi: 10.1097/ICO.0B013E3180DE1C38.

363. Gupta, P. K., Vora, G. K., Matossian, C., Kim, M., Stinnett, S., Outcomes of intense pulsed light therapy for treatment of evaporative dry eye disease. *Can. J. Ophthalmol.* **2016**, *51*, 4, 249–253. doi: 10.1016/J.JCJO.2016.01.005.

364. Salwowska, N. M., Bebenek, K. A., Żądło, D. A., Wcisło-Dziadecka, D. L., Physiochemical properties and application of hyaluronic acid: a systematic review. *J. Cosmet. Dermatol.* **2016**, *15*, 4, 520–526. doi: 10.1111/JOCD.12237.

365. Ritch, R., Natural compounds: evidence for a protective role in eye disease. *Can. J. Ophthalmol.* **2007**, *42*, 3, 425–438. doi: 10.3129/CAN.J.OPHTHALMOL.I07-044.

366. Memarzadeh, E., Luther, T., Heidari-Soureshjani, S., Effect and mechanisms of medicinal plants on dry eye disease: A systematic review. *J. Clin. Diagnostic Res.* **2018**, *12*, 9, NE01–NE04. doi: 10.7860/JCDR/2018/36409.12042.

367. Peng, Q. H., Yao, X. L., Wu, Q. L., Tan, H. Y., Zhang, J. R., Effects of extract of Buddleja officinalis eye drops on androgen receptors of lacrimal gland cells of castrated rats with dry eye. *Int. J. Ophthalmol.* **2010**, *3*, 1, 48. doi: 10.3980/J.ISSN.2222-3959.2010.01.10.

368. Chien, K. J. *et al.*, Effects of Lycium barbarum (goji berry) on dry eye disease in rats. *Mol. Med. Rep.* **2018**, *17*, 1, 818. doi: 10.3892/MMR.2017.7947.

369. Kim, C. S., Jo, K., Lee, I. S., Kim, J., Topical Application of Apricot Kernel Extract Improves Dry Eye Symptoms in a Unilateral Exorbital Lacrimal Gland Excision Mouse. *Nutrients* **2016**, *8*, 11, 750–760. doi: 10.3390/NU8110750.

370. Kang, S. W. *et al.*, A standardized extract of Rhynchosia volubilis Lour. exerts a protective effect on benzalkonium chloride-induced mouse dry eye model. *J.*

Ethnopharmacol. **2018**, *215*91–100. doi: 10.1016/J.JEP.2017.12.041.

371. Choi, W. *et al.*, Therapeutic Efficacy of Topically Applied Antioxidant Medicinal Plant Extracts in a Mouse Model of Experimental Dry Eye. *Oxid. Med. Cell. Longev.* **2016**, *2016*. doi: 10.1155/2016/4727415.

372. Choi, W. *et al.*, Clinical Effect of Antioxidant Glasses Containing Extracts of Medicinal Plants in Patients with Dry Eye Disease: A Multi-Center, Prospective, Randomized, Double-Blind, Placebo-Controlled Trial. *PLoS One* **2015**, *10*, 10, e0139761. doi: 10.1371/JOURNAL.PONE.0139761.

373. Cui, L. *et al.*, Experimental and Clinical Applications of Chamaecyparis obtusa Extracts in Dry Eye Disease. *Oxid. Med. Cell. Longev.* **2017**, *2017*. doi: 10.1155/2017/4523673.

374. Choi, S. Y., Eom, Y., Kim, J. Y., Jang, D. H., Song, J. S., Kim, H. M., Effect of natural extract eye drops in dry eye disease rats. *Int. J. Ophthalmol.* **2020**, *13*, 7, 1030. doi: 10.18240/IJO.2020.07.02.

375. Haji-Ali-Nili, N. *et al.*, Effect of a Natural Eye Drop, Made of Plantago Ovata Mucilage on Improvement of Dry Eye Symptoms: A Randomized, Double-blind Clinical Trial. *Iran. J. Pharm. Res.* **2019**, *18*, 3, 1611. doi: 10.22037/IJPR.2019.1100717.

376. Ang, B. C. H., Sng, J. J., Wang, P. X. H., Htoon, H. M., Tong, L. H. T., Sodium Hyaluronate in the Treatment of Dry Eye Syndrome: A Systematic Review and Meta-Analysis. *Sci. Rep.* **2017**, *7*, 1, 1–14. doi: 10.1038/s41598-017-08534-5.

377. Yokoi, N., Komuro, A., Nishida, K., Kinoshita, S., Effectiveness of hyaluronan on corneal epithelial barrier function in dry eye. *Br. J. Ophthalmol.* **1997**, *81*, 7, 533–536. doi: 10.1136/bjo.81.7.533.

378. Limberg, M. B., McCaa, C., Kissling, G. E., Kaufman, H. E., Topical application of hyaluronic acid and chondroitin sulfate in the treatment of dry eyes. *Am. J. Ophthalmol.* **1987**, *103*, 2, 194–197. doi: 10.1016/S0002-9394(14)74226-6.

379. Kulovesi, P., Rantamäki, A. H., Holopainen, J. M., Surface Properties of Artificial Tear Film Lipid Layers: Effects of Wax Esters. *Invest. Ophthalmol. Vis. Sci.* **2014**, *55*, 7, 4448–

4454. doi: 10.1167/IOVS.14-14122.

380. Chen, H.-B., Yamabayashi, S., Ou, B., Tanaka, Y., Ohno, S., Tsukahara, S., Structure and composition of rat precorneal tear film. A study by an in vivo cryofixation. *Invest. Ophthalmol. Vis. Sci.* **1997**, *38*, 2, 381–387.

381. Rieger, G., Lipid-containing eye drops: a step closer to natural tears. *Ophthalmologica* **1990**, *201*, 4, 206–212. doi: 10.1159/000310154.

382. Choi, J. H., Kim, J. H., Li, Z., Oh, H. J., Ahn, K. Y., Yoon, K. C., Efficacy of the Mineral Oil and Hyaluronic Acid Mixture Eye Drops in Murine Dry Eye. *Korean J. Ophthalmol.* **2015**, *29*, 2, 137. doi: 10.3341/KJO.2015.29.2.131.

383. Tomosugi, N., Kitagawa, K., Takahashi, N., Sugai, S., Ishikawat, I., Diagnostic potential of tear proteomic patterns in Sjögren's syndrome. *J. Proteome Res.* **2005**, *4*, 3, 820–825. doi: 10.1021/PR0497576.

384. Grus, F. H. *et al.*, SELDI-TOF-MS ProteinChip array profiling of tears from patients with dry eye. *Invest. Ophthalmol. Vis. Sci.* **2005**, *46*, 3, 863–876. doi: 10.1167/IOVS.04-0448.

385. Versura, P. *et al.*, Tear proteomics in evaporative dry eye disease. *Eye (Lond).* **2010**, *24*, 8, 1396–1402. doi: 10.1038/EYE.2010.7.

386. Higuchi, A., Inoue, H., Kaneko, Y., Oonishi, E., Tsubota, K., Selenium-binding lactoferrin is taken into corneal epithelial cells by a receptor and prevents corneal damage in dry eye model animals. *Sci. Rep.* **2016**, *6*, 1, 1–9. doi: 10.1038/srep36903.

387. Oliverio, G. W., Spinella, R., Postorino, E. I., Inferrera, L., Aragona, E., Aragona, P., Safety and tolerability of an eye drop based on 0.6% Povidone-iodine nanoemulsion in dry eye patients. *J. Ocul. Pharmacol. Ther.* **2021**, *37*, 2, 90–96. doi: 10.1089/JOP.2020.0085/ASSET/IMAGES/LARGE/JOP.2020.0085_FIGURE1.JPEG.

388. Amrane, M. *et al.*, Ocular tolerability and efficacy of a cationic emulsion in patients with mild to moderate dry eye disease – A randomised comparative study. *J. Fr. Ophtalmol.* **2014**, *37*, 8, 589–598. doi: 10.1016/J.JFO.2014.05.001.

389. Zhang, L. M., Kong, T., Aqueous polysaccharide blends based on hydroxypropyl guar

gum and carboxymethyl cellulose: synergistic viscosity and thixotropic properties. *Colloid Polym. Sci.* **2006**, *2*, 285, 145–151. doi: 10.1007/S00396-006-1530-7.

390. González De Castilla, A., Bittner, J. P., Müller, S., Jakobtorweihen, S., Smirnova, I., Thermodynamic and Transport Properties Modeling of Deep Eutectic Solvents: A Review on gE-Models, Equations of State, and Molecular Dynamics. *J. Chem. Eng. Data* **2020**, *65*, 3, 943–967. doi: 10.1021/acs.jced.9b00548.

391. Calogirou, A., Larsen, B. R., Kotzias, D., Gas-phase terpene oxidation products: A review. *Atmos. Environ.* **1999**, *33*, 9, 1423–1439. doi: 10.1016/S1352-2310(98)00277-5.

392. Gonzalez-Burgos, E., Gomez-Serranillos, M. P., Terpene Compounds in Nature: A Review of Their Potential Antioxidant Activity. *Curr. Med. Chem.* **2012**, *19*, 31, 5319–5341. doi: 10.2174/092986712803833335.

393. De Cássia Da Silveira E Sá, R., Andrade, L. N., De Sousa, D. P., A review on anti-inflammatory activity of monoterpenes. *Molecules* **2013**, *18*, 1, 1227–1254. doi: 10.3390/molecules18011227.

394. Huang, L., Bai, J., Yang, H., Liu, J., Cui, H., Combined use of borneol or menthol with labrasol promotes penetration of baicalin through rabbit cornea in vitro. *Pak. J. Pharm. Sci.* **2015**, *28*, 1, 1–7.

395. Liu, J., Fu, S., Wei, N., Hou, Y., Zhang, X., Cui, H., The effects of combined menthol and borneol on fluconazole permeation through the cornea ex vivo. *Eur. J. Pharmacol.* **2012**, *688*, 1–3, 1–5. doi: 10.1016/j.ejphar.2011.12.007.

396. Qi, H. P. *et al.*, In vitro evaluation of enhancing effect of borneol on transcorneal permeation of compounds with different hydrophilicities and molecular sizes. *Eur. J. Pharmacol.* **2013**, *705*, 1–3, 20–25. doi: 10.1016/j.ejphar.2013.02.031.

397. Mohammadi-Samani, S., Yousefi, G., Mohammadi, F., Ahmadi, F., Meloxicam transdermal delivery: Effect of eutectic point on the rate and extent of skin permeation. *Iran. J. Basic Med. Sci.* **2014**, *17*, 2, 112–118.

398. Stott, P. W., Williams, A. C., Barry, B. W., Transdermal delivery from eutectic systems:

Enhanced permeation of a model drug, ibuprofen. *J. Control. Release* **1998**, *50*, 1–3, 297–308. doi: 10.1016/S0168-3659(97)00153-3.

399. Silva, L. P. *et al.*, Design and characterization of sugar-based deep eutectic solvents using COSMO-RS. *ACS Sustain. Chem. Eng.* **2018**, *6*, 8, 10724–10734. doi: 10.1021/acssuschemeng.8b02042.

400. Martins, M. A. R., Pinho, S. P., Coutinho, J. A. P., Insights into the Nature of Eutectic and Deep Eutectic Mixtures. *J. Solution Chem.* **2019**, *48*, 7, 962–982. doi: 10.1007/s10953-018-0793-1.

401. Taherzadeh, M., Haghbakhsh, R., Duarte, A. R. C., Raeissi, S., Generalized Model to Estimate the Refractive Indices of Deep Eutectic Solvents. *J. Chem. Eng. Data* **2020**, *65*, 8, 3965–3976. doi: 10.1021/acs.jced.0c00308.

402. Haghbakhsh, R., Taherzadeh, M., Duarte, A. R. C., Raeissi, S., A general model for the surface tensions of deep eutectic solvents. *J. Mol. Liq.* **2020**, *307*112972. doi: 10.1016/j.molliq.2020.112972.

403. Fredenslund, A., Jones, R. L., Prausnitz, J. M., Group-contribution estimation of activity coefficients in nonideal liquid mixtures. *AIChE J.* **1975**, *21*, 6, 1086–1099. doi: 10.1002/aic.690210607.

404. Klamt, A., Conductor-like screening model for real solvents: A new approach to the quantitative calculation of solvation phenomena. *J. Phys. Chem.* **1995**, *99*, 7, 2224–2235. doi: 10.1021/j100007a062.

405. Klamt, A., Jonas, V., Bürger, T., Lohrenz, J. C. W., Refinement and parametrization of COSMO-RS. *J. Phys. Chem. A* **1998**, *102*, 26, 5074–5085. doi: 10.1021/jp980017s.

406. Bakirtzi, C., Triantafyllidou, K., Makris, D. P., Novel lactic acid-based natural deep eutectic solvents: Efficiency in the ultrasound-assisted extraction of antioxidant polyphenols from common native Greek medicinal plants. *J. Appl. Res. Med. Aromat. Plants* **2016**, *3*, 3, 120–127. doi: 10.1016/J.JARMAP.2016.03.003.

407. Liew, S. Q., Ngoh, G. C., Yusoff, R., Teoh, W. H., Acid and Deep Eutectic Solvent (DES)

extraction of pectin from pomelo (Citrus grandis (L.) Osbeck) peels. *Biocatal. Agric. Biotechnol.* **2018**, *13*1–11. doi: 10.1016/j.bcab.2017.11.001.

408. González, C. G., Mustafa, N. R., Wilson, E. G., Verpoorte, R., Choi, Y. H., Application of natural deep eutectic solvents for the “green”extraction of vanillin from vanilla pods. *Flavour Fragr. J.* **2018**, *33*, 1, 91–96. doi: 10.1002/ffj.3425.

409. Haghbakhsh, R., Bardool, R., Bakhtyari, A., Duarte, A. R. C., Raeissi, S., Simple and global correlation for the densities of deep eutectic solvents. *J. Mol. Liq.* **2019**, *296*111830. doi: 10.1016/j.molliq.2019.111830.

410. Valderrama, J. O., Sanga, W. W., Lazzús, J. A., Critical properties, normal boiling temperature, and acentric factor of another 200 ionic liquids. *Ind. Eng. Chem. Res.* **2008**, *47*, 4, 1318–1330. doi: 10.1021/ie071055d.

411. Mirza, N. R., Nicholas, N. J., Wu, Y., Kentish, S., Stevens, G. W., Estimation of Normal Boiling Temperatures, Critical Properties, and Acentric Factors of Deep Eutectic Solvents. *J. Chem. Eng. Data* **2015**, *60*, 6, 1844–1854. doi: 10.1021/acs.jced.5b00046.

412. Labinov, S. D., Sand, J. R., An analytical method of predicting Lee-Kesler-Plöcker equation-of-state binary interaction coefficients. *Int. J. Thermophys.* **1995**, *16*, 6, 1393–1411. doi: 10.1007/BF02083548.

413. Prausnitz, J. M., Lichtenthaler, R. N., Azevedo, E. G. de, *Molecular thermodynamics of fluid-phase equilibria.* Prentice Hall PTR, 1999.

414. Okuniewski, M., Paduszy, K., Domanska, U. M., Phase Diagrams in Representative Terpenoid Systems — Measurements and Calculations with Leading Thermodynamic Models Phase Diagrams in Representative Terpenoid Systems — Measurements and Calculations with Leading Thermodynamic Models. *Ind. Eng. Chem. Res.* **2017**, *56*, 34, 9753–9761. doi: 10.1021/acs.iecr.7b02207.

415. Kim, H., Evaluation of UNIFAC group interaction parameters using properties based on quantum mechanical calculations. , 2005.

416. Tiegs, D., Gmehling, J., Rasmussen, P., Fredenslund, A., Vapor—Liquid Equilibria by

UNIFAC Group Contribution. 4. Revision and Extension. *Ind. Eng. Chem. Res.* **1987**, *26*, 1, 159–161. doi: 10.1021/ie00061a030.

417. Magnussen, T., Rasmussen, P., Fredenslund, A., Unifac Parameter Table for Prediction of Liquid-Liquid Equilibria. *Ind. Eng. Chem. Process Des. Dev.* **1981**, *20*, 2, 331–339. doi: 10.1021/i200013a024.

418. Jain, M., Attarde, D., Gupta, S. K., Estimation of unknown UNIFAC interaction parameters between thiophene and olefin, and thiol and olefin functional groups. *Fluid Phase Equilib.* **2017**, *442*81–86. doi: 10.1016/j.fluid.2017.03.019.

419. Voutsas, E. C., Tassios, D. P., Analysis of the UNIFAC-Type Group-Contribution Models at the Highly Dilute Region. 1. Limitations of the Combinatorial and Residual Expressions. *Ind. Eng. Chem. Res.* **1997**, *36*, 11, 4965–4972. doi: 10.1021/ie960770c.

420. Gmehling, J., Li, J., Schiller, M., A Modified UNIFAC Model. 2. Present Parameter Matrix and Results for Different Thermodynamic Properties. *Ind. Eng. Chem. Res.* **1993**, *32*, 1, 178–193. doi: 10.1021/ie00013a024.

421. Oracz, P., Góral, M., Wilczek-Vera, G., Warycha, S., Vapour-liquid equilibria. X. The ternary system cyclohexane-methanol-acetone at 293.15 and 303.15 K. *Fluid Phase Equilib.* **1996**, *126*, 1, 71–92. doi: 10.1016/S0378-3812(96)03126-3.

422. Hansen, H. K., Rasmussen, P., Fredenslund, A., Schiller, M., Gmehling, J., Vapor-Liquid Equilibria by UNIFAC Group Contribution. 5. Revision and Extension. *Ind. Eng. Chem. Res.* **1991**, *30*, 10, 2352–2355. doi: 10.1021/ie00058a017.

423. Eckert, F., Klamt, A., Fast Solvent Screening via Quantum Chemistry: COSMO-RS Approach. *AIChE J.* **2002**, *48*, 2, 369–385. doi: 10.1002/aic.690480220.

424. Klamt, A., Statistical thermodynamics of interacting surfaces. , in *Cosmo-Rs*, 2005, 59–81.

425. Bakhtyari, A., Haghbakhsh, R., Duarte, A. R. C., Raeissi, S., A simple model for the viscosities of deep eutectic solvents. *Fluid Phase Equilib.* **2020**, *521*112662. doi: 10.1016/j.fluid.2020.112662.

426. Leron, R. B., Soriano, A. N., Li, M. H., Densities and refractive indices of the deep eutectic solvents (choline chloride+ethylene glycol or glycerol) and their aqueous mixtures at the temperature ranging from 298.15 to 333.15K. *J. Taiwan Inst. Chem. Eng.* **2012**, *43*, 4, 551–557. doi: 10.1016/j.jtice.2012.01.007.

427. Bonem, J. M., *Chemical Projects Scale Up*. Elsevier, 2018. doi: 10.1016/C2016-0-02123-X.

428. Ghaedi, H., Ayoub, M., Sufian, S., Shariff, A. M., Lal, B., The study on temperature dependence of viscosity and surface tension of several Phosphonium-based deep eutectic solvents. *J. Mol. Liq.* **2017**, *241*500–510. doi: 10.1016/j.molliq.2017.06.024.

429. Freire, M. G., Carvalho, P. J., Fernandes, A. M., Marrucho, I. M., Queimada, A. J., Coutinho, J. A. P., Surface tensions of imidazolium based ionic liquids: Anion, cation, temperature and water effect. *J. Colloid Interface Sci.* **2007**, *314*, 2, 621–630. doi: 10.1016/j.jcis.2007.06.003.

430. Wang, X., Lu, X., Zhou, Q., Zhao, Y., Li, X., Zhang, S., Database and new models based on a group contribution method to predict the refractive index of ionic liquids. *Phys. Chem. Chem. Phys.* **2017**, *19*, 30, 19967–19974. doi: 10.1039/c7cp03214e.

431. Piñaro, Á., Brocos, P., Amigo, A., Pintos, M., Bravo, R., Surface tensions and refractive indices of (tetrahydrofuran + n-alkanes) at T = 298.15 K. *J. Chem. Thermodyn.* **1999**, *31*, 7, 931–942. doi: 10.1006/jcht.1999.0517.

432. Popescu, C. M., Popescu, M. C., Vasile, C., Structural analysis of photodegraded lime wood by means of FT-IR and 2D IR correlation spectroscopy. *Int. J. Biol. Macromol.* **2011**, *48*, 4, 667–675. doi: 10.1016/j.ijbiomac.2011.02.009.

433. Manivannan, M., Rajendran, S., Investigation of inhibitive action of urea-Zn2+ system in the corrosion control of carbon steel in sea water. *Int. J. Eng. Sci. Technol.* **2011**, *3*, 11, 8048–8060.

434. Zhang, Q., De Oliveira Vigier, K., Royer, S., Jérôme, F., Deep eutectic solvents: Syntheses, properties and applications. *Chem. Soc. Rev.* **2012**, *41*, 21, 7108–7146. doi: 10.1039/c2cs35178a.

435. Charisiadis, P., Kontogianni, V. G., Tsiafoulis, C. G., Tzakos, A. G., Siskos, M., Gerothanassis, I. P., 1H-NMR as a structural and analytical tool of intra- and intermolecular hydrogen bonds of phenol-containing natural products and model compounds. , *Molecules*, *19*, 9, . MDPI AG, 13643–13682, Sep. 02, 2014. doi: 10.3390/molecules190913643.

436. Rodrigues, L. A. *et al.*, Terpene-Based Natural Deep Eutectic Systems as Efficient Solvents to Recover Astaxanthin from Brown Crab Shell Residues. *ACS Sustain. Chem. Eng.* **2020**, *8*, 5, 2246–2259. doi: 10.1021/acssuschemeng.9b06283.

437. Li, Y. *et al.*, An insight into the extraction of transition metal ions by picolinamides associated with intramolecular hydrogen bonding and rotational isomerization. *RSC Adv.* **2014**, *4*, 56, 29702–29714. doi: 10.1039/c4ra02030h.

438. Alhadid, A., Mokrushina, L., Minceva, M., Formation of glassy phases and polymorphism in deep eutectic solvents. *J. Mol. Liq.* **2020**, *314*113667. doi: 10.1016/j.molliq.2020.113667.

439. Bezold, F., Minceva, M., Liquid-liquid equilibria of n-heptane, methanol and deep eutectic solvents composed of carboxylic acid and monocyclic terpenes. *Fluid Phase Equilib.* **2018**, *477*98–106. doi: 10.1016/j.fluid.2018.08.020.

440. Rycerz, L., Practical remarks concerning phase diagrams determination on the basis of differential scanning calorimetry measurements. , in *Journal of Thermal Analysis and Calorimetry*, Jul. 2013, *113*, 1, , 231–238. doi: 10.1007/s10973-013-3097-0.

441. Chemat, F., Anjum, H., Shariff, A. M., Kumar, P., Murugesan, T., Thermal and physical properties of (Choline chloride + urea + l-arginine) deep eutectic solvents. *J. Mol. Liq.* **2016**, *218*301–308. doi: 10.1016/j.molliq.2016.02.062.

442. Food and Agriculture Organization, *World fisheries and aquaculture*. 2018. Accessed: Aug. 27, 2019. [Online]. Available: www.fao.org/publications

443. Govindharaj, M., Roopavath, U. K., Rath, S. N., Valorization of discarded Marine Eel fish skin for collagen extraction as a 3D printable blue biomaterial for tissue engineering. *J. Clean. Prod.* **2019**, *230*412–419. doi: 10.1016/j.jclepro.2019.05.082.

444. Khan, R. A., Natural products chemistry: The emerging trends and prospective goals. *Saudi Pharm. J.* **2018**, *26*, 5, 739–753. doi: 10.1016/J.JSPS.2018.02.015.

445. Nehete, J. Y., Bhambar, R. S., Narkhede, M. R., Gawali, S. R., Natural proteins: Sources, isolation, characterization and applications. *Pharmacogn. Rev.* **2013**, *7*, 14, 107–116. doi: 10.4103/0973-7847.120508.

446. Yamada, Y. *et al.*, Anti-hypertensive activity of genetically modified soybean seeds accumulating novokinin. *Peptides* **2008**, *29*, 3, 331–337. doi: 10.1016/J.PEPTIDES.2007.11.018.

447. Alvarez, A. M. R., Rodríguez, M. L. G., Lipids in pharmaceutical and cosmetic preparations. *Grasas y Aceites* **2000**, *51*, 1–2, 74–96. doi: 10.3989/GYA.2000.V51.I1-2.409.

448. Hoang, H. T., Moon, J.-Y., Lee, Y.-C., Natural Antioxidants from Plant Extracts in Skincare Cosmetics: Recent Applications, Challenges and Perspectives. *Cosmetics* **2021**, *8*, 4, 130. doi: 10.3390/COSMETICS8040106.

449. Ahsan, H., Ahad, A., Siddiqui, W. A., A review of characterization of tocotrienols from plant oils and foods. *J. Chem. Biol.* **2015**, *8*, 2, 59. doi: 10.1007/S12154-014-0127-8.

450. Fiedor, J., Burda, K., Potential Role of Carotenoids as Antioxidants in Human Health and Disease. *Nutrients* **2014**, *6*, 2, 488. doi: 10.3390/NU6020466.

451. Valcarcel, J., Novoa-Carballal, R., Pérez-Martín, R. I., Reis, R. L., Vázquez, J. A., Glycosaminoglycans from marine sources as therapeutic agents. *Biotechnol. Adv.* **2017**, *35*, 6, 711–725. doi: 10.1016/j.biotechadv.2017.07.008.

452. Kim, S.-K., Mendis, E., Bioactive compounds from marine processing byproducts - A review. *Food Res. Int.* **2006**, *39*383–393. doi: 10.1016/j.foodres.2005.10.010.

453. Abbott, A. P., Capper, G., Davies, D. L., Rasheed, R. K., Tambyrajah, V., Novel solvent properties of choline chloride/urea mixtures. *Chem. Commun.* **2003**, 1, 70–71. doi: 10.1039/B210714G.

454. Ünlü, A. E., Arlkaya, A., Takaç, S., Use of deep eutectic solvents as catalyst: A mini-

review. *Green Process. Synth.* **2019**, *8*, 1, 355–372. doi: 10.1515/gps-2019-0003.

455. Zeng, Q., Wang, Y., Huang, Y., Ding, X., Chen, J., Xu, K., Deep eutectic solvents as novel extraction media for protein partitioning. *Analyst* **2014**, *139*, 10, 2565–2573. doi: 10.1039/c3an02235h.

456. Piccirillo, C. *et al.*, Extraction and characterisation of apatite- and tricalcium phosphate-based materials from cod fish bones. *Mater. Sci. Eng. C* **2013**, *33*, 1, 103–110. doi: 10.1016/J.MSEC.2012.08.014.

457. Ferraro, V., Carvalho, A. P., Piccirillo, C., Santos, M. M., Paula, P. M., E. Pintado, M., Extraction of high added value biological compounds from sardine, sardine-type fish and mackerel canning residues — A review. *Mater. Sci. Eng. C* **2013**, *33*, 6, 3111–3120. doi: 10.1016/J.MSEC.2013.04.003.

458. Medina Uzcátegui, L. U., Vergara, K., Martínez Bordes, G., Sustainable alternatives for by-products derived from industrial mussel processing: A critical review. *Waste Manag. Res. J. a Sustain. Circ. Econ.* **2021**, 1–16. doi: 10.1177/0734242X21996808.

459. Bligh, E. G., Dyer, W. J., A rapid method of total lipid extraction and purification. *Can. J. Biochem. Physiol.* **1959**, *37*, 8, 911–917. doi: 10.1139/o59-099.

460. Harrysson, H., Hayes, M., Eimer, F., Carlsson, N. G., Toth, G. B., Undeland, I., Production of protein extracts from Swedish red, green, and brown seaweeds, Porphyra umbilicalis Kützing, Ulva lactuca Linnaeus, and Saccharina latissima (Linnaeus) J. V. Lamouroux using three different methods. *J. Appl. Phycol.* **2018**, *30*, 6, 3565–3580. doi: 10.1007/S10811-018-1481-7/TABLES/4.

461. Galland-Irmouli, A. V. *et al.*, Nutritional value of proteins from edible seaweed Palmaria palmata (dulse). *J. Nutr. Biochem.* **1999**, *10*, 6, 353–359. doi: 10.1016/S0955-2863(99)00014-5.

462. Lowry, O. H., Rosebrough, N. J., Farr, A. L., Randall, R. J., Protein measurement with the Folin phenol reagent. *J. Biol. Chem.* **1951**, *193*, 1, 265–275. doi: 10.1016/S0021-9258(19)52451-6.

463. Barbarino, E., Lourenço, S. O., An evaluation of methods for extraction and quantification of protein from marine macro- and microalgae. *J. Appl. Phycol.* **2005**, *17*, 5, 447–460. doi: 10.1007/S10811-005-1641-4.

464. Volpi, N., Hyaluronic acid and chondroitin sulfate unsaturated disaccharides analysis by high-performance liquid chromatography and fluorimetric detection with dansylhydrazine. *Anal. Biochem.* **2000**, *277*, 1, 19–24. doi: 10.1006/abio.1999.4366.

465. Dong, Y., Yan, W., Zhang, X. Di, Dai, Z. Y., Zhang, Y. Q., Steam Explosion-Assisted Extraction of Protein from Fish Backbones and Effect of Enzymatic Hydrolysis on the Extracts. *Foods* **2021**, *10*, 8, 1942. doi: 10.3390/FOODS10081942.

466. Toppe, J., Albrektsen, S., Hope, B., Aksnes, A., Chemical composition, mineral content and amino acid and lipid profiles in bones from various fish species. *Comp. Biochem. Physiol. Part B Biochem. Mol. Biol.* **2007**, *146*, 3, 395–401. doi: 10.1016/J.CBPB.2006.11.020.

467. Fernández, A., Grienke, U., Soler-Vila, A., Guihéneuf, F., Stengel, D. B., Tasdemir, D., Seasonal and geographical variations in the biochemical composition of the blue mussel (Mytilus edulis L.) from Ireland. *Food Chem.* **2015**, *17*743–52. doi: 10.1016/J.FOODCHEM.2014.12.062.

468. Trilaksani, W., Riyanto, B., Wahyuningsih, T., Characterization and Antioxidant Activity of Hyaluronan from Vitreous Humor of Yellowfin Tuna Eye (Thunnus albacares). *J. Pengolah. Has. Perikan. Indones.* **2019**, *22*, 3, . doi: 10.17844/jphpi.v22i3.29126.

469. Abdallah, M. M. *et al.*, Potential Ophthalmological Application of Extracts Obtained from Tuna Vitreous Humor Using Lactic Acid-Based Deep Eutectic Systems. *Foods* **2022**, *11*, 3, 157. doi: 10.3390/FOODS11030342.

470. Şahin, S., Kurtulbaş, E., Bilgin, M., Special designed deep eutectic solvents for the recovery of high added-value products from olive leaf: a sustainable environment for bioactive materials. *Prep. Biochem. Biotechnol.* **2020**, *51*, 5, 422–429. doi: 10.1080/10826068.2020.1824162.

471. Rondon-Berrios, H. *et al.*, Urea for the Treatment of Hyponatremia. *Clin. J. Am. Soc.*

Nephrol. **2018**, *13*, 11, 1627–1632. doi: 10.2215/CJN.04020318.

472. Huttunen, J. K., Fructose in medicine. *Postgrad. Med. J.* **1971**, *47*, 552, 654. doi: 10.1136/PGMJ.47.552.654.

473. Boomsma, B., Bikker, E., Lansdaal, E., Stuut, P., L-Lactic Acid-A Safe Antimicrobial for Home-and Personal Care Formulations. *SOFW-Journal* **2015**, *141*, 10, 2–5.

474. Wang, C., Chang, T., Yang, H., Cui, M., Antibacterial mechanism of lactic acid on physiological and morphological properties of Salmonella Enteritidis, Escherichia coli and Listeria monocytogenes. *Food Control* **2015**, *47*231–236. doi: 10.1016/J.FOODCONT.2014.06.034.

475. Yoshimura, K. *et al.*, Effect of Lactic Acid Content into on during Miconazole Eye Drops to be Used for Infection Preventive. *J. Drug Res. Dev.* **2021**, *7*, 1, 1–7. doi: 10.16966/2470-1009.160.

476. Barclay, T., Ginic-Markovic, M., Cooper, P., Petrovsky, N., The chemistry and sources of fructose and their effect on its utility and health implications. *J. Excipients Food Chem.* **2012**, *3*, 2, 67–82.

477. Schütte, E., Reim, M., Fructose Metabolism of the Cornea. *Ophthalmic Res.* **1976**, *8*, 6, 434–437. doi: 10.1159/000264851.

478. Kinoshita, J. H., Physiological chemistry of the eye. *Arch. Ophthalmol.* **1962**, *68*, 4, 554–570. doi: 10.1001/ARCHOPHT.1962.00960030558024.

479. Galin, M. A., Aizawa, F., McLean, J. M., Urea as an Osmotic Ocular Hypotensive Agent in Glaucoma. *AMA. Arch. Ophthalmol.* **1959**, *62*, 3, 347–352. doi: 10.1001/ARCHOPHT.1959.04220030003001.

480. Gandhi, G. M., Anasuya, S. R., Kawathekar, P., Bhaskarmall, Krishnamurthy, K. R., Urea in the management of advanced malignancies (Preliminary report). *J. Surg. Oncol.* **1977**, *9*, 2, 139–146. doi: 10.1002/JSO.2930090207.

481. Fredriksson, T., Gip, L., Urea creams in the treatment of dry skin and hand dermatitis. *Int. J. Dermatol.* **1975**, *14*, 6, 442–444. doi: 10.1111/J.1365-4362.1975.TB00137.X.

482. Sharma, A., Keisham, N. K., Sharma, A., Correlation between Urea Levels in Lacrimal Fluid and Patho-Physiology of Dry Eye Syndromes. *IOSR J. Dent. Med. Sci.* **2020**, *19*29–34. doi: 10.9790/0853-1908142934.

483. Jäger, K., Kielstein, H., Dunse, M., Nass, N., Paulsen, F., Sel, S., Enzymes of urea synthesis are expressed at the ocular surface, and decreased urea in the tear fluid is associated with dry-eye syndrome. *Graefe's Arch. Clin. Exp. Ophthalmol.* **2013**, *251*, 8, 1995–2002. doi: 10.1007/S00417-013-2391-7.

484. Manda, G., Mocanu, M. A., Marin, D. E., Taranu, I., Dual Effects Exerted in Vitro by Micromolar Concentrations of Deoxynivalenol on Undifferentiated Caco-2 Cells. *Toxins (Basel).* **2015**, *7*, 2, 593–603. doi: 10.3390/TOXINS7020593.

485. Sambruy, Y., Ferruzza, S., Ranaldi, G., De Angelis, I., Intestinal Cell Culture Models: Applications in Toxicology and Pharmacology. *Cell Biol. Toxicol.* **2001**, *17*, 4, 301–317. doi: 10.1023/A:1012533316609.

486. Serra, A. T., Seabra, I. J., Braga, M. E. M., Bronze, M. R., De Sousa, H. C., Duarte, C. M. M., Processing cherries (Prunus avium) using supercritical fluid technology. Part 1: Recovery of extract fractions rich in bioactive compounds. *J. Supercrit. Fluids* **2010**, *55*, 1, 184–191. doi: 10.1016/J.SUPFLU.2010.06.005.

487. Huang, D., Ou, B., Hampsch-Woodill, M., Flanagan, J. A., Prior, R. L., High-throughput assay of oxygen radical absorbance capacity (ORAC) using a multichannel liquid handling system coupled with a microplate fluorescence reader in 96-well format. *J. Agric. Food Chem.* **2002**, *50*, 16, 4437–4444. doi: 10.1021/JF0201529.

488. Feliciano, R. P. *et al.*, Phenolic content and antioxidant activity of moscatel dessert wines from the setúbal region in portugal. *Food Anal. Methods* **2009**, *2*, 2, 149–161. doi: 10.1007/S12161-008-9059-7.

489. Waitz, J. A., *Methods for Dilution Antimicrobial Susceptibility Tests for Bacteria That Grow Aerobically*, Tenth. CLSI document No. M07-A10. Clinical and Laboratory Standards Institute: Wayne, Pennsylvania, 1990.

490. Cano-Sancho, G., González-Arias, C. A., Ramos, A. J., Sanchis, V., Fernández-Cruz, M.

L., Cytotoxicity of the mycotoxins deoxynivalenol and ochratoxin A on Caco-2 cell line in presence of resveratrol. *Toxicol. Vitr.* **2015**, *29*, 7, 1639–1646. doi: 10.1016/J.TIV.2015.06.020.

491. Bony, S., Carcelen, M., Olivier, L., Devaux, A., Genotoxicity assessment of deoxynivalenol in the Caco-2 cell line model using the Comet assay. *Toxicol. Lett.* **2006**, *166*, 1, 67–76. doi: 10.1016/J.TOXLET.2006.04.010.

492. Marchel, M., Cieśliński, H., Boczkaj, G., Deep eutectic solvents microbial toxicity: Current state of art and critical evaluation of testing methods. *J. Hazard. Mater.* **2022**, *425*127963. doi: 10.1016/J.JHAZMAT.2021.127963.

Funding acknowledgment

The authors acknowledge the financial support received from the European Union's H2020-MSCA program, IT-DED^3 project grant agreement: 765608.

iNOVA4Health—UIDB/04462/2020 and UIDP/04462/2020, a program financially supported by Fundação para a Ciência e Tecnologia/Ministério da Ciência, Tecnologia e Ensino Superior, through national funds is acknowledged.

Funding from INTERFACE Programme, through the Innovation, Technology and Circular Economy Fund (FITEC), is gratefully acknowledged.

ITQB-UNL | Av. da República, 2780-157 Oeiras, Portugal
Tel (+351) 214 469 100 | Fax (+351) 214 411 277

www.itqb.unl.pt